NTNU

Norwegian University of
Science and Technology

Cost-Optimization of the Safety Factor for Design of Mooring Lines with Bayesian Networks

Eivind Rindal

Civil and Environmental Engineering
Submission date: June 2018
Supervisor: Jochen Kohler, KT
Co-supervisor: Kjell Larsen, Statoil/NTNU

Norwegian University of Science and Technology
Department of Structural Engineering

Department of Structural Engineering
Faculty of Engineering
NTNU- Norwegian University of Science and Technology

ACCESSIBILITY

OPEN

MASTER THESIS 2018

SUBJECT AREA:	DATE:	NO. OF PAGES:
Structural Reliability	June 8 2018	13 + 74 + 9

TITLE:

Cost-Optimization of the Safety Factor for Design of Mooring Lines with Bayesian Networks

BY:

Eivind Rindal

SUMMARY:
This Thesis investigates how aspects of mooring line design and integrity management of mooring lines can be coupled with decision theory and structural reliability methods to address the optimal safety factor based on risk-informed cost optimization. Three research objectives have been formulated to aid achieving the overarching objective: (1) to represent the current design practice as a decision graph; (2) to represent the current inspection and maintenance routines as a decision graph; (3) to assess the sensitivity of decision outcomes towards the various influencing variables, and estimate the gain of acquiring additional information. Relevant events, decision alternatives, consequences, random variables and their associated uncertainties have to be explored upfront as a prerequisite for the modeling.

The software GeNIe is used to create decision graphs for the design phase. The resulting networks represent the ultimate and accidental limit state. The fatigue limit state is not addressed in this study. The series effect of the line components is neglected, and the decisions kept to a minimum, accounting only for the grade, diameter, and consequence class. Cost-optimization curves are derived from the decision graphs. Results show that the optimal safety factors, in general, are below the values provided by ISO 19901-7.

An attempt is made to model the inspection phase as dynamic decision graph in GeNIe. Since dynamic decision graphs are not supported in the software, two potential solutions are pursued. The first approach is to create an unrolled version of the network, and the second approach is to use chance nodes as proxies for the decision nodes and to subsequently compute the expected cost manually. It is concluded that both approaches are not feasible without considerable effort; therefore, further investigation of the topic is suspended.

A sensitivity analysis with respect to the failure event is conducted for the design phase networks. Diameter is found to be the most influential parameter, followed by the loads, corrosion rates, and chosen grades. The value of information analysis shows a larger expected gain when the system effects are neglected. This may be due to the assumed independence for corrosion rates and service life between the mooring lines. When system effects are neglected, it is preferred to obtain perfect information on the loads or corrosion rates, while when accounted for, observing loads is the least preferred strategy.

RESPONSIBLE TEACHER: Professor Jochen Köhler

SUPERVISORS: Professor Jochen Köhler, Ajunct Professor Kjell Larsen

CARRIED OUT AT: The Department of Structural Engineering, NTNU

Abstract

The structural integrity of mooring lines is critical for the safety of offshore facilities. In recent years, concerns have been raised in the offshore industry about the high failure rates compared to the design expectations, in particular in the first years of service. This motivates a review of the design procedures and inspection and maintenance policies. Research is to be conducted to provide insight into the causes of failure as support for better decision-making.

This Thesis investigates how aspects of mooring line design and integrity management of mooring lines can be coupled with decision theory and structural reliability methods to address the optimal safety factor based on risk-informed cost-optimization. Three research objectives have been formulated to aid achieving the overarching objective: (1) to represent the current design practice as a decision graph; (2) to represent the current inspection and maintenance routines as a decision graph; (3) to assess the sensitivity of decision outcomes towards the various influencing variables, and estimate the gain of acquiring additional information. Relevant events, decision alternatives, consequences, random variables and their associated uncertainties have to be explored upfront as a prerequisite for the modeling.

The software GeNIe is used to create decision graphs for the design phase. The resulting networks represent the ultimate and accidental limit state. The fatigue limit state is not addressed in this study. The series effect of the line components is neglected, and the decisions kept to a minimum, accounting only for the grade, diameter, and consequence class. Cost-optimization curves are derived from the decision graphs. Results show that the optimal safety factors, in general, are below the values provided by ISO 19901-7.

An attempt is made to model the inspection phase as dynamic decision graph in GeNIe. Since dynamic decision graphs are not supported in the software, two potential solutions are pursued. The first approach is to create an unrolled version of the network, and the second approach is to use chance nodes as proxies for the decision nodes and to subsequently compute the expected cost manually. It is concluded that both approaches are not feasible without considerable effort; therefore, further investigation of the topic is suspended.

A sensitivity analysis with respect to the failure event is conducted for the design phase networks. Diameter is found to be the most influential parameter, followed by the loads, corrosion rates, and chosen grades. The value of information analysis shows a larger expected gain when the system effects are neglected. This may be due to the assumed independence for corrosion rates and service life between the mooring lines. When system effects are neglected, it is preferred to obtain perfect information on the loads or corrosion rates, while when accounted for, observing loads is the least preferred strategy.

Sammendrag

Den strukturelle integriteten til forankringsliner er avgjørende for sikkerheten til offshoreanlegg. I de siste årene er det observert høyere feilrater enn forventet, spesielt i de første årene av levetiden. Dette motiverer en gjennomgang av dimensjonering og inspeksjons- og vedlikeholdsrutiner, for å øke forståelsen for årsakene til linebrudd og dermed gi støtte for bedre beslutningstaking.

Denne avhandlingen undersøker hvordan aspekter fra dimensjonering og integritetsstyring av forankringsliner kan kombineres med beslutningsteori og pålitelighetsmetoder for bestemme den kostnadsoptimale sikkerhetsfaktoren. Tre delmål har blitt formulert for å bidra til å oppnå det overordnede målet: (1) å representere den nåværende dimensjoneringspraksis som et beslutningsdiagram; (2) å representere de nåværende inspeksjons- og vedlikeholdsrutiner som et beslutningsdiagram; (3) å utføre en sensitivitetsanalyse av de resulterende beslutningsdiagrammene, og å estimere verdien av å innhente ytterligere informasjon. Relevante hendelser, beslutningsalternativer, konsekvenser, tilfeldige variabler og tilhørende usikkerheter må identifiseres på forhånd som en forutsetning for modelleringen.

Programmet GeNIe er brukt til å lage beslutningsdiagrammer for dimensjoneringen. De resulterende nettverkene representerer bruddgrense- og ulykkegrensetilstanden. Utmattingsgrensetilstanden er ikke undersøkt i denne avhandlingen. Serieffekten av linekomponentene er neglisjert, og kun beslutninger om stålkvalitet, diameter og konsekvensklasse er inkludert. Kostnadsoptimaliseringskurver generert fra beslutningdiagrammene viser at de optimale sikkerhetsfaktorene generelt sett er lavere enn verdiene gitt i ISO 19901-7.

Det er forsøkt å modellere inspeksjonsrutiner som et dynamisk beslutningsdiagram i GeNIe. Da dynamiske beslutningsdiagrammer ikke støttes av programvaren, er to potensielle løsninger utforsket. Den første tilnærmingen er å konvertere nettverket til et vanlig beslutningsdiagram, og den andre tilnærmingen er å benytte sannsynlighetsnoder som stedfortreder for beslutningsnodene og for å så manuelt beregne den forventede kostnaden. Det er konkludert at begge tilnærminger ikke er gjennomførbare uten betydelig innsats, derfor er ikke emnet undersøkt videre.

En sensitivitetsanalyse er gjennomført for dimensjoneringsmodellene. Det er vist at diameter er den mest innflytelsesrike parameteren, etterfulgt av last, korrosjonsrater og stålkvalitet. De estimerte avkastningene for ytterligere informasjon er størst når systemeffektene av forankringssytemet er neglisjert. Dette kan skyldes av at korrosjonsrater og levetid for forankringslinene er antatt uavhengig. Når systemeffekter er neglisjert er det foretrukket å innhente ytterligere informasjon om belastningene eller korrosjonsratene, mens når de er medregnet er innhenting av informasjon om last det minst foretrukne alternativet.

Preface

This MSc Thesis is conducted for the Department of Structural Engineering at The Norwegian University of Science and Technology (NTNU), as a prerequisite for achieving a master's degree. The work presented in this Thesis has been carried out from mid January to the start of June, 2018.

The target audience for this Thesis is engineers or people with a similar technical background, with prior knowledge about statistics and structural engineering. Although this Thesis concerns offshore mooring lines, no prior knowledge about this topic is needed, as this is covered in its introductory chapters.

I would like to express my gratitude to my supervisors, Professor Jochen Köhler at NTNU, and adjunct professor Kjell Larsen at NTNU and Equinor Research Center, who gave support and valuable advice throughout the whole project. I would also like to thank Ph.D. candidate Jorge Mendoza Espinoza at NTNU for the detailed feedback he provided during the project.

Furthermore, I would like to thank Håkon Dahle for our productive cooperation at NTNU and UC Berkeley, but also for being a good travel companion and friend. Last but not least, I would like to thank my parents for their support and advice during all these years.

Eivind Rindal

Norwegian University of Science and Technology
Trondheim, June 8, 2018

Contents

Nomenclature

A_m	Added Mass
a	Action
B	Linear Damping
B_v	Viscous Damping
C_F	Cost of Failure
C_I	Cost of Inspection
C_R	Cost of Replacement
C_t	Stiffness
c	C-factor
d	Diameter
δ	Corroded Diameter
e	Experiment Alternative
$F_x\,(t)$	Excitation Forces
$f_{X,Y}$	Joint Probability Density Function for X and Y
$g\,(R,S)$	Limit State Function
m	Mass
$P\,(A)$	Probability of A
$P\,(A \mid E)$	Probability of A Conditional on E
$P\,(A,E)$	Joint Probability of A and E
$P'\,(A)$	Prior Probability of A
$P''\,(A)$	Posterior Probability of A
P_F	Probability of Failure
$R\,(t)$	Resistance
R_C	Minimum Breaking Strength
R_{Corr}	Corrosion Rate
$S\,(t)$	Load
S_L	Service Life
SF	Safety Factor
S_C	Most Probable Maximum
θ	State
u	Utility
W	Weight
Z	Experiment Outcome

Abbreviations

ALS	Accidental Limit State
CPT	Conditional Probability Table
DAG	Directed Acyclic Graph
DOF	Degrees of Freedom
DP	Dynamic Positioning
EUR	Euro
FLS	Fatigue Limit State
FPSO	Floating Production, Storage, and Offloading Unit
GBP	Pound Sterling
JIP	Joint Industry Project
LF	Low-Frequency
MAUT	Multiple-Attribute Utility Theory
MCMC	Markov Chain Monte Carlo
MNOK	Million Norwegian Kroner
MBS	Minimum Breaking Strength
MPI	Magnetic Particle Inspection
MPM	Most Probable Maximum
NDT	Non-Destructive Testing
PDF	Probability Density Function
PMF	Probability Mass Function
PSA	Petroleum Safety Authority
SPM	Single Point Mooring
SRB	Sulphur Reducing Bacteria
Std	Standard Deviation
ULS	Ultimate Limit State
USD	United States Dollar
WF	Wave-Frequency

1 Introduction

Mooring lines are a common solution for stationkeeping of offshore structures on the Norwegian continental shelf. Their main purpose is to limit the horizontal offset to avoid damage to the risers, umbilicals and other equipment, and to maintain a safe distance to other offshore structures. A mooring line failure is an undesirable event because it may lead to a halt of production, damage to assets and the environment and loss of human lives. After years of decline, the number of recorded incidents have started to increase, with as many as 16 mooring line failures occurring between 2010 and 2014 (Kvitrud 2014). The relative high failure rates prompt a review of the current design procedure and the inspection and maintenance routines.

A significant amount of research is being conducted on the topic of mooring line failures, such as the recently commenced LifeMoor project and the ongoing NorMoor joint industry project (JIP). NorMoor JIP includes participants from oil companies, engineering companies, rig-owners, manufacturers and marine authorities, and covers the Gulf of Mexico, Brazil, and Northern Europe. The project aims to calibrate the safety factors to ensure an appropriate target reliability level. The safety factors for the ultimate and accidental limit states were calibrated in phase 1-2 (2012-2016), and fatigue limit state calibration is ongoing and will be completed in 2019 (Okkenhaug et al. 2017).

This Thesis approaches the calibration of safety factors in a top-down manner. It is sought after developing accurate and robust risk-based decision networks. For that purpose, relevant regulations and routines are reviewed and complemented with literature on Bayesian networks in the context of structural reliability. The resulting models may act as starting points for incremental improvements in the field when better sub-models for representing the relevant processes are developed. As the industry is pursuing operations in deeper and colder waters in new frontiers, such as the Arctics, the risk-based decision networks suggested in this Thesis, might prove to be an effective tool to maintain safety for personnel, property and the environment.

1.1 Research Topics and Goals

The objective of the Thesis is to analyze and represent the current practice of mooring line design and inspection and maintenance routines and to describe the relevant events, decisions, consequences and the associated uncertainties, and how the various factors influence the decision outcome. Three major research goals have been formulated to achieve this objective:

1. ***How can the current design practice be represented as a decision graph?*** The relevant guidelines for the design of mooring lines are given in ISO 19901-7 and DVNGL-OS-E301. Based on these documents, the relation between the variables relevant for the design can be determined and structured in a Bayesian network or decision graph in a suitable program such as GeNIe. The arising limit state functions may be evaluated by various methods for assessing structural reliability, such as FORM/SORM and Monte

Carlo sampling in order to determine the *conditional probability tables* (CPTs) needed for modeling with Bayesian networks. The continuous nodes arising from continuous random variables in the limit state functions need to be discretized and subsequently removed to ensure exact inference as described in Daniel Straub (2009) and Daniel Straub and Der Kiureghian (2010). The consequences of the different alternatives must be determined by expert opinion or estimated based on the available data.

2. ***How can the current inspection and maintenance routines be represented as a decision graph?*** ISO 19901-7, DVNGL-OS-E301 and experts from Equinor give insight on the current inspection and maintenance routines. By using the methods described in Daniel Straub (2009), a dynamic Bayesian network can be created to show how the deterioration of the mooring lines develops over time and how actions and evidence affect the optimal policy. The intention is to further enhance the network to system scale, modeling the deterioration of several mooring lines, inspired by the network used to model Dutch highway bridges in Alex Kosgodagan et al. (2015). The dynamic Bayesian network need initial and transitional probabilities as input. These probabilities can be assessed as performed in Kosgodagan et al. (2015) or based on structural reliability methods.

3. ***What is the expected value of acquiring additional information for the decision-maker?*** The aim of the value of information analysis is to investigate if the decision-maker, in this case Equinor, should invest in more extensive research and *in situ* data acquisition on particular fields to reduce the uncertainty. This analysis can be performed as explained in Thomas Dyhre Nielsen and Jensen (2009). A sensitivity analysis will determine how strongly the parameters in the network influence the outcome, thus revealing the critical areas for further enhancements. The sensitivity analysis and its implementation as an algorithm are described in detail in Castillo et al. (1997) and Kjærulff and van der Gaag (2000), respectively.

1.2 Limitations

This Thesis is limited to cover modeling of the ultimate limit state and to some degree the accidental limit state. The effects of fatigue are not accounted for in the resulting networks. Also, the series effect arising from the mooring line components is assumed to be negligible. The consequence of this assumption is discussed in the conclusion of Chapter 4. Furthermore, this Thesis is limited to a simple representation of the load distributions.

1.3 Thesis Layout

In Chapter 2, theoretical background of the characteristics of mooring lines is presented, such as the different configurations, components, failure rates and potential consequences of failure. The chapter also contains a literature review of the current design practice, and the inspection and maintenance policy. Chapter 3 covers the relevant theoretical background of Bayesian

networks and decision graphs in the context of structural reliability, and a literature review on research on the topic. The current design practice of mooring lines is represented as a risk-based design problem in Chapter 4. Similar to the previous chapter, a decision graph of the current inspection and maintenance routines are given in Chapter 5. In Chapter 6, a value of information analysis is conducted to investigate how potential improvements of the network or the inspection methods will benefit the decision-maker. A sensitivity study of the network parameters is also conducted in this chapter. Finally, Chapter 7 will summarize the Thesis, provide the general conclusions and present an outlook on further research on the topic.

2 Review of Mooring Line Characteristics

This chapter introduces basic concepts of mooring line characteristics, design, and inspection routines, as a prerequisite for later chapters, in particular, Chapter 4 and Chapter 5. First, the different offshore structures are introduced, and the various concepts of mooring system layouts are discussed. This is followed by an introduction to the different components usually found in a mooring line. Then, a brief description of mooring line design and inspection routines are presented. In the end, the chapter discusses failure rates and potential consequences, before concluding with a summary.

2.1 Types of Structures

There are numerous different types of offshore structures, ranging from platforms fixed on the seabed to semi-submersible structures. Figure 1 illustrates the most common types of platforms, from the left: jacket; gravity platform; semi-submersible; floating production, storage and offloading unit (FPSO); and a tension leg platform. All the different types of platforms are required to keep stationary for shorter or more extended periods of time. For semi-submersible or FPSO platforms, this requirement is usually fulfilled through the use of dynamic positioning (DP), mooring systems or a combination of the two. A more thorough review of the different platform types is given in Keshavarz (2011).

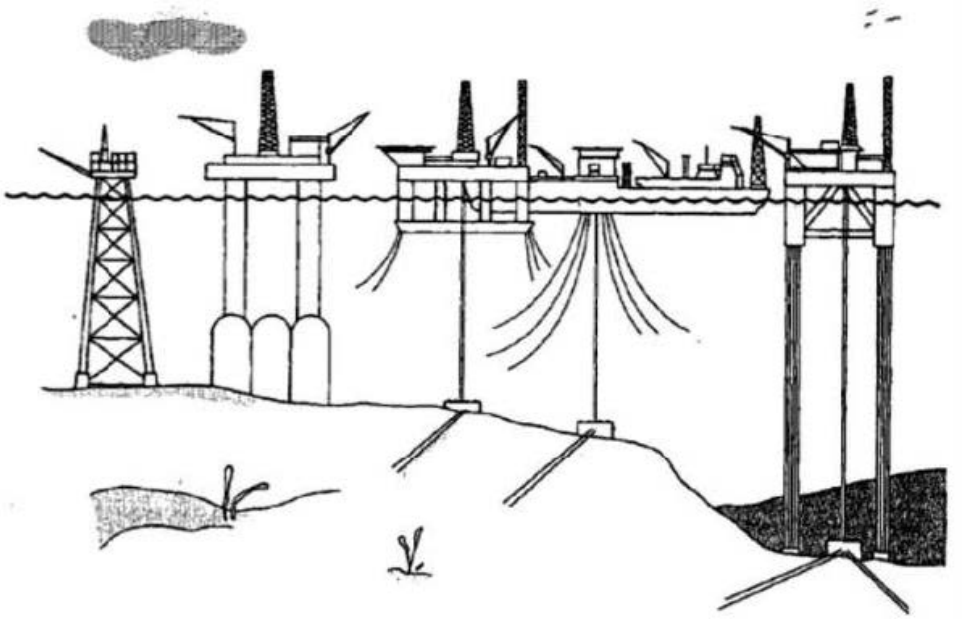

Figure 1: Different types of offshore structures (Faltinsen 1993, p. 2)

2.2 Mooring Line Systems

There are several kinds of mooring systems available to handle the vastly different locations and weather-systems, platform types and mooring durations. A mooring system consists of several

mooring lines, normally between 12 to 20 (Larsen 2017). The system can be characterized by how it connects the offshore structure to the seabed. A spread mooring system is connected to multiple points on the platform, thus fixing the orientation of the platform. Due to its simplicity, it is a common solution for semi-submersibles in relatively calm waters. Single point mooring (SPM) is a more common solution for FPSOs, as they are usually ship shaped, whereas a spread mooring system leads to higher demand on the mooring system. An SPM system has all mooring lines connected to a turret, which can be internally or externally integrated with the platform, and it acts as a point of rotation. This allows the platform to weather-vane, thus reducing the total load on the mooring system. However, it is a more complex solution because its ability to rotate makes it necessary to connect the risers (pipes that transport hydrocarbons) and umbilicals (pipes that contain hydraulic wires, electric wires, and fiber optics) to the turret in addition to the mooring lines (Noble Denton Europe 2006). An illustration of an internal turret is given in Figure 2.

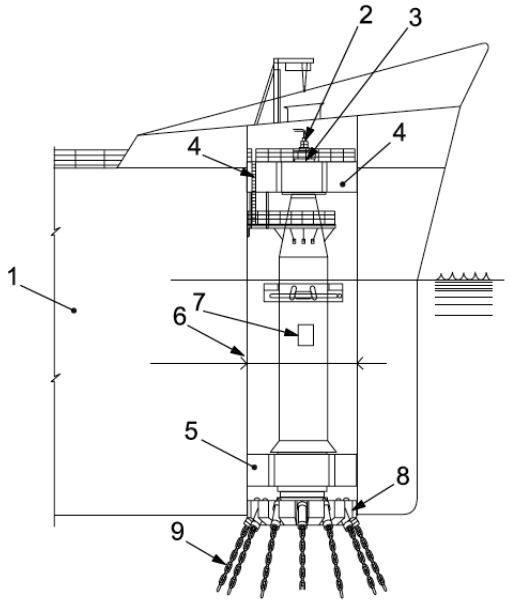

Figure 2: Schematic of an internal turret (ISO 19901-7, p. 58)

Furthermore, the mooring system can be categorized by how it generates the resisting forces. The most common types of configuration are called catenary and taut leg. Illustrations of catenary and taut leg configurations are shown in Figure 3(a) and Figure 3(b) respectively.

As suggested by its name, the catenary mooring lines form a curve and are not fully stretched. In this configuration, the restoring forces are generated by the self-weight of the mooring line and friction against the seabed. To be effective, a substantial length of the line, normally a chain segment, rests on the seabed (Chakrabarti 2005). The catenary configuration is suitable for relatively shallow waters, as it requires a large amount of chain and space at the seabed, limiting space available for other installations on the seabed and increasing the risk for a clash

between the mooring lines and pipelines (Keshavarz 2011). Catenary lines are commonly used on the Norwegian continental shelf.

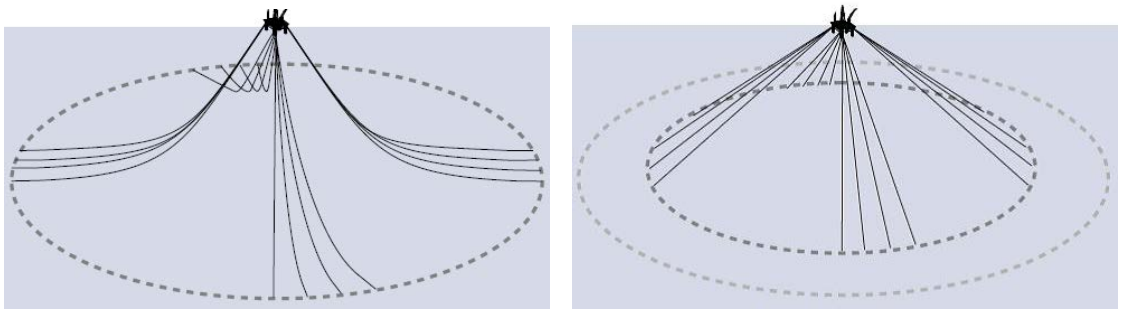

(a) Catenary mooring system (b) Taut leg mooring system

Figure 3: Different mooring systems (Noble Denton Europe 2006, p. 28-29)

In contrast, taut leg lines are fully stretched from the platform to the attachment point on the seabed. This makes the configuration more suitable for deep waters where self-weight is a restraint, and in areas where there is limited space on the seabed due to pipelines and sub-sea structures. It is essential that the lines are long and elastic enough to develop sufficient capacity to absorb the motions of the platform without overloading from the dynamic excitation (Chakrabarti 2005).

Regardless of how the lines are attached or generate resisting forces, they can be clustered or evenly spread out. Evenly spread mooring lines are the most simple solution, but there might be other factors to consider that makes clustered lines the more optimal solution. For instance, the layout of the risers and sub-sea structures governs this decision, as a collision with the mooring lines must be avoided. In addition, it might be favorable to group the mooring lines in clusters if the weather tends to have a specific direction (Chakrabarti 2005).

2.3 Mooring Line Components

To govern certain properties, for example, geometric or elastic stiffness and self-weight, it is common to segment the mooring lines. A common mooring line often consists of several components such as chain segments, steel wires, synthetic ropes, buoys, and anchors. Figure 4 illustrates a segmented catenary mooring line. The chain segments are often used in the areas with the highest corrosion and wear rates, which is where the mooring line rests on the seabed, called the *touch down zone* or *trash zone*, and the surface area called the *splash zone*. In the trash zone, the lifting and lowering of the catenary chain due to the motions of the platform causes it to slam onto the seabed resulting in mechanical damage and wear (Hoel 2016). In the trash zone, *sulphur reducing bacteria* (SRB) makes this a highly corrosive environment, while in the splash zone this is caused by the high oxygen level (Tømmervåg 2016).

The mooring lines are attached to the seabed with anchors, which have different properties depending on the type. Drag anchors can sustain high horizontal loads but are vulnerable to lateral loading; therefore, they are only suitable for catenary mooring lines (Hoel 2016). On the other hand, piled anchors or suction anchors can sustain both horizontal and vertical loads associated with the taut leg configuration (Noble Denton Europe 2006). For spread mooring systems, the mooring lines are connected to the structure through a fairlead or a trumpet to guide and control them. The contact between the line and trumpet or fairlead subjects the lines to heavy wear, as seen on some of the chain links. Therefore, the tension in the line is often adjusted slightly to even out the wear over all the mooring lines (Keshavarz 2011).

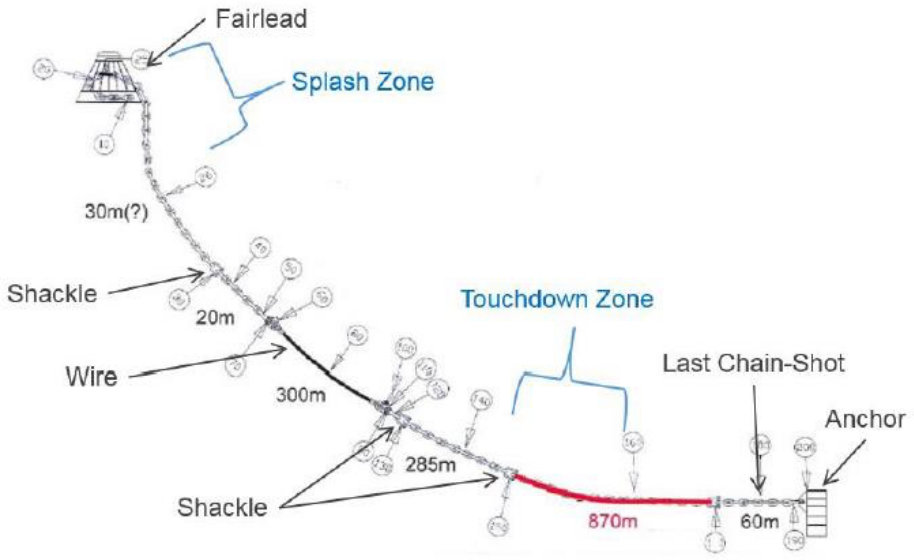

Figure 4: Schematic of a segmented mooring line (Tømmervåg 2016, p. 8)

2.3.1 Chains

Mooring lines often consist of substantial lengths of chain segments. The chain links are produced by bending steel bars into shape and welding the plane sections together. The exact dimensions are difficult to establish because of plastic deformation that takes place during the production, but the bent section tends to have a reduced diameter (Tømmervåg 2016). Therefore, tolerances for geometry and diameter are specified in DNVGL-OS-E302 and IACS W22. The links are subsequently subjected to proof loading, which they must sustain without fracture, to ensure that the links are of sufficient quality. The manufacturing process and quality control are described in detail in the Rämnes Bruk Product Catalogue.

The links in the chain can be of the studded (also called studlink) or the studless type as illustrated in Figure 5. The main difference between them is the transverse stud found in the studded type. There are advantages and disadvantages for the different types; while a studless link is

lighter and easier to handle than a studlink and has a longer fatigue life, the studlink has greater stiffness and is less likely to twist, but the stud could make defects in the material harder to discover during inspection (Chakrabarti 2005).

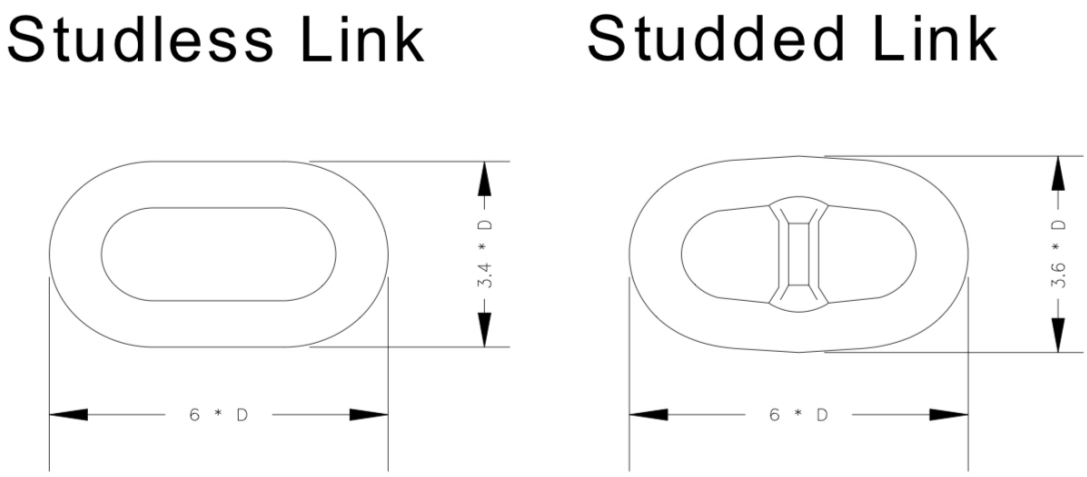

Figure 5: Illustration of a studless link and studded link (Noble Denton Europe 2006, p. 40)

There are currently five different steel grades in use in the offshore industry: R3, R3S, R4, R4S, and R5. Their minimum requirements are given in Table 1. Special care ought to be used when selecting the steel grade of the chain. While a low tensile strength might lead to insufficient capacity, high tensile strength steel has been observed to be more susceptible to hydrogen-assisted cracking (Kvitrud 2014). Because of this, Equinor has specified a maximum yield strength and ultimate strength for R5 but does normally not use a higher steel grade than R4S (Bache 2017).

Table 1: Min. mechanical properties for chain cables (adapted from DNVGL-OS-E302, p. 27)

Grade	**Yield Stress [MPa]**	**Tensile Strength [MPa]**	**Elongation [%]**	**Reduction of Area [%]**
R3	410	690	17	50
R3S	490	770	15	50
R4	580	860	12	50
R4S	700	960	12	50
R5	760	1000	12	50

2.3.2 Steel Wire Rope

Wire ropes are suitable as a component in mooring lines, as they have high yield strength, but relatively low self-weight (Larsen 2015). They are often used in the water span, where the low abrasion characteristics do not hinder its use. Steel wire ropes consist of one or more strands, which is individual wires wound in a helical pattern. Single-strand wire ropes are primarily

used for permanent moorings (mooring period longer than five years), and multi-strand wire ropes are most common in temporary moorings (Keshavarz 2011).

The wire ropes are required to be fully protected against corrosion to preserve the fatigue capacity of the wire ropes exhibit in the air. This protection is normally done by sheathing with a polyurethane coating, adding a coating of sacrificial wires or galvanizing. Special care ought to be used during the installation phase, as bending of the wire rope severely reduces its fatigue life (ISO 19901-7, DNVGL-OS-E304).

2.3.3 Synthetic Fiber Rope

The industry has experienced increased use of synthetic fiber ropes, especially polyester ropes, but other high-tech fibers exist. The ropes provide high elasticity and have a low self-weight. The fiber used for the ropes is made from visco-elastic materials; therefore, the stiffness is not constant but varies with load magnitude, number of cycles and frequency. Besides, the fibers may creep as their age increases (Noble Denton Europe 2006).

The main remaining technical issue for synthetic fiber rope is its low external abrasion resistance. Due to this, the rope can only be used in the water span, so it stays clear of contact with the seabed or fairlead (Larsen 2015).

2.4 Design of Mooring Systems

Mooring line design is an essential barrier against mooring line failure, and to ensure integrity throughout the planned service life. The chosen system depends on location, type of operation, duration, the consequence of failure, and the total cost. Details about the design of mooring systems are given in DVNGL-OS-E301 and ISO 19901-7.

Mooring lines are designed to resist all known loads with a sufficient margin. This requirement is called the design format, formulated as $S_C \cdot SF \leq R_C$ and illustrated in Figure 6, where S_c and R_c refer to *most probable maximum* (MPM) and *minimum breaking strength* (MBS), respectively. If it is exceeded, the structure is in a state which no longer fulfills the relevant design criteria. The design format is equivalent to the limit state function, formulated in mathematical terms as $g = R - S$, where R represents resistance, and S represents the load. When the limit state function is equal to zero, it defines the boundary between the safe domain and the failure domain. The probability of failure may be expressed through the limit state function as $P_F = P\left(R - S \leq 0\right) = \iint_{R \leq S} f_{R,S}\left(r, s\right) drds$, where $f_{R,S}$ is the joint probability density function.

There are three design limit states to be satisfied (DVNGL-OS-E301):

- *Ultimate Limit State* (ULS): Design against overload for an intact mooring system subjected to extreme weather conditions. It means that the MBS must exceed the MPM scaled by a safety factor

- *Accidental Limit State* (ALS): Design against overload for a damaged system subjected to extreme weather conditions. This check is to ensure that the system can endure a failure of one or two (depending on the consequence class) mooring lines of sub-standard quality
- *Fatigue Limit State* (FLS): Design against fatigue failure so all mooring lines can withstand the accumulated damage, taking all possible sea states into account

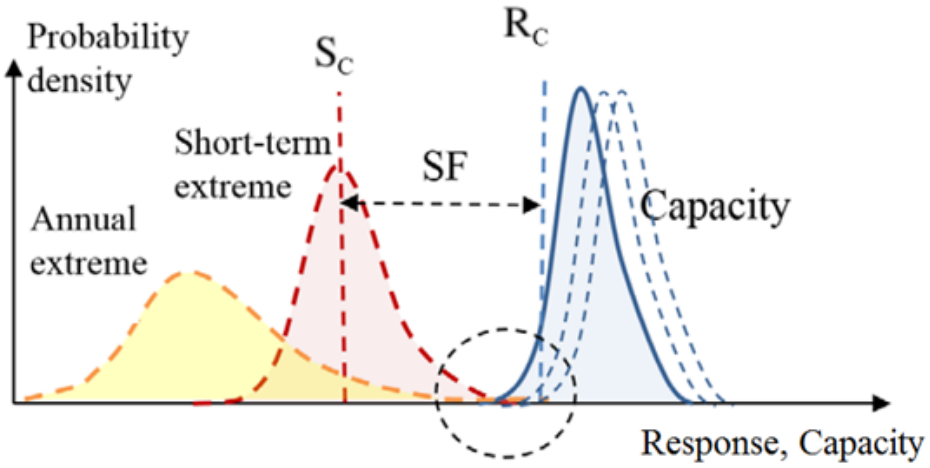

Figure 6: Illustration of the design format (Larsen 2015)

The safety factors take different values depending on the type of analysis and consequence class. There are three consequence classes given in ISO 19901-7 which apply for ULS and ALS. In this Thesis, it is chosen to not distinguish between class 2 and 3 and to only refer to stricter class 3. The two consequence classes used in this Thesis are listed below.

- Class 1: The survival condition, where mooring system failure is unlikely to lead to unacceptable consequences such as loss of life, collision with an adjacent platform, an uncontrolled outflow of oil or gas, capsize or sinking
- Class 3: The standby condition, where mooring system failure may well lead to unacceptable consequences of the types mentioned in class 1

For the fatigue limit state, the concept of consequence classes is not used. Instead, the system is checked for both single line failure and multiple line failures.

2.4.1 Loads

For mooring line tension, the floater motions at the top end are the governing excitation mechanism (Larsen 2015). The motion of the floater is governed mainly by forces generated by winds, waves, and currents, but it is required to take marine growth, tide and storm surges, earthquakes, temperature differences, and snow and ice into account where it is applicable (DVNGL-OS-E301). The effect of the motion of the floater on the mooring lines is illustrated in Figure 7.

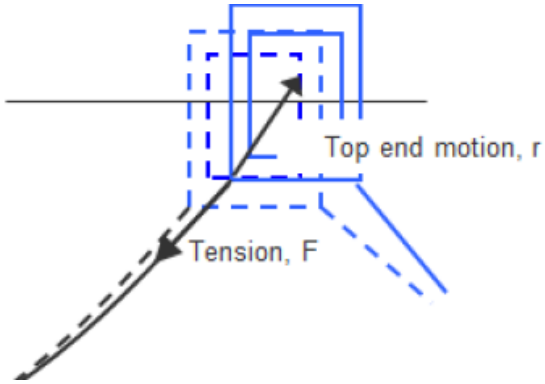

Figure 7: The effect of the top end motion on the mooring line (Larsen 2015)

Normally, sea states with return periods of 100 years are used to evaluate the wave loads. Different combinations of *significant wave height* and *peak wave period* along the *100-year contour line* are used to ensure that the mooring system is properly designed. An example of a 100-year contour line is illustrated in Figure 8. The chosen sea states are applied together with the corresponding states for wind and current (DVNGL-OS-E301).

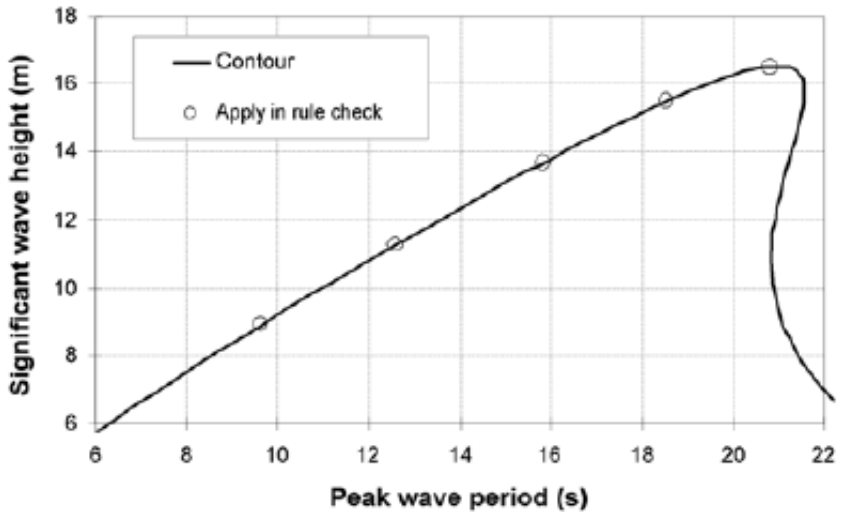

Figure 8: Contour lines for the sea state (DVNGL-OS-E301, p. 19)

For the wind loads, a mean wind speed of 10 m above the water surface with a 100-year return period is used. The wind load is treated as a steady component in combination with a time-varying component known as the gust, which is described by a wind gust spectrum (DVNGL-OS-E301).

The current is described by the surface current speed with a 10-year return period, which is taken from the marginal distribution of current speeds. The loads which are applied in mooring line response calculations for ULS and ALS have to include the most unfavorable combination of wind, wave and current with the 100-year return period. Both the intensity and direction have to be included in the calculations (DVNGL-OS-E301).

For the analysis, the loads are subdivided into excitation regimes given in Table 2.

Table 2: Excitation regimes for loads (adapted from Larsen (2015, p. 19))

	Mean	**Low-Frequency: (30-500s)**	**Wave-Frequency: (5-30s)**
Wave	Mean wave drift force	Wave drift	1st order forces
Wind	Mean wind speed	Wind gust	
Current	Mean current speed		

2.4.2 Analysis

There are three main types of analysis for the design of mooring lines; static, quasi-static and dynamic.

The static analysis is often carried out in the very initial stages of the mooring system design. In this analysis, only the mean components of the loads are used, and fluid forces on the mooring lines are neglected. The calculations use an equivalent linear stiffness to asses the relation between platform offset and tensile forces in the mooring lines. The maximum dynamic offsets are estimated, and the line configurations are checked with crude calculations (Chakrabarti 2005).

The quasi-static analysis is generally more complex than the static counterpart. The most important differences are that the quasi-static analysis involves a non-linear stiffness for catenary lines, and the equation of motion given in Equation (1) is integrated in the time-domain for the six *degrees of freedom* (DOF) a naturally buoyant platform as illustrated in Figure 9. Also, the quasi-static analysis includes effects of added mass and damping. In general, there are two different methods to be used; time-domain simulation or frequency response method. The time-domain simulation uses the low-frequency (LF) and wave-frequency (WF) forces generated by waves, and the mean components of the wind and current. The mooring stiffness is used without considering line dynamics. The frequency response method uses a linear stiffness for the mooring lines, and the dynamic responses are calculated for a single-DOF system subjected to the LF motions from waves and wind. (Chakrabarti 2005).

The main difference between dynamic and quasi-static analysis is that velocity dependent forces (viscous drag) and acceleration-dependent forces (inertia) of the line is included. The dynamic analysis is usually performed on a system that results from the static analysis, and it includes the LF motions from waves and wind and the WF motions from waves. To analyze the lines, they are decomposed into many straight elements with linear shape functions, where the mass and added mass are lumped at the ends of the bars. In general, the motions of the platforms are computed independently from the estimates of the line dynamics, except for deep-water moorings, where the interactions need to be considered. The damping influences the calculated

response greatly. Therefore, the damping in the system needs to be estimated before the analysis is conducted. However, there is no universal agreement on the values of mooring damping (Chakrabarti 2005).

The motion of the platform for a single DOF[1] is described by the equation:

$$(m + A_m) \cdot \ddot{x} + B \cdot \dot{x} + B_v \cdot \dot{x} \cdot |\dot{x}| + C_t \cdot x = F_x(t) \tag{1}$$

where m, A_m, B, B_v , C_t and $F_x(t)$ is mass, added mass, linear damping, viscous damping, stiffness and excitation forces, respectively. Furthermore, x refers to the DOF, $\dot{x}$ is velocity, and $\ddot{x}$ is acceleration.

Table 1 in ISO 19901-7 gives the recommended types of analysis. DVNGL-OS-E301 requires a dynamic analysis, except for cases where it can be demonstrated that the line dynamics can be neglected, where the quasi-static analysis can be used. From the analysis, the extreme loads are sampled to a Gumbel II distribution. In general, MPM is the greatest value from a three-hour storm.

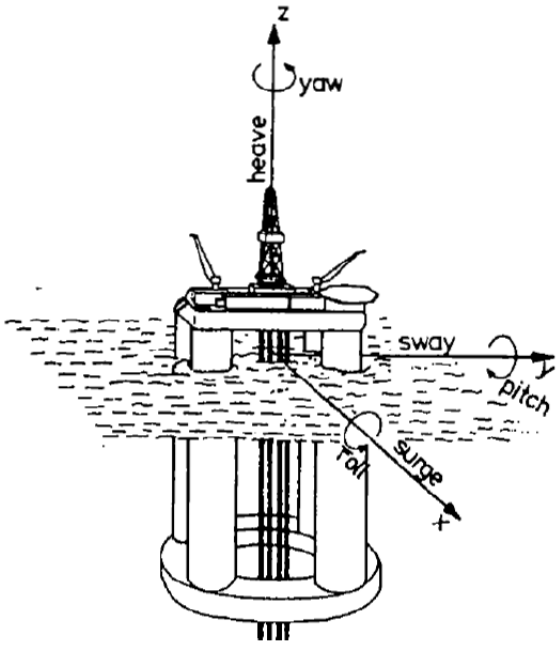

Figure 9: DOFs for a naturally buoyant platform (Faltinsen 1993, p. 3)

2.5 Inspection and Maintenance Routines

It is necessary to control the operation phase and perform condition monitoring to ensure mooring line integrity. This is achieved through regular inspections of the mooring lines. The requirements for inspection are given from the Norwegian Maritime Authority (2009) and in

[1] In this case *surge*, which is the DOF in x direction as shown in Figure 9

DNVGL-RU-OU-0101 for DNV GL classified structures. Since most permanent platforms are not DNV GL classified, the companies have developed their company-specific inspection guidelines based on their own and industry experience.

The inspection routine for mooring chain depends on its age. The inspection is usually a mix of a visual inspection, measurements of diameter and electrode potential, ultrasound testing or other *non-destructive inspection* (NDT) methods such as *magnetic particle inspection* (MPI).

According to DNVGL-RU-OU-0101, a chain which are less than 20 years old with no previous failures, and proper documentation and service history, is surveyed with the following inspection routine:

- 100% visual examination
- 5% NDT on the general chain
- 20% NDT on the chain which has been in the way of fairleads over last 5 years
- 20% NDT on the chain which will be in the way of fairleads over next 5 years

This is increased to include mechanical testing of each length of chain and NDT increased to cover 20% of the whole chain, if there is no history or documentation available.

The following applies to a chain that is older than 20 years (DNVGL-RU-OU-0101, Norwegian Maritime Authority 2009):

- If all documentation is available, and there are no reported failures and only minor repairs performed, then the mooring line can be inspected with the routine outlined above
- If no documentation is available, then the chain shall be subjected to minimum 20% NDT and tested mechanically for all lengths
- If documentation shows that the mooring line has been defective, then the NDT shall be increased to 100% in the areas where the defects are found
- The chains must be re-certified every 2.5 years, by using MPI or similar inspection methods on all the available surfaces over the whole length

For the steel wire ropes, and fiber rope, the inspection consists solely of a visual examination, with a special emphasis on external wear and deformation over the whole length, and general damages in the termination area (DNVGL-RU-OU-0101).

In practice, a line is fully inspected every four years. However, the upper parts, which includes the fairlead and platform chain, are inspected every year. In the event of a line failure, the whole system is inspected . The inspection program is altered if any damage is found on the mooring lines. The conducted maintenance varies from case to case.

2.6 Mooring Line Failure

A mooring line failure is defined as *"an occurrence of the loss of connectivity of a mooring line between the attached point on the vessel and the seabed, occurring at a substantially different time to another single line failure event on that facility"* (Fontaine et al. 2014, p. 1). Current regulation require flotels and production facilities to tolerate the loss of two lines, while other structures must withstand a failure of a single mooring line (Petroleum Safety Authority Norway 2016). If a failure occurs, the normal procedure is to shut down the operation until the cause of failure is established. Normally, the facility can continue operation up to weather conditions with a one-year return period, but a repair procedure is immediately commenced. A controlled shutdown decreases the potential consequences, and according to the regulation, requires lower safety factors compared to a fully operative platform (Petroleum Safety Authority Norway 2017a) (Petroleum Safety Authority Norway 2017b). However, a mooring line failure will cause a redistribution of loads that will increase the demand on the remaining lines, thus increasing the risk of a progressive failure.

2.6.1 Failure Rates

In the last five years, only three mooring line failures have occurred during operation of the structures. According to the Norwegian Petroleum Safety Authority (PSA), initiatives and measures from the industry have contributed to the number of undesirable events being reduced. Some of these measures are listed below. The reported incidents of mooring line failure on the Norwegian continental shelf between 2000 and 2017 are presented in Figure 10. Normalization of the number failures by the number of devices with anchoring does not change the tendencies illustrated in the figure (PSA 2018).

- Increased expertise in the industry
- Wave loads have been corrected
- Torsion in the anchor lines is reduced by using special equipment during the installation
- Increased knowledge of the effect of using steel wire rope
- Improved the protection of fiber rope
- Improved use of appropriate equipment

Several surveys have been conducted to investigate the cause of failure experienced in the industry (Kvitrud 2014) (Fontaine et al. 2014) (K.-t. Ma et al. 2013). The surveys show that the mooring line failure rates form a characteristic curve called the *bathtub curve*, illustrated in Figure 11. This curve shows that the mooring lines exhibit a high infant mortality rate, which may be caused by damages from the production or installation. According to one survey, as many as half of the reported mooring line failures occurred within the first five years of the planned

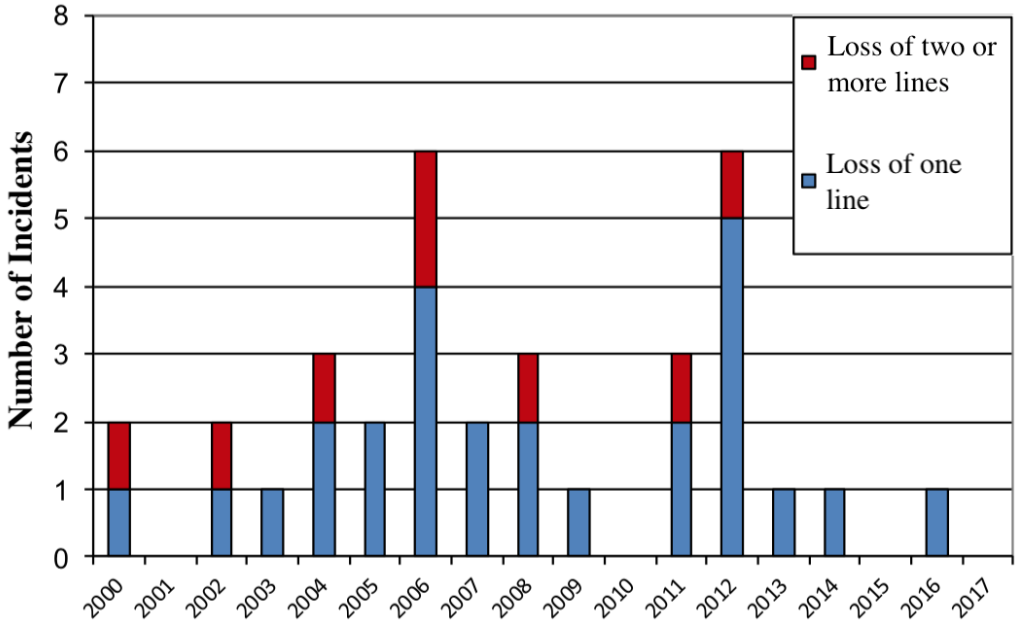

Figure 10: Reported incidents on the Norwegian continental shelf (PSA 2018, p. 96)

service life (K.-t. Ma et al. 2013). The curve shows that the failure rate decreases over time after installation until it flattens out. This plateau is characterized by the occurrence of random failures. As the mooring lines begin to reach the end of their service life, the failure rate increases again, this time due to the degradation mechanism that deteriorates their structural integrity.

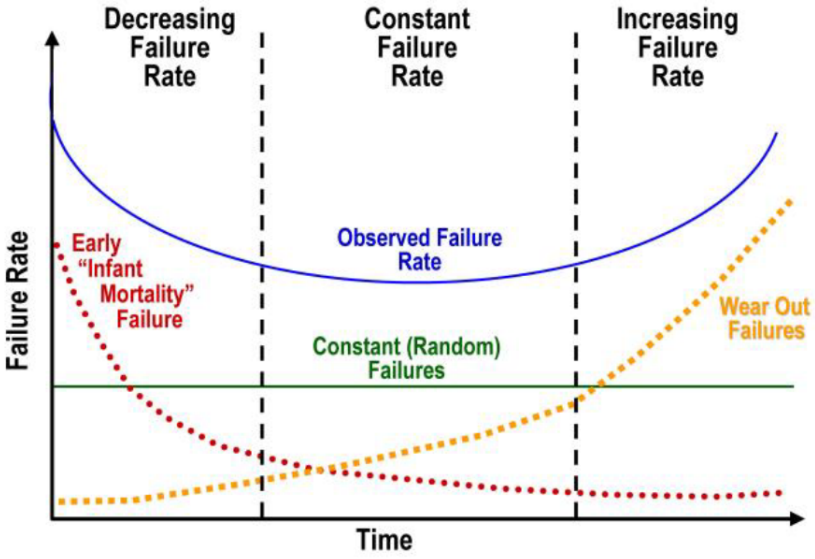

Figure 11: The bathtub curve (Smedley and Petruska 2014, p. 3)

2.6.2 Potential Consequences

The different estimates of the consequences from a mooring line failure vary widely. In general, the consequences can be grouped into one of four groups: loss of human lives, pollution, assets, and reputation. While it is hard to asses the cost of human life, pollution, and loss of reputation, previous failures may provide the order of magnitude of the cost of losing the asset.

The Gryphon Alpha incident may serve as an example of how costly a progressive mooring line failure may be. During a storm, four of the ten mooring lines and the DP system failed, which caused the FPSO to drift 180 meters off location. The drift-off caused severe damage to the risers, and gas was subsequently detected in the turret. Luckily, no crew members sustained serious injuries. The insurance costs were estimated to be in the range of 440 million GBP (Maersk 2011).

For a single line failure on the Norwegian continental shelf, one can assume that the cost of acquiring and installing a new mooring line, is taken to be about 20 million Norwegian Kroner (MNOK). On average, a platform on the Norwegian continental shelf produces on average between 50,000 to 200,000 barrels a day. One barrel of *Brent crude* is about 60 USD or 500 NOK (December 2017), which means that a halt of the production costs 25-100 MNOK per day. Assuming a three-day downtime to gain control of the situation and assess the cause of failure and integrity of the remaining mooring lines, means that the total cost may be in the range 95 MNOK to 320 MNOK.

2.7 Summary

This chapter opens with an introduction of the different type of offshore structures before it moves on to introduce key aspects of mooring system characteristics, such as single point mooring, spread mooring, catenary lines and taut leg configuration. This is followed by a brief introduction of mooring line components with an emphasis on chain links. Thereafter, the design phase and inspection and maintenance routines are explained, to facilitate the development of appropriate models in later chapters. The chapter concludes with a brief description of historical failure rates and potential consequences.

3 Review of Decision Theory

This chapter introduces fundamental concepts of decision theory that are required to fully understand the networks created and analyzed in Chapter 4, Chapter 5 and Chapter 6. The chapter starts with a brief introduction to uncertainty and utility theory, before decision trees, Bayesian networks, dynamic Bayesian networks, and decision graphs are introduced. A short literature review on Bayesian networks in the context of structural reliability is presented at the end of the chapter.

3.1 Decision Theory

The ability to make good and well-informed decisions is one of the most important skills an engineer can possess, as they may have a major and lasting impact on society. However, it has been observed through empirical studies that humans behave irrationally, thus proving the need for a framework that can aid rational, consistent decision-making (Kahneman and Tversky 2013). This framework must enable the engineer in identifying the optimal decision alternative in accordance with a set of objectives[2] and constraints. Ultimately, decision theory provides the necessary foundation on which this framework can be formalized.

3.2 Uncertainty

If there is no uncertainty related to the variables and outcomes in a decision problem, finding the optimal decision is a trivial task. However, since our knowledge is imperfect, all decisions contains some elements of uncertainty. Therefore, decision-making involves accepting some uncertainty. This uncertainty can be categorized as aleatoric or epistemic uncertainty. Aleatoric uncertainty is related to the randomness of nature, which is the reason why outcomes of identical experiments will be different each time the experiment is run. Epistemic uncertainty relates to what we could potentially know, but in reality, do not know. This kind of uncertainty can be reduced through additional research of the relevant phenomena. However, these additional measurements or improvements are related to costs, which need to be accounted for in the decision analysis. The value of this additional information can be quantified through a *preposterior* analysis described later in this chapter.

Uncertainty is described by the probability that a specific event will occur, quantified as a number between zero and one. If the probability of an event is zero or one, it is said to be deterministic, as there is no uncertainty related to whether the event will occur or not. A probability of zero can be interpreted as it being impossible for the event to occur. A higher number would suggest the event is more likely to occur. A probability of one means that the event will happen *almost surely* (Grädel et al. 2007). Probability can be interpreted as subjective or objective. The

[2]Note that the set of objectives depends on the point of view of the client

most popular way to view objective probability is that the probability is described by the relative frequency of the outcomes when the experiment is repeated in the long run(Hájek 2003). Subjective probability can be viewed as a degree of belief, exemplified by expert opinion. In Bayesian statistics, subjective and objective probabilities can be combined to reduce the uncertainties regarding the system.

3.3 Utility

It is necessary to quantify the potential consequences of a decision problem to assess the optimality of the decision alternatives. A unique metric has to be introduced to compare the different attributes present in the problem, such as safety, money and ecological health, before the decision analysis may be conducted. This metric is called *utility*, denoted as *u* in the literature. The basic principle of utility theory developed by Von Neumann and Morgenstern states that the utility is quantified in a manner that a decision is preferred over another if the expected utility of the former is larger than the expected utility of the latter (Von Neumann and Morgenstern 2007).

In some cases, the utility can be described in monetary units, but this is not always the case nor always desirable. To illustrate this, consider the consequence of loss for a given company. It can be assumed that a small loss does not have a significant impact on a company. However, if the loss is doubled the company may start to feel the consequences, as it might have to lay off workers or take other measures to cope with the loss. Therefore, the consequences are experienced as more severe than for half the loss. Conversely, if one were to gain a significant amount of money, the double of that amount is not twice as good (Daniel Straub 2015). It follows that both loss and gain can be described as a non-linear curve, called the *utility curve*. The shape of the utility curve varies with the size of a company and their resistance against financial loss. This effect is called the *size effect* of the utility curve, and it is illustrated in Figure 12(a).

Many decision problems involve multiple attributes, which provides a need for an extension of utility theory. This demand resulted in the development of *Multiple-Attribute Utility Theory* (MAUT). When multiple attributes are relevant to the decision problem, it is essential to describe the utility by a joint utility function. The so-called indifference curves are developed by keeping the joint utility function constant. These curves are useful to understand the decision-makers preference for the attributes. The indifference curves illustrate that, for some combination, more of attribute X_1 and less of X_2 is equivalent for the decision-maker to a combination where the reverse is true, as illustrated in Figure 12(b) (Keeney and Raiffa 1993). The use of MAUT is problematic when the attributes are related to safety and expenses, as critics have claimed that expressing these different attributes with the same utility is not ethical. However, it is a necessity to express the preference of the attributes explicitly, to make rational, consistent decisions. Ultimately, decisions have to be made, which implies accepting a trade-off between the different attributes (Daniel Straub 2015).

In this Thesis, the utility is represented by a linear function since the cost-optimization of the safety factors is conducted from a regulative perspective. Consequently, the utility and monetary units are interchangeable terms throughout the rest of the Thesis.

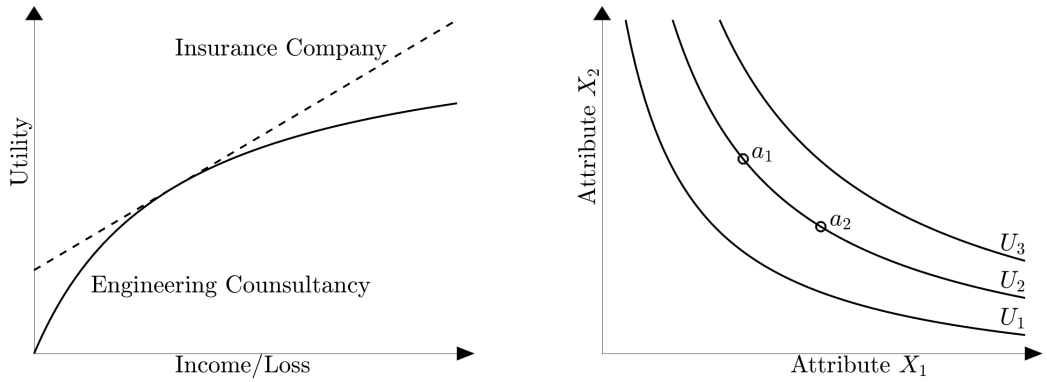

(a) Utility curves

(b) Indifference curves

Figure 12: Adapted from Daniel Straub (2015)

3.4 Decision Tree

Decision problems are often represented graphically, usually as a *decision tree*. A decision tree is a simple framework to determine the optimal strategy to maximize the expected utility. The decision tree in its simplest form consists of decision alternatives, system states, and utilities, represented as a, θ and u respectively, as illustrated in Figure 13. The decision alternatives and the system outcomes can be described as discrete or continuous variables or a combination of both. It is assumed that different decision alternatives will change the state of the system and that this is reflected in the uncertainties (Benjamin and Cornell 2014). Therefore, the probability that a certain state θ will occur is conditional on the chosen decision alternative, i.e. $P(\theta_i \mid a_j)$. Similarly, the utility is conditional on the chosen decision alternative and the state of the system. When all the different states and utilities are mapped in the decision tree, it is then solved from right to left, where the expected utility for each decision branch is calculated. The optimal decision is then found as the branch with the maximum expected utility.

$$P(A \mid E) = \frac{P(E \mid A) \cdot P(A)}{P(E)} \tag{2}$$

A decision tree can be used for *prior*, *posterior* and *preposterior* analysis (Benjamin and Cornell 2014). A prior analysis relies on the initial uncertainties for the system, i.e. no measurements are performed for the specific problem to reduce the uncertainties. The initial uncertainty is called the prior uncertainty, denoted $P'(\theta)$. In contrast, posterior analysis updates the uncertainty with new information through the use of Bayes' Theorem. Bayes' theorem describes the probability of an event A occurring, given that event E has already occurred, through the

relationship given in Equation (2). If event E describes the observed evidence, then the theorem provides a method to quantify the following reduction in uncertainty on the event A. This updated probability, called the posterior probability, denoted $P''(\theta)$, is used instead of the prior probability in the decision tree.

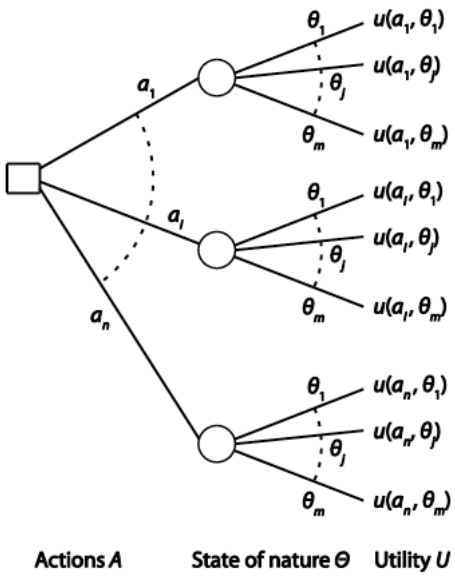

Figure 13: Generic prior decision tree (Daniel Straub 2015, K:9)

The reduction of the uncertainty increases the accuracy of the decision analysis. This benefit, called *value of information*, can be quantified through a preposterior analysis (Benjamin and Cornell 2014). The preposterior analysis introduces the variables e and Z as experiment alternatives and experiment outcomes, respectively. A generic preposterior decision tree is illustrated in Figure 14. The analysis aims to choose the optimal experiment alternative, by comparing the expected values of each branch in the decision tree. As for the prior and posterior analysis, the optimal decision is the decision associated with the branch that yields the highest expected utility.

While the advantages of the decision tree analysis are plenty, the method also suffers from certain drawbacks. For instance, the creator of the decision tree must have a good understanding of the system, to model the dependencies as close to reality as possible. It is, even for the experts, cumbersome to model the different causal relations between the variables and to incorporate evidence into the model. However, the main problem for decision trees is their exponential nature (Daniel Straub 2015). For this reason, even simple systems will quickly make the calculations so computationally expensive that an analysis of a realistic model is impractical.

3.5 Bayesian Networks

A *Bayesian network* can be used to estimate the likelihood of the outcomes and their expected utilities in a system, and it is a more robust way of representing a decision problem than a

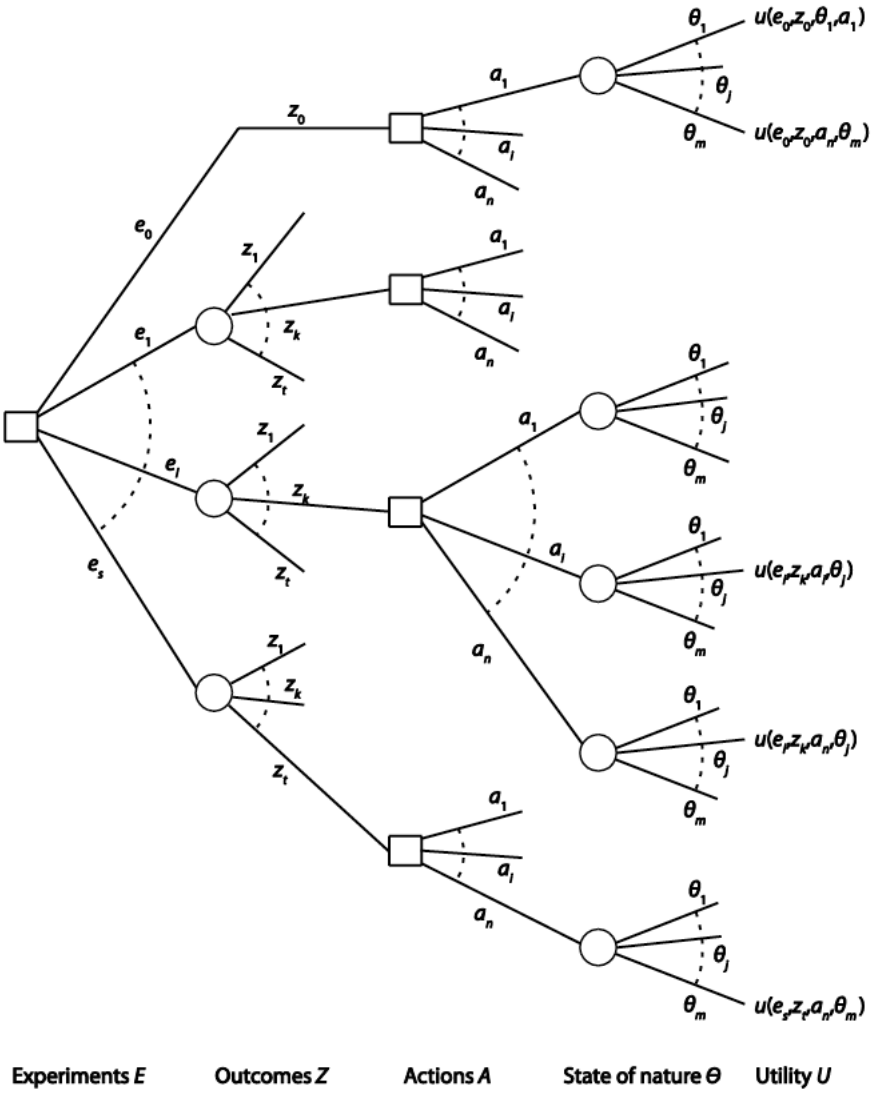

Figure 14: Generic preposterior decision tree (Daniel Straub 2015, K:17)

decision tree. A Bayesian network consists of nodes and arcs where the nodes can represent states, conditions, decisions or utilities and the arcs models dependencies. There are several advantages of using a Bayesian network over a decision tree. For instance, the graphical representation of the dependence structure between variables makes it easy for humans to interpret, even for non-experts. New information can easily be introduced as evidence to update the uncertainties (Huckl n.d.). Moreover, as explained later in this section, techniques can be used to reduce the number of calculations, so the computational cost is reduced.

A *causal network* is a *directed acyclic graph*, or DAG, which consist of nodes and arcs, illustrated in Figure 15. Since the arcs in the network represent causal relations, they must be directed, and they are not allowed to form a loop between the nodes (Pearl 2014). Causal networks can be viewed as a mapping of causality in a system. It is useful to investigate the flow of information in causal networks because it behaves similarly for Bayesian networks. However, it is important to note that causal networks are not equal to a Bayesian network. The main dif-

ference between them is that Bayesian networks include a probabilistic aspect, which requires the rules for Bayesian networks to be more strict.

The causal relationship between the nodes is described in a similar way to that of a family. In Figure 15 the node *A* is said to be the *parent* of node *C*. Similarly, node *C* is the *child* of node *A*. *D*, which is a child of *C*, is called *descendant* of *A*, and *A* is the *ancestor* of *D*.

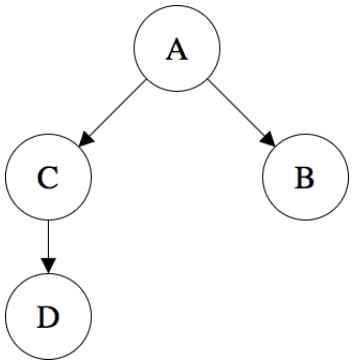

Figure 15: A causal network (adapted from Daniel Straub 2015)

If there is no path between two nodes, they are said to be D-separated (Pearl 2014). For Bayesian networks, the D-separation property of the model is used to reduce the complexity of the calculations. The three connection types which are illustrated in Figure 16 govern the D-separation properties in the networks:

- A serial connection consists of three nodes, where the first node influences the second which in turn influences the third. Figure 16(a) illustrates a serial connection. Information can be passed from X_1 to X_2 or from X_2 to X_1 via X_3, that is, evidence about X_1 influences X_2 and vice versa. Evidence about X_3 blocks X_1 and X_2 from influencing another. X_1 and X_2 are then called to be D-separated.

- A diverging connection consists of one parent node and two or more children. The simplest case with three nodes is illustrated in Figure 16(b). When evidence about one of the children is observed, the information can pass through the parent over to the other children. When evidence about the parent is observed, it is not possible to receive more information for the remaining children by observing one of them. Thus, the children X_1 and X_2 are then called to be D-separated.

- A converging connection consists of one child and two or more parents, illustrated with three nodes in Figure 16(c). In contrast to serial and diverging connections, the connection is D-separated before any evidence is received in the system. This means that the parents, X_1 and X_2, are D-separated when there is no evidence about the child X_3. When evidence is received about the child, the parents become conditionally dependent, and information can pass between them.

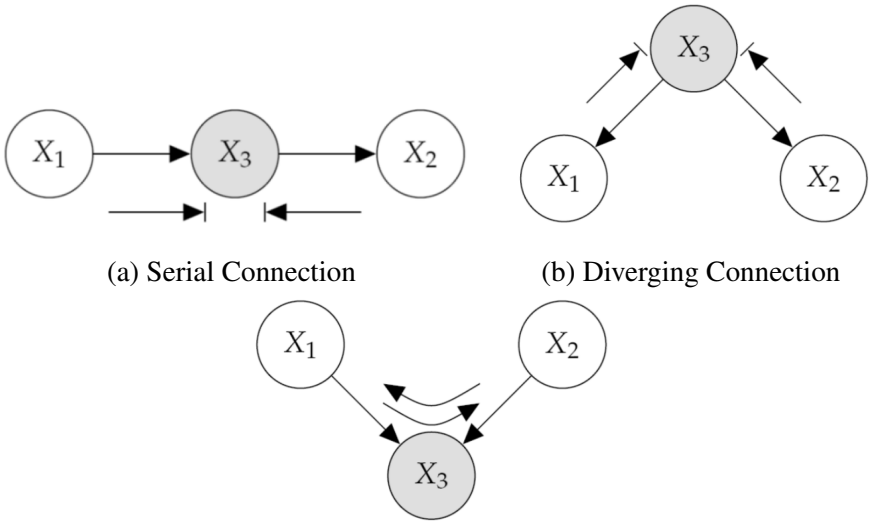

(a) Serial Connection

(b) Diverging Connection

(c) Converging Connection

Figure 16: Information flow when X_3 is observed (Huckl n.d.)

Another essential term is the so-called *Markov blanket*. A Markov blanket for a node is defined as the parents, children, and nodes it shares children with. From the D-separation properties it can be inferred that when all nodes in the Markov blanket for node *A* has received evidence, *A* is D-separated from the other nodes in the system (Thomas Dyhre Nielsen and Jensen 2009). An example of a Markov blanket is given in Figure 17.

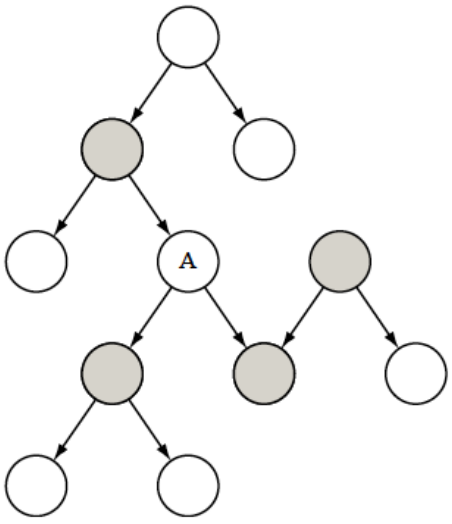

Figure 17: The gray nodes mark the Markov blanket for node A (Daniel Straub 2015, I:9)

A Bayesian network, similar to a causal network, consists of nodes and arcs that form a DAG. In contrast, the nodes represent random variables with a number of mutually exclusive states. For each of these variables a conditional probability is assigned, where the node is conditional on its parents. The full probabilistic model is described by the joint *probability mass function* (PMF)

or the joint *probability density function* (PDF), depending on whether the variables are discrete or continuous. Explicit construction of this joint PMF/PDF quickly becomes cumbersome. If the probabilistic chain rule is used, the joint PMF/PDF can be expressed as:

$$P(A_n, ..., A_1) = P(A_n \mid A_{n-1}, ..., A_1) \cdot P(A_{n-1} \mid A_{n-2}, ..., A_1) ... \cdot P(A_2 \mid A_1) \cdot P(A_1) \quad (3)$$

This does not simplify the expression. However, in probability theory, two events, *A* and *E*, are statistically independent if the probability of *A* is not affected by whether the event *E* has occurred, i.e. $P(A \mid E) = P(A)$. If the two events are independent, their joint PMF/PDF can be described as $P(A, E) = P(A) \cdot P(E)$. By considering the properties of the Markov blanket, several of the variables can be described independently. This significantly reduces the number of probabilities that need to be quantified; thus the computational effort is reduced. By using this, the expression in Equation (3) is reduced to the expression given in Equation (4) where $pa(A)$ denotes the set that contains the parents of *A*.

$$P(A_n, \ldots, A_1) = \prod_{i=1}^{n} P[A_i \mid pa(A_1)] \quad (4)$$

It is worth to note that the arcs in the Bayesian networks do not need to represent causal relations unlike that of the causal networks. This could be the case if a diagnostic rather than a causal network is preferred, or that it is not possible to determine the causal relationship between all the variables. In the latter case, a network can still be established. However, it is essential to check that the D-separation properties of the network correspond to the true dependence between the variables. Nonetheless, Bayesian networks are best when causal relationships are modeled, as non-causal Bayesian networks are more prone to modeling errors and often lead to more links between the variables, resulting in increased complexity of the network (Daniel Straub 2015).

While Bayesian networks can be formulated for continuous random variables or a mix between discrete and continuous random variables (so-called *hybrid Bayesian networks*), only Bayesian networks modeled with discrete variables are considered in this Thesis[3]. This is because exact inference is only possible in some cases of the continuous and hybrid networks. It is possible to circumvent this by either discretizing the continuous random variables or by using approximate methods such as *Markov Chain Monte Carlo* (MCMC). For a more in-depth view of hybrid Bayesian networks, the reader can refer to Langseth, Thomas D Nielsen, et al. (2009) and Daniel Straub and Der Kiureghian (2010).

3.6 Dynamic Bayesian Networks

Dynamic Bayesian networks can be used when some or all of the random variables in the system are time-dependent. In a dynamic Bayesian network the random variables are discretized in time steps. The simplest version of a dynamic Bayesian network is the *Markov chain*, where all

[3] Except for the auxiliary networks used to quantify the decision graphs in Chapter 4

variables have exactly one parent except for the first ancestor, and all variables are a parent to exactly one variable except for the last descendant, as illustrated in Figure 18(a). The Markov chain fulfills the Markov property, which means that the future state is independent of the past state, given that we know the present state of the system. This can also be deducted from the D-separation properties of a serial connection, where evidence about the present state makes the past state and the future state independent. Few processes fulfill the Markov assumption perfectly, but it can reasonably be assumed to apply for the deterioration of structures, traffic models, and time-variant loads (Daniel Straub 2015).

A Markov chain is described by the initial probabilities and the transitional (conditional) probabilities of the system. If the transitional probabilities are equal for each time step, the Markov chain is said to be homogeneous. For some processes, the future state is dependent on the present state and the past state. This can be modeled as a second-order Markov chain, shown in Figure 18(b), where the network has a memory of two instances. According to Daniel Straub (2015), it is often preferable to have a dynamic Bayesian network that fulfills the first-order Markov property. In many cases, this can be achieved by adding additional variables to the network and re-arranging the arcs, as illustrated in Figure 18(c). Dynamic Bayesian networks are often shown in a compact form for convenience, where a dashed arrow with a number indicates the dependencies in time and space. This compact representation is shown in Figure 18(d).

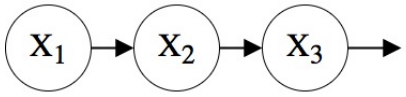

(a) Markov chain

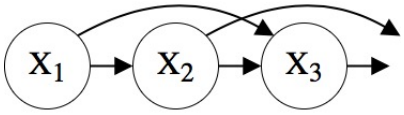

(b) Second-order Markov chain

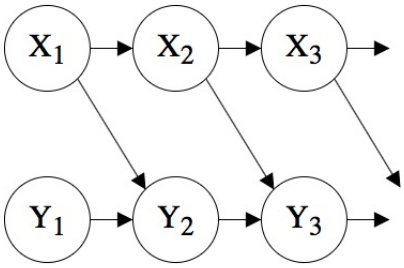

(c) First-order solution of Figure 18(b)

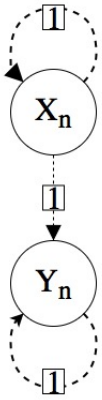

(d) Compact representation of Figure 18(c)

Figure 18: Different examples of Markov chains (adapted from Daniel Straub 2015)

3.7 Critical Appraisal

A Bayesian network approach for risk-based decisions has several advantages. As already mentioned, it is easier to grasp the causal relations for a Bayesian network compared to a decision

tree. It is also more flexible in utilizing information and more robust in terms of possible scenarios that can be modeled than for a decision tree (Huckl n.d.). Besides, several different sources of probability can be used as a basis for the calculations; for example, expert opinion, observed frequencies, and physical or logical models of the process. This means that the Bayesian network can incorporate state-of-the-art knowledge to model the process in the best way possible. New information is easily introduced into the system to reduce the uncertainties and improve the foundation for the decision-maker (Huckl n.d.).

The main limitation for Bayesian networks is that they require an in-depth understanding of the system to describe the causal relations and dependencies adequately. This is highlighted by the fact that the most common mistake is to underestimate the statistical dependence between the variables[4]. This requirement makes it almost impossible for a non-expert to create, use and maintain a detailed Bayesian network adequately. Besides, most software only works with discrete variables, which means that continuous variables have to be discretized so they can be implemented into the network. This introduces a modeling error in the network. Bayesian networks are also subject to certain algorithm limitations; the required computational cost increases as the number of nodes increase. This means that larger problems cannot be exact inferred by the use of Bayesian networks. If the problem becomes too demanding, then MCMC simulation or other approximate methods can be used (Daniel Straub 2015).

3.8 Decision Graphs

Bayesian networks can be further enhanced into *decision graphs* (also called *influence diagrams*). A decision graph is a Bayesian network supplemented with additional nodes that represent the decisions that have to be made in the system, as well as the utilities. Conventionally, square nodes represent decisions (also called actions), oval nodes represent random variables, and diamond-shaped nodes represent utilities. While utility nodes cannot have any children[5], they can be children of decision nodes and or random variables. Decision nodes can be both parent and child to a random variable and vice verse. In contrast to Bayesian networks where causality is preferable but not a necessity, decision graphs have to be modeled so that the dependence structure is causal (Daniel Straub 2015). This is because the actions selected in the decision nodes change the probabilistic nodes; thus the results taken from a non-causal network are not valid. Finally, an order of the decision nodes needs to be assumed as it influences the result.

Decision graphs are particularly useful for finding an optimal strategy for a decision problem where there are several decisions to be made. An example of this is the preposterior analysis. Figure 19 illustrates how the generic preposterior decision tree from Figure 14 can be simplified into a preposterior decision graph. Decision graphs are favored over decision trees because it is

[4] which can be mitigated by including more ancestors

[5] Except for other utility nodes when MAUT is considered

often straightforward to determine the value of information through a preposterior analysis of a decision graph in suitable software.

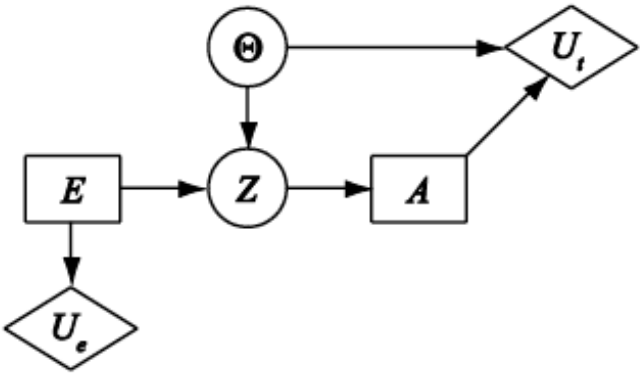

Figure 19: Generic preposterior decision graph (Daniel Straub 2015, K:21)

3.9 Software

There is various software available for evaluating discrete Bayesian networks and performing MCMC simulations. The most common products are listed below. Detailed knowledge about the algorithms behind the programs is not needed for this Thesis.

- GeNIe, BayesFusion - Developed at *University of Pittsburgh*. GeNIe provides a graphical interface for Bayesian networks and dynamic Bayesian networks. Its engine, called Smile, is compatible with C++. The software is free for academic use under certain conditions.
  - `http://www.bayesfusion.com/download`
- FullBNT - Developed by Kevin Murphy at *University of California, Berkeley*. FullBNT is a MATLAB code for inference in Bayesian networks.
  - `http://www.github.com/bayesnet/bnt`
- Hugin - Commercial bayesian network software developer and provider. It has been used successfully in a number of cases in various fields.
  - `http://www.hugin.com`
- Winbugs - Developed by *MRC Biostatistics*, *University of Cambridge* and *Imperial College School of Medicine*. It is an free, open source software useful for performing MCMC simulations.
  - `http://www.winbugs-development.mrc-bsu.cam.ac.uk`

3.10 Literature Review

This Thesis suggests networks based on previous work on Bayesian networks and decision graphs, which is a modeling tool originally developed in computer science, with important contributions by Pearl (2014), Thomas Dyhre Nielsen and Jensen (2009), and Russell and Norvig (2016). Bayesian networks gained widespread attention during the 90s when both the industry and research institutions used it as a framework for building systems that mimic the human ability of reasoning and decision-making (Thomas Dyhre Nielsen and Jensen 2009). Recently, Bayesian networks have also been applied to engineering risk and reliability analysis (see Faber et al. 2002, Friis-Hansen 2004, Grêt-Regamey and Straub 2006, Langseth and Portinale 2007). While the early models were limited by the available computational power, the continued advances in the field enable the analysis of greater and more complex decision problems.

The most significant advancements in Bayesian Networks relevant to the topic of this Thesis can be structured into two themes. The first theme is how to monitor a large population of structures based on the state of a few samples from the population, based on a few parameters. This requires the decision-maker to use the new information available about the state of some structures, to update the prediction about the rest. The second theme concerns the effort of combining structural reliability methods, which usually deals with continuous random variables and low probabilities of failure, with the Bayesian networks updating possibilities.

3.10.1 Bayesian Networks in the Context of Structural Reliability

1. ***Application of decision graph modeling on current design practice***
   The guidelines for the design of mooring lines given in ISO 19901-7 and DVNGL-OS-E301 give the necessary background information to develop limit state functions for the design phase. A better understanding of how to combine the structural reliability methods and Bayesian modeling is required for the project. Daniel Straub and Der Kiureghian (2010) covers the development of hybrid Bayesian networks, termed *enhanced Bayesian networks*, and how this network is reduced to a network that only contains discrete nodes through a node reduction algorithm. The paper also discusses how different modeling strategies can affect the complexity of the outcome network. Recommendation on how continuous nodes arising from the limit state functions can be discretized consistently is given in Daniel Straub (2009). The assessment of the posterior distribution trough structural reliability methods is covered in Daniel Straub and Papaioannou (2014). This paper also provides examples where this Bayesian updating method is applied.

2. ***Application of decision graph modeling on current inspection and maintenance routines***
   Practical insight on how the inspection and maintenance are given by reports and expert statements provided by Equinor. Since this topic involves deterioration and monitoring of mooring lines, a deeper understanding of dynamic Bayesian network modeling is sought

after. Daniel Straub (2009) covers the deterioration processes through dynamic Bayesian networks. In addition, the article gives recommendations on how to implement observations in the models and provides examples of deterioration modeling. Kosgodagan et al. (2015) investigates how transitional probabilities for a Markov chain network can be assessed using expert judgment. This is used for a numerical example for a set of Dutch highway steel bridges with correlated traffic load. This is further developed in Alex Kosgodagan et al. (2015), which covers the modeling of a set of Dutch bridges as a dynamic decision graph. Attema et al. (2017) investigate the efficiency of monitoring a specific detail of a bridge to assess the state of similar, un-monitored details in the same bridge by using Bayesian networks to update the predicted crack growth. In this paper, it is concluded that this strategy significantly decreases the uncertainty of the crack growth prediction and may provide valuable information about the degradation of the bridge.

3.11 Summary

The chapter opens with a passage concerning the necessity of decision theory, and how it can aid consistent and rational decision-making. To properly describe the strength of decision theory, the abstract concepts of utility and uncertainty are introduced. Furthermore, decision analysis is introduced through the description of decision trees. The difference between prior, posterior and preposterior analysis is explained. The concept of causal networks is introduced, which is subsequently developed into Bayesian networks and ultimately, to decision graphs. Important terminology regarding these tools are introduced, such as the kind-ship relations between the nodes, D-separation property, Markov blanket, and Markov assumption. Furthermore, a short introduction on dynamic Bayesian networks is given. A critical appraisal and sources of relevant software, both commercial and open source, are presented near the end of the chapter. The chapter concludes with a short and concise literature review on Bayesian network modeling techniques and applications on engineering problems.

4 Modeling the Design Phase

This chapter focuses on how the design of mooring lines can be represented as a risk-based decision problem, and how corresponding networks in GeNIe can be developed. The chapter can be roughly subdivided into three parts, where the first part, Sections 4.1, 4.2, and 4.3, describes the development of the two main networks that the work resulted in, as well as their underlying assumptions. The second part, Sections 4.4 and 4.5, focuses on the assumptions made in order to quantify the nodes, and how they are quantified. The third part, Sections 4.6 and 4.7, investigates the optimal solution for the design and discusses the results. The chapter is concluded with a summary.

4.1 Limit State Function

Recall from Section 2.4 that a limit state function equal to zero describes the boundary between the safe domain and the failure domain. In this chapter, the limit state function is written as $g = R(t) - S(t) \leq 0$, where $S(t)$ and $R(t)$ represent the load and resistance, respectively. Note that the resistance and loads are written as time-dependent, since both the load and the resistance do not remain constant throughout the service life as illustrated in Figure 20.

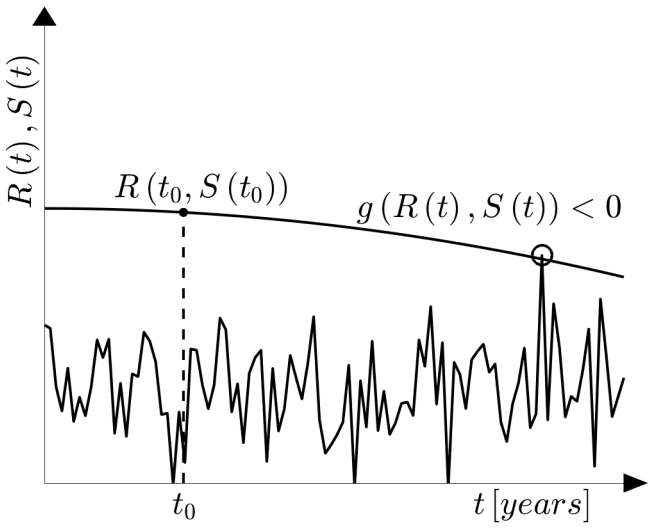

Figure 20: Time-dependent limit state function

The time-dependence of the resistance and the loads, shown in Figure 20, is the main cause for neglecting fatigue modeling in this Thesis. The accumulated fatigue damage is dependent on the number of load reversals the mooring line is subjected to, and thus, the elapsed time. In contrast to the FLS design, the ULS and ALS design is assumed to be time-independent as it is adequate to verify that the expected resistance in the final year of the service life is sufficient to withstand the loads generated by the 100-year storm[6]. Therefore, the challenge is

[6]storm with a 100-year return period, ref. Section 2.4.1

to develop a network that is capable of representing a combination of a time-dependent and a time-independent problem. However, this challenge is too complex for this Thesis. Thus it is decided not to pursue this further.

4.2 The ULS Network

4.2.1 Assumptions for the ULS Network

Before the networks are developed, the underlying assumptions have to be stated. To avoid complex networks that cannot be easily quantified or analyzed, the number of decisions is kept to a minimum. Therefore, the only decisions included in the networks are: diameter, grade, and consequence class. This means that the effect of the chosen mooring system configuration is implicitly accounted for in the load distribution (i.e. the distribution is conditional on the chosen configuration). The mooring lines are assumed to consist of chain segments, to simplify the modeling further. It is assumed that it is sufficient to neglect the series effect for the mooring chain links and to only look at the most loaded link. The effect of this assumption is discussed in Section 4.7. As stated in Section 1.2, the modeling of FLS is out of scope for this Thesis. The networks are so far only applicable for a permanent mooring.

A principle widely applied in this and following chapters is that multiple events can be clustered or lumped into one event, with a more uncertain outcome, and that events that are relevant for the decisions have to be modeled in finer detail. This approximation will be the cause of some errors in the networks. Nevertheless, the networks might be useful for investigating the general tendencies of the system.

Recall from Section 3.8 that the oval nodes are called chance nodes, and represents uncertainty, usually described by a distribution. The square nodes represent choice or decision nodes. The diamond-shaped nodes are called consequence nodes or utility nodes. The following convention is defined to ease the readability of the Thesis: node names are written in italic; the failure nodes in the networks are colored red; the logical switches in the networks are colored yellow.

4.2.2 Limit State Network

From the general definition of the limit state function, a simple Bayesian network is developed. The network consists of three nodes, where the two parents, *Resistance* and *Loads*, cause *Failure*, which describes whether the system fails or survives given the state of the parents. This simple network, referred to as the Limit State Network, is shown in Figure 21.

4.2.3 Loads

The node *Loads* describes both the pre-tension and external loads caused by weather. The node can be expanded further into a branch, for instance by including the cause of the load-

ing, typically wind, waves, and current, and the direction of the cause. Choices that affect the load distribution such as configuration and type of mooring system could also be included here. However, it is beyond the scope of this Thesis to develop a weather model, and derive the mooring line tensions from this. Instead, the loads are assumed to be represented by a Gumbel II distribution, which accounts for all potential mooring systems and configurations. This Gumbel II distribution is approximated with a Weibull distribution, to ease the discretization and quantification of the networks. For the subsequent networks, the loads are assumed to be independent of chosen diameter and grade, which means that direct forces from interactions between the mooring lines and the water are neglected and that the pre-tension is independent of the resistance. The distribution for *Loads* is referred to as Loads I in Table 4. In this Thesis, the node *Loads* is not expanded further into a branch.

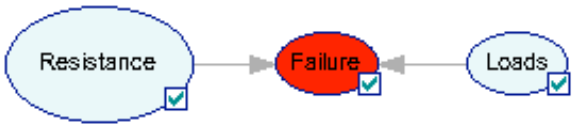

Figure 21: The Limit State Network

4.2.4 Resistance

In order to develop the network further, *Resistance* is expanded by introducing the two decision nodes *Diameter* and *Grade*, and the two chance nodes *Service Life* and *Corrosion Rate* that together reflect the uncertainty in decrease of the cross-section due to uniform corrosion. In addition, there is uncertainty related to the manufactured diameter of the chain links, as explained in Section 2.3. The combined effect of the uncertainty from manufacturing and corrosion is modeled by introducing a child node called *Corroded Diameter*, which has *Diameter*, *Service Life* and *Corrosion Rate* as parents. Alternatively, this can be modeled by having two chance nodes that separate the uncertainty from the manufacturing and the corrosion processes.

Next, the chance nodes *Minimum Breaking Strength* and *Resistance* are included. The *Minimum Breaking Strength* is a child of *Corroded Diameter* and *Grade* as shown in the relation given in Equation (5). It is itself parent of *Resistance* to reflect that the links are produced with overstrength, so it is ensured that most chain links do not fail when the loading is less than MBS[7]. In addition to *Loads*, the *Resistance* is parent to *Failure*. The resulting network is shown in Figure 22.

4.2.5 Consequences

The next step is to expand the network by including the costs and potential consequences. The *Production Cost* is related to the diameter and the grade, and it is therefore a child of the

[7]This is also ensured by subjecting the chain links to a proof load, which is 70% of MBS

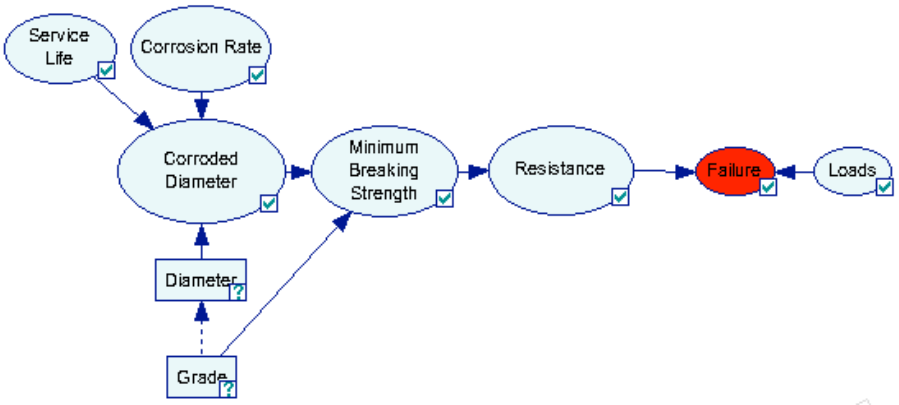

Figure 22: Limit State Network where the resistance is expanded

nodes *Diameter* and *Grade*. It is decided to model it as two separate branches to model the consequence of failure more accurately. The first branch consists solely of the node *Failure Cost*, which accounts for the consequence of a single mooring line failure. The second branch contains the chance node *System Failure* which describes the system failure conditional on a single mooring line failure, and the node *System Failure Cost* which accounts for the cost associated with this event. In addition, the node *Consequence Class* is added to make it easier to account for different scenarios. The final network is shown in Figure 23. Note that an order of the decision nodes has to be assumed and specified. For this network, it is assumed that the consequence class is chosen before grade, which is chosen before diameter.

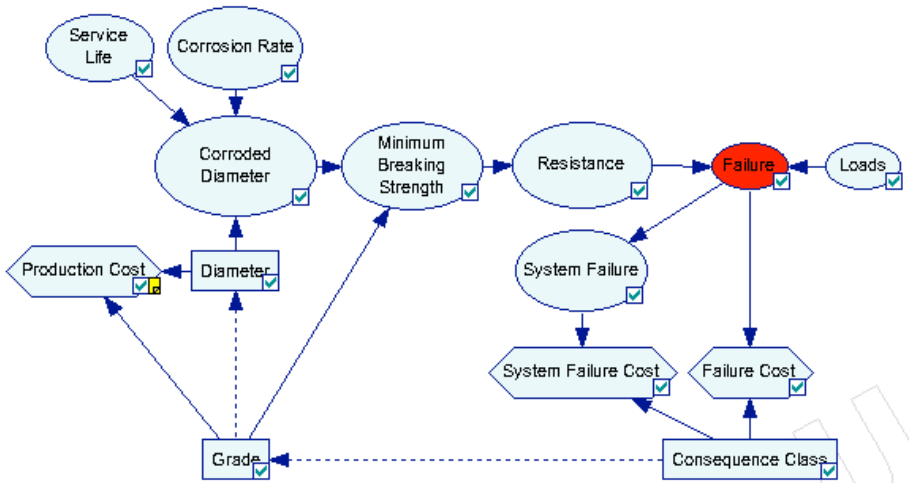

Figure 23: The ULS Network

4.2.6 The Safety Factor Network

A second version of the network is also established, shown in Figure 24, where the main difference is that the decision node *Diameter* is replaced with the decision node *Safety Factor*, and the chance node *Corroded Diameter* is removed but implicitly accounted for through the node

Minimum Breaking Strength. This network is created to directly show how the optimal safety factor varies for different cases. The safety factor is easier to interpret directly compared to diameter since the optimal safety factor is a unitless parameter that refers to the optimal ratio between resistance and load.

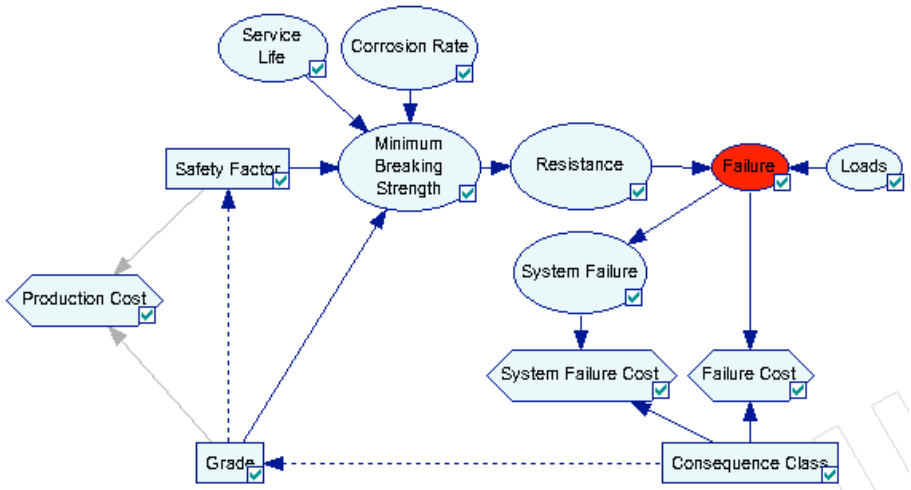

Figure 24: The Safety Factor Network

4.3 The Progressive Failure Network

The second main network to be developed is the Progressive Failure Network. The objective of this network is to illustrate how a parallel system like the mooring system behaves during a failure scenario, where the load is redistributed to the remaining lines, thus increasing the demand and therefore the probability of failure. Since it involves multiple lines, the case where evidence suggests that one of the lines has a low resistance corresponds to the ALS design. The ALS design assumes that the realization of a weak line is independent from the condition of the remaining lines. This assumption can be evaluated by introducing mutual ancestors to resistance nodes, to account for the correlation caused by production and location-specific events. This implies, that once the network is properly quantified, it may be used to show trends outside the design spectrum.

The primary challenge with the network is to model the redistribution of loads due to a failure. The network has to include a resistance node, a load node and a failure node for all mooring lines. Since the load is redistributed conditional on the failure event, it can be inferred that the failure nodes are parents to all other load nodes. However, this violates the requirement that the network must be acyclic, as explained in Section 3.5. The cyclic reference problem is illustrated in Figure 25 for two mooring lines.

A possible solution to this problem is to introduce logical switches and model the problem similar to a dynamic Bayesian network, where the time steps are defined by mooring line failure rather than a distinct period. The purpose of the logical switches is to simplify the graph and

reduce the number of arcs[8], but they are not strictly necessary from a modeling perspective. The complete network for three mooring lines is shown in Figure 26.

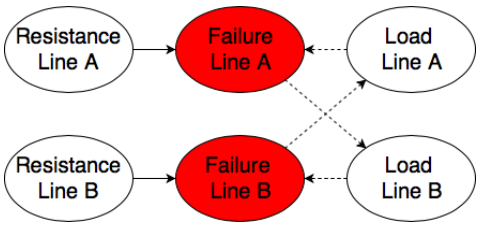

Figure 25: The dotted arcs mark the cyclic reference

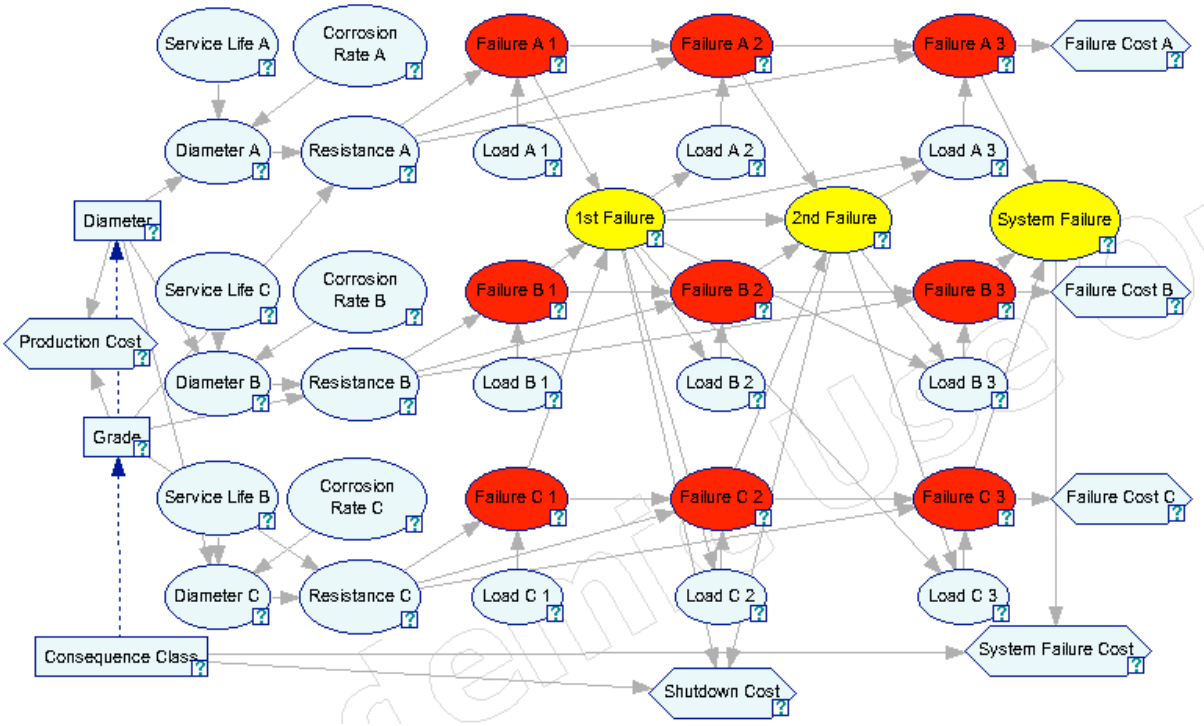

Figure 26: The Progressive Failure Network for three mooring lines

4.3.1 Assumptions for the Progressive Failure Network

Similar to the ULS Network, the Progressive Failure Network requires a set of initial assumptions. All of the assumptions made in Section 4.2.1 are still valid. An essential assumption for the Progressive Failure Network is that only one mooring line failure may occur in each time step. In addition, the corrosion rate and service life of each mooring line are assumed independent. This corresponds to observations from inspections, where corrosion between mooring lines, and even within a single mooring line, varies considerably. The service life of each mooring line is assumed to be independent since it is unlikely that they are replaced at the same time.

[8]For n mooring lines, a logical switch reduces the number of arcs between two consecutive time steps from n^2 to $3n$

Furthermore, the mooring lines are assumed to be equally designed. As a final assumption, the failure scenario takes place during a relatively short time-span, for example, a storm, which means that the resistance is unchanged between the time steps, and the mooring lines are not replaced once they have failed.

4.3.2 Joint Limit State Network

The Limit State Network, shown in Figure 21, serves as a starting point for the Progressive Failure Network. The network is duplicated two times, so each of the three mooring lines are represented. Since the resistance of a line is assumed unchanged throughout the time-span, except if the line fails, only one resistance node per line is needed, and it is connected to the three failure events. Furthermore, the failure events in the first time step are connected to loads in the second time step via the first logical switch, to model the redistribution of loads. The loads in the second time step are defined as the original distribution (called Loads I in Table 4)[9] if the logical switch registers that no failure occurs in the first time step. However, if one of the mooring lines fails, the switch passes the information on to the load nodes in the second time step, which uses a different distribution to model the higher loads (called Loads II in Table 4). In addition, the failure events in the second time step are dependent on their respective failure events in the first time step, so a failed line stays failed.

The same procedure is also applied from the second time step to the third. An essential addition to the network is to include dependencies from the first failure switch to the loads in the third time step, and from the first failure switch to the second failure switch. This is done so that the network can represent the second redistribution of loads (called Loads III in Table 4), which only occurs if a failure happens in the first and the second time step. If a failure occurs in only one of them, the loads should be represented by the second distribution. The resulting network, referred to as the Joint Limit State Network, is shown in Figure 27.

4.3.3 Resistance

The resistances of the mooring lines are expanded similarly to the ULS Network or Safety Factor Network as explained in Section 4.2.4. To reduce the size of the Progressive Failure Network, the effects modeled by the nodes *Minimum Breaking Strength* and *Resistance* in the ULS Network are lumped into a single node called *Resistance*. Since the design is assumed to be equal for all the mooring lines, only one decision node for diameter and grade is needed. Ultimately, three *Service Life* nodes and *Corrosion Rate* nodes are included, due to the assumption that service life and corrosion rates are independent for each mooring line. This expanded network is shown in Figure 28.

[9] Gumbel II approximated as Weibull

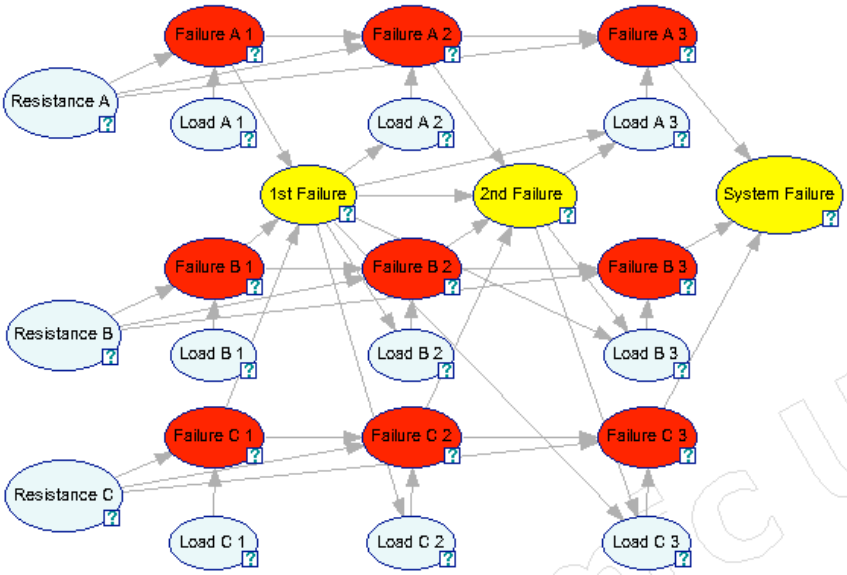

Figure 27: The Joint Limit State Network

4.3.4 Consequences

The consequences are added by attaching *Failure Cost* nodes to the last failure event for each mooring line, and a node called *Shutdown Cost* to the two failure switches. This is to avoid modeling a case where each mooring line failure causes separate shutdowns. The final failure switch, called *System Failure*, only shows a failure if all three mooring lines have failed; thus the *System Failure Cost* is attached to this node. This means that if all the lines fail, the consequence is the added cost of all the mooring line failures, the shutdown and the cost of system failure. In addition, a choice node called *Consequence Class* is added to ease the analysis of different scenarios. Finally, *Production Cost* is added, which is a child of *Diameter* and *Grade*, and has the same values used for the ULS Network. The final network is already shown in Figure 26.

4.4 Distributions and Assumptions

Distributions have to be assigned to the nodes so that they can be discretized and quantified. In general, the distributions are assumed from information provided by Equinor.

The loads are assumed to be Gumbel II distributed, with a location parameter corresponding to the MPM and a coefficient of variation of 10%. The MPM for *Loads* in the ULS Network is taken as MBS/2.2, with MBS computed from Equation (5), where δ is diameter compensated for expected corrosion and c is the c-factor given in Table 3 (Rämnes Bruk Product Catalogue). Grade R4 and a corroded diameter of 128 mm are used for the assessment of the load since it corresponds to the predicted diameter of the mooring lines of Troll B at the end of the service life.

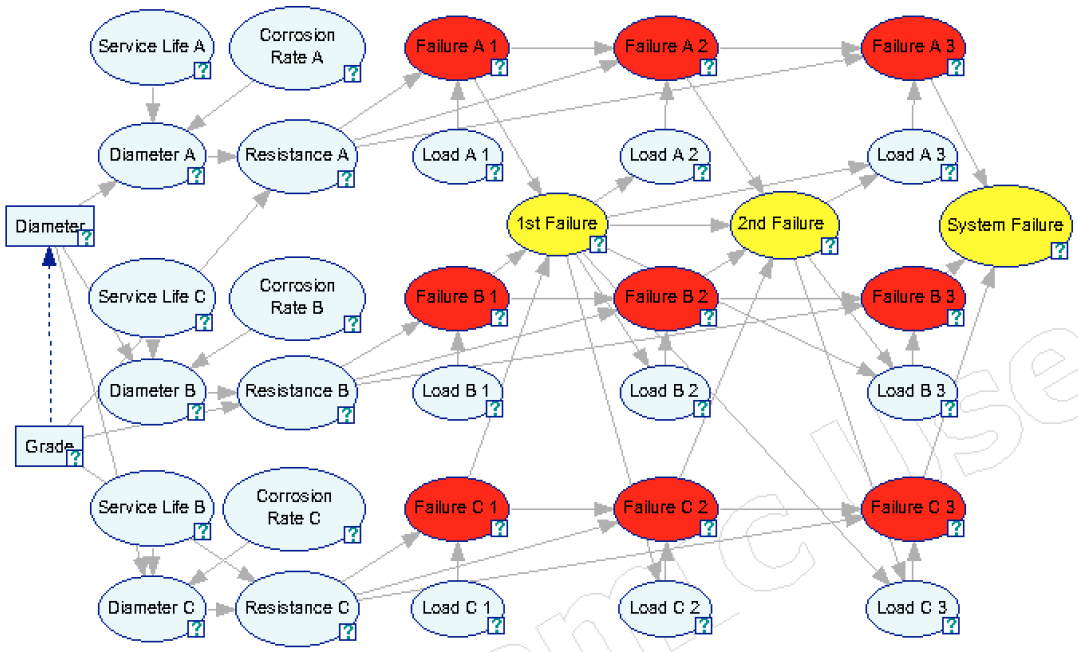

Figure 28: The Joint Limit State Network where the resistance is expanded

For the Progressive Failure Network, the loads are assumed to be distributed with an MPM of MBS/2.2 (Loads I), MBS/1.5 (Loads II) and MBS/1.0 (Loads III) for no failures, one failure, and two failures, respectively.

$$\text{MBS}\,[\text{kN}] = c\,[\text{-}] \cdot \delta^{\,2}\,\left[\text{mm}^2\right] \cdot (44 - 0.08 \cdot \delta\,[\text{mm}]) \tag{5}$$

Table 3: C-factor and price for the different grades

Grade	**R3**	**R3S**	**R4**	**R4S**	**R5**
C-Factor [-]	0.0223	0.0249	0.0274	0.0304	0.032
Cost per kg [EUR]	5.1	5.4	5.7	6	6.3

Since the networks are created solely for permanent mooring, only one distribution is needed for *Service Life*. It is assumed that the distribution is Normal with a mean of 30 years and that 1 out of 20 mooring lines has a service life that is less or equal to 25 years.

Allowances for corrosion rates are given in ISO 19901-7. For the splash and trash zones, the allowance is 0.2-0.8 mm/year. These rates are chosen as the basis for the corrosion rate in the network, and it is modeled as a Lognormal distribution with a mean corresponding to 0.5 mm/year and a standard deviation of 0.2 mm/year. This means that the probability of exceeding the allowances specified in ISO 19901-7 is less than 1%.

The choices for diameter is restricted to 80-180 mm, as this roughly corresponds to the common sizes of chain links. The *Corroded Diameter* is given by the manufactured (also called nominal)

diameter subtracted by the corrosion rates multiplied with service life. The nominal diameter is assumed to be Normally distributed with a mean corresponding to the chosen nominal diameter and a coefficient of variation of 15%. This is summarized in Equation (6), where R_{Corr} represents corrosion rate, and S_L represents service life.

$$\delta\,[\text{mm}] = \text{Normal}\left(d\,[\text{mm}]\,, 0.015 \cdot d\,[\text{mm}]\right) - R_{\text{Corr}}\,[\text{mm/year}] \cdot S_L\,[\text{years}] \tag{6}$$

For single mooring chain links, NorMoor JIP uses a Normal distribution with mean equal to MBS scaled by 1.1 and a coefficient of variation of 4% based on previously performed breaking tests. This assumption is deemed suitable for these networks.

Table 4 summarizes the different distributions assumed for nodes in the networks.

Table 4: Assumed distributions for chance nodes in the networks

Node Name	**Distribution**	**Mean** (Scale)	**Std** (Shape)	**Unit**
Loads I	Weibull	(7,000)	(5.43)	kN
Loads II	Weibull	(12,600)	(5.43)	kN
Loads III	Weibull	(15,000)	(5.43)	kN
Service Life	Normal	30	3.0398	years
Corrosion Rate	Lognormal	ln(0.5)	0.2	mm/year
MBS	Equation (5)	-	-	kN
Corroded Diameter	Equation (6)	-	-	mm
Resistance	Normal	1.1 MBS	0.044 MBS	kN

The cost of production is computed from grade and weight. The weight of the mooring chain, denoted W, is calculated from Equation (7), where d is the nominal diameter in millimeter (Rämnes Bruk Product Catalogue). The cost for each grade is given in Table 3. Since all the mooring lines are assumed to be of identical design, the total production cost is computed for 12 lines, each 1,000 m long, using a conversion rate of 9.6 NOK/EUR.

$$W\,[\text{kg/m}] = 0.0219 \cdot d^2\,\left[\text{mm}^2\right] \tag{7}$$

The failure cost and system failure cost differs for consequence class 1 and consequence class 3. Consequence class 1 is primarily used for survival situations of temporary moorings, where no production takes place. Because of this, the cost of failure is assumed to be 20 MNOK, corresponding to the cost of purchasing and installing a new 1,000 m long mooring line. The system failure cost is assumed to be the failure cost of all the 12 lines, i.e. 240 MNOK. For consequence class 3, the failure cost for one mooring line is assumed to be 170 MNOK, based on a three-day shutdown, a production of 100,000 barrels per day, 60 USD per barrel (total 150 MNOK) in addition to the cost of purchasing and installing 1,000 m of chain. The system

failure cost for consequence class 3 is taken to be 5,000 MNOK, as this is roughly in the same range as the cost of the Gryphon Alpha incident. It is assumed that the probability for system failure is 90%, given that a mooring line has failed due to overload in the ULS Network.

For the Progressive Failure Network, the first mooring line failure triggers the cost of shutdown, assumed to be 150 MNOK for consequence class 3. Since consequence class 1 is for the survival condition, no production takes place. Therefore the cost of a shutdown is assumed to be zero for consequence class 1. Thus, the cost of mooring line failure only includes the cost of acquiring and re-installing the mooring line, assumed to be 20 MNOK. The cost of system failure is similar to the ULS Network, that is, 240 MNOK for consequence class 1 and 5,000 MNOK for consequence class 3. The assumed costs are summarized in Table 5.

Table 5: Assumed cost of failure for the consequence classes

Node Name	**Consequence Class 1 [MNOK]**	**Consequence Class 3 [MNOK]**
Failure Cost (ULS)	20	240
System Failure Cost (ULS)	170	5,000
Shutdown Cost	0	150
Failure Cost (A/B/C)	20	20
System Failure Cost	240	5,000

4.5 Quantifying the Nodes

The next step to get the networks operational is to quantify the nodes appropriately. A Monte Carlo sampling method is suggested to achieve this, because of its simplicity. The general method with examples is explained below.

1. Assign distribution to chance nodes without parents. Choose appropriate intervals for the different distributions and evaluate the CPT by using cumulative density functions

   - Node X is assigned a distribution and discretized in n intervals where $I_0, I_1 \dots I_n$ denote the boundaries. The CPT is created by computing $P_i = P\left(I_{i-1} \leq X \leq I_i\right)$ for all $i \in (1, 2 \dots n)$

2. Formulate functions that describe the relations between the parents and their children

   - Node Y is related to node X through the function $Y = f\left(X\right)$

3. Choose appropriate intervals to discretize the children. The limit state functions are established by subtracting the upper bound of each intervals from the functions resulting from Step 2

- Node Y is discretized in m intervals where $J_0, J_1 \dots J_m$ denote the boundaries. The limit state function is $g_j = f(X) - J_j$ for all $j \in (1, 2 \dots m)$

4. Sample from all discretization-intervals of the parents and evaluate the limit state functions

   - Generate k samples from interval i with boundaries (I_{i-1}, I_i) for node X and evaluate $g_j (I_{i-1} \leq X \leq I_i)$

5. Compute the probability of having a value lower than the upper bound by taking the number of negative realizations of the limit state function and dividing it by the total number of realizations

   - $P(Y \leq J_j \mid I_{i-1} \leq X \leq I_i) \approx \{g_j (I_{i-1} \leq X \leq I_i) \leq 0\}/k$

6. Subtract by the probability of having a value lower than the lower bound. The result described the probability of having a value within the specified interval, and it is conditional on the intervals of the parents

   - The CPT for Y is computed through $P(J_{i-1} \leq Y \leq J_j \mid I_{i-1} \leq X \leq I_i) = P(Y_j \leq J_j) - P(J_{i-1} \leq Y_j)$ for all $i \in (1, 2 \dots n), j \in (1, 2 \dots m)$

7. If necessary, repeat Step 2-6

The challenge with this approach is apparent when a node has one or more parents described by non-linear distributions. To sample from a specific interval of the non-linear distributions, one would have to sample from the distributions for the whole set of ancestors. This is troublesome for the tails, as realizations for this region are less likely to occur. Because of this, a significant number of realizations would have to be sampled before a sufficient amount of valid samples are generated to ensure accuracy. This would undoubtedly be time-consuming, thus decreasing the robustness of the networks.

Fortunately, GeNIe has functionality that enables the use of Monte Carlo sampling to evaluate the CPTs. By replacing the chance nodes in the networks with equation nodes, it is possible to specify the distributions and the relationship between the nodes in the system. Since equation nodes in GeNIe do not support Gumbel distributions, the upper tail is approximated with a Weibull distribution fitted to the 95 and 99 percentiles.

To quantify the equation nodes, they have to be truncated (given bounds) and discretized. Currently, GeNIe does not support continuous nodes in combination with utility and decision nodes. Hence, a continuous auxiliary network consisting solely of equation and chance nodes is created for each network, where the chance nodes serve as proxies for the decision nodes. The nodes are then quantified as explained in the Appendix.

Note that the truncation of the distributions discards any extreme realizations which lead to a loss of information about the tail distribution. This leads to an underestimation of the conditional probabilities and may have an impact on the results since the probability of failure is generally caused by an exceptionally low realization of the resistance, and an exceptionally high realization of the load.

4.5.1 Quantifying the Safety Factor Network

The Safety Factor Network is quantified with an auxiliary network as described in the Section 4.5, but with a few changes in the procedure. The range of choices for safety factor is carefully calibrated so it yields valid nominal diameters. The relation between safety factor and diameter is inverted to get the diameter as a function of grade and safety factor. It is found that GeNIe does not run with the inverted function, possibly due to its complexity.

Instead, the valid section of the inverted function is approximated with a quadratic polynomial. Since the safety factor and c-factor are proportional, the relationship between their ratio and the diameter can be expressed with a single function and thereby further simplify the problem. This function is subsequently used to compute the diameter from a range of safety factors and grades to quantify the production costs. The general procedure is summarized below:

1. Subtract the expected value of loss due to corrosion from the valid range of nominal diameters (in this case, 80-180 mm)

2. Compute a set of MBS values from the corroded diameters and divide by MPM of the load to get the corresponding set of safety factors

3. Divide the set of safety factors by their corresponding c-factor used to generate them to get a single curve for the relation between diameter and safety factor

4. Fit a quadratic polynomial to the section of the inversion of this curve that reproduces the valid range of diameters

5. Determine the boundaries for the set of safety factors that can be used as choices by finding the minimum safety factor with grade R5 and the maximum with grade R3

6. Create a chance node with uniform probability for the outcomes to serve as a proxy for the decision

7. Use a double *switch* or *choose* statement in an equation node to reproduce values for the nominal diameters given safety factor and c-factors. The resulting auxiliary network is then quantified as explained in the Appendix.

4.6 Parameter Study

A parameter study is conducted for the ULS Network and the Progressive Failure Network to determine the optimal safety factor based on cost-optimization. From the networks, it is possible to plot the expected cost for all diameters and grades. The safety factor is calculated from diameter, grade, and MPM, and plotted against the expected costs. The parameter study is not conducted for the Safety Factor Network, as it is a variant of the ULS Network and therefore yields no additional information.

The cost-optimization curves shown in this section consists of two contributions: the *risk*, which is the probability multiplied by the consequences, and the *mitigation cost*, which is the cost of decreasing the risk, usually performed by increasing the strength of the member. In the networks, the mitigation cost is described by the node *Production Cost*. The optimal decision is found where the total expected costs are minimized. The area to its left, where the risk is higher than the mitigation cost, is referred to as the *risk dominated area*. The area to its right, where the opposite is true, is referred to as the *mitigation cost dominated area*. This is illustrated in Figure 29.

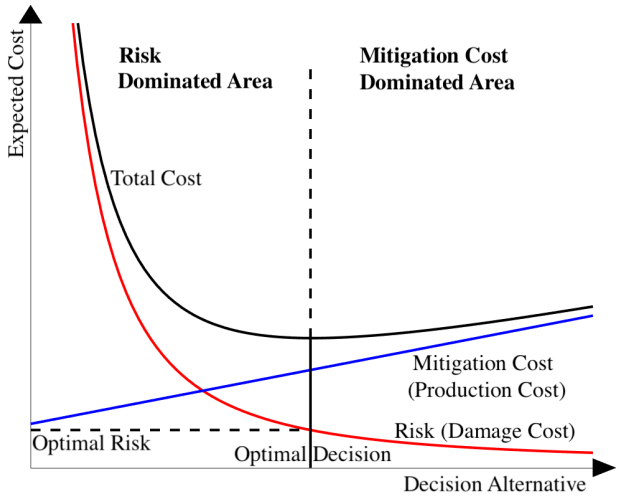

Figure 29: Generic cost-optimization curve

4.6.1 Parameter Study for the ULS Network

Figure 30(a) and Figure 30(b) show the cost-optimization curves for consequence classes 1 and 3, respectively. From these curves, it is observed that grade R4S is optimal for both classes, with minimal expected costs of 190 MNOK (102.5 mm diameter), and 313 MNOK (128.5 mm diameter). Note that the gradients of the curves the risk dominated region is much higher for consequence class 3 compared to consequence class 1. Since the probabilities of failure are equal for both cases, the difference in the gradients must be due to the higher failure costs for

consequence class 3. In the mitigation cost dominated region, the gradients of the curves are the same for both consequence classes, since the mitigation costs are independent of the class.

The expected costs for the safety factor are plotted in Figure 30(c) and Figure 30(d) for consequence classes 1 and 3. The vertical lines indicate the optimal safety factors for each grade. It is observed from the figures that the optimal solution for consequence class 1 is between 1.2 and 1.3. For consequence class 3, the optimal safety factor is between 1.8 and 2.05. In both cases, the optimal safety factor is lower than the values specified by ISO 19901-7, which is 1.5 and 2.2 for intact condition and single mooring line failure respectively.

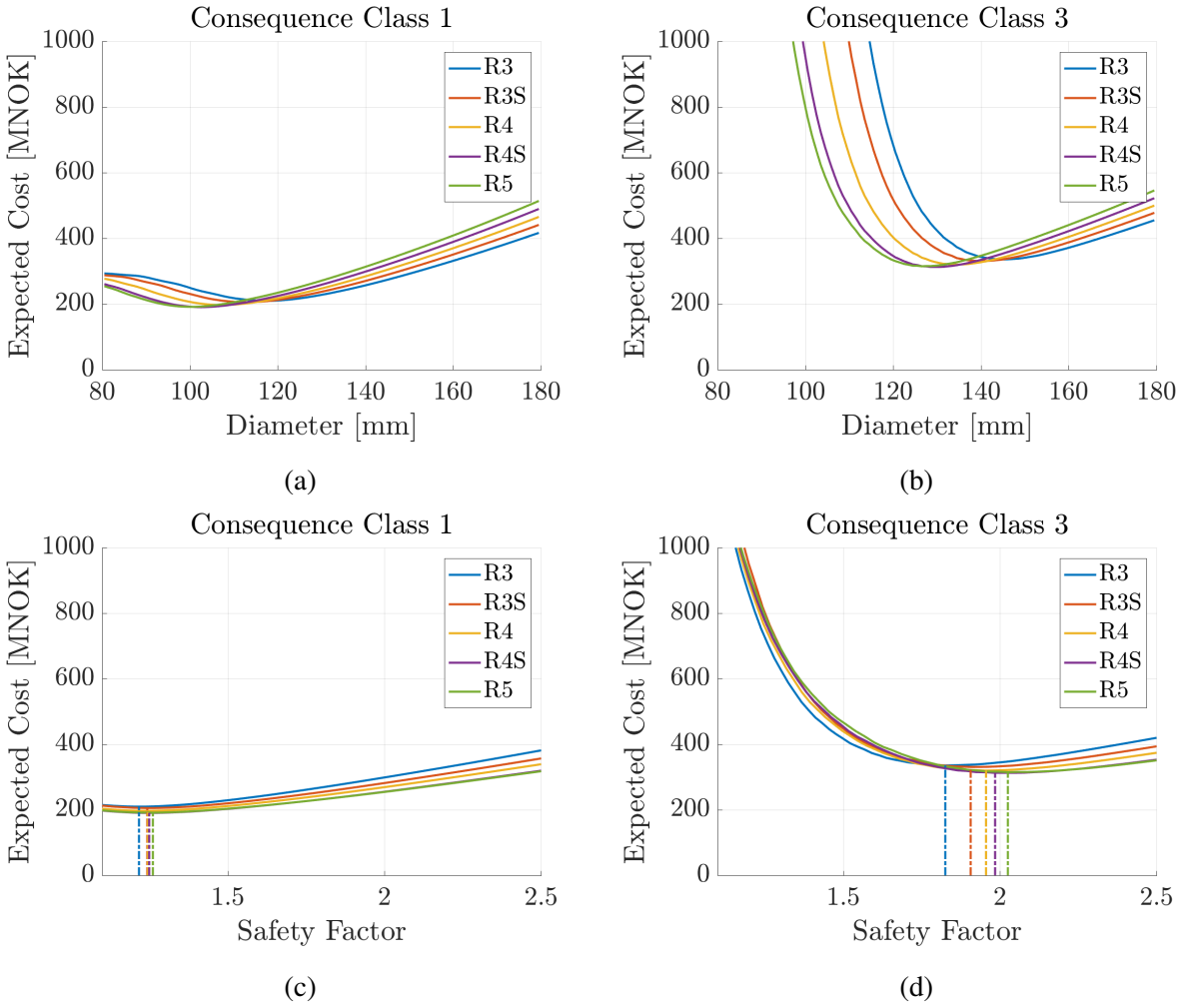

Figure 30: Expected Costs from the ULS Network

4.6.2 Parameter Study for the Progressive Failure Network

The cost-optimization curves for the Progressive Failure Network are shown in Figure 31(a) and Figure 31(b). The optimal values are 216 MNOK, 112.5 mm, R4S and 268 MNOK, 126.5 mm, R4S for consequence classes 1 and 3, respectively. The curves in the figures show certain similarities to their counterparts for the ULS Network, such as the steep decrease of expected

costs in the risk dominated region for consequence class 3, followed by the gentle increase in the mitigation cost dominated region. However, there is one noticeable difference between the plots for the Progressive Failure Network and ULS Network; there is a ”bulge” in the graph in the risk dominated area for consequence class 1, where the curvatures changes and the lines converge as the diameter decreases. It can be observed that the value it converges to is the sum of the production and installment cost and the consequence of a mooring system failure. This can be explained by the fact that the low diameters cause the failure probability to be close to one. Therefore, the risk, which is the product of the consequences and the failure probability, is almost equal to the consequences of failure. It is likely that this effect would be present in the other figures if the axes were unbounded.

Figure 31(c) and Figure 31(d) show the expected costs and the safety factor indication lines for all grades and consequence classes. It is observed from Figure 31(c) that the optimal safety factor is in the same range as the value specified by ISO 19901-7. However, the optimal safety factor is still too low for consequence class 3, as it is between 1.8 and 1.95.

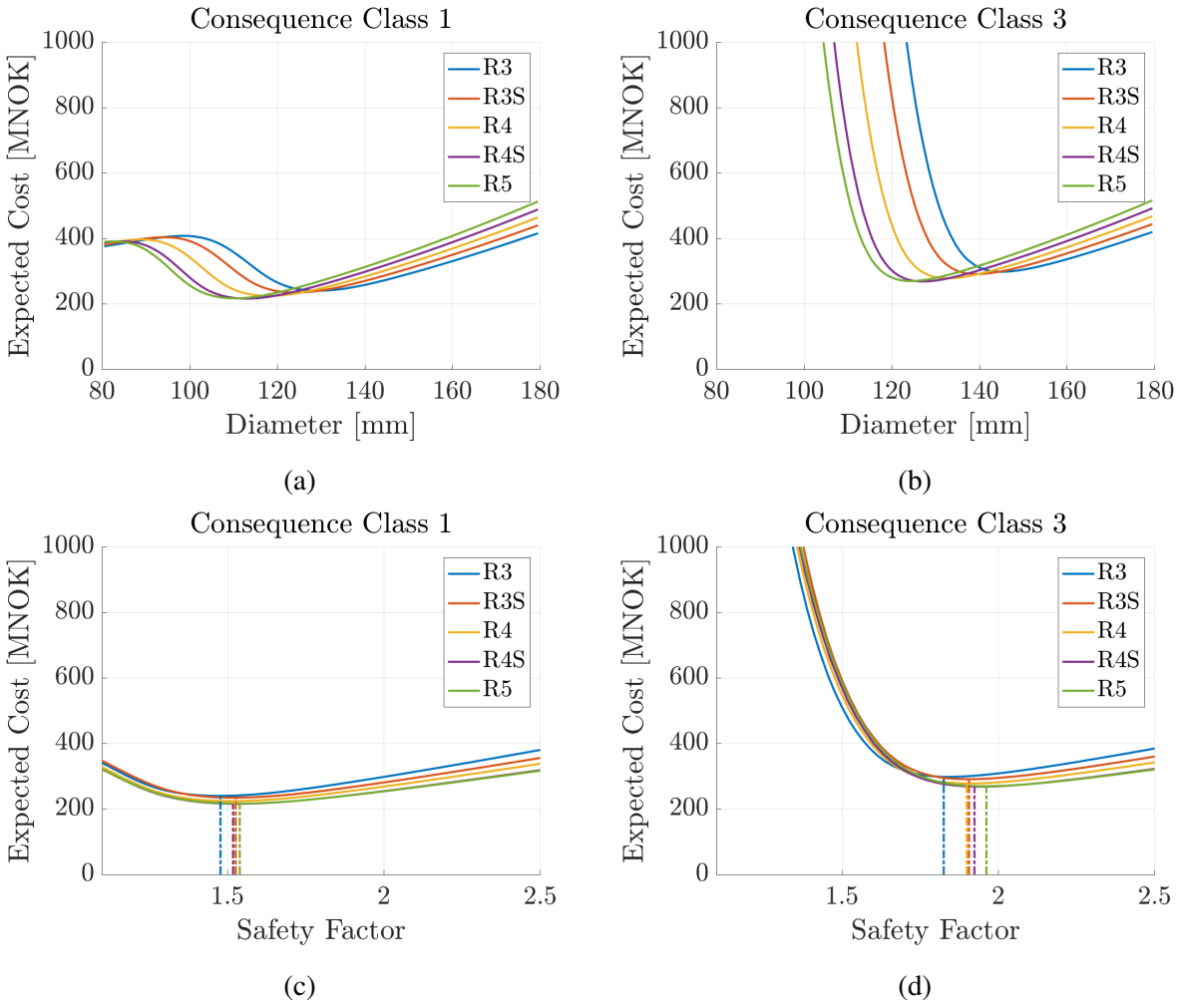

Figure 31: Expected Costs from the Progressive Failure Network

4.7 Discussion

The parameter study carried out in the previous section shows that the optimal safety factors are in most cases lower than the safety factors provided by ISO 19901-7. This discrepancy may be a consequence of neglecting the series effect of the chain links, where a failure of one link yields the failure of the mooring line. If the resistance of the links is independent, i.e. there is no correlation between them, the system reliability decreases. Since it is almost impossible to estimate the correlation, the uncorrelated and fully correlated cases serve as bounds, which is stated in mathematical terms in Equation (8) where $Comp, i$ refers to a chain link of the mooring line, and Sys refers to the mooring line.

$$\max_{i=1}^{n} \{P_F\left(Comp, i\right)\} \leq P_F(Sys) \leq 1 - \prod_{i=1}^{n} \left(1 - P_F\left(Comp, i\right)\right) \tag{8}$$

It is expected that the resistance of the chain links in a mooring line is correlated to some degree. This correlation may be caused by the production or the environmental conditions that the mooring lines are subjected to. Since it is assumed in this Thesis that the mooring line resistance is equal to the component resistance[10], it is reasonable to conclude that resistance for each mooring line is overestimated. By introducing correlation between the chain links, the system resistance would decrease and therefore increase the probability of failure and the risk. This would cause an increase in the optimal safety factor. However, without a reasonable estimate of the correlation, the absolute value of the increase remains unknown.

Based on the scatter of the optimal safety factor it may be suggested that the safety factors provided in the design standards should be dependent on the steel grade. However, this cannot be concluded at present, since the dependency of the loads on the resistance is not accounted for in the networks.

4.8 Summary

This chapter concerns the modeling of the design phase. Before the networks are developed, the underlying assumptions are established. In general, it is assumed that the series effect of the mooring chain could be neglected, so it is sufficient to consider the most loaded link, and that loading is independent of the design. Two main networks referred to as the ULS Network and the Progressive Failure Network are developed from the limit state function. Furthermore, the quantification of the nodes is explained, before a brief parameter study is conducted. The results show that the optimal safety factor for the ULS Network is 1.2-1.3 and 1.8-2.05, for consequence classes 1 and 3, respectively. This is lower than 1.5 for the survival scenario, and 2.2 for the operational scenario provided in ISO 19901-7. For the Progressive Failure Network, the optimal value is 1.5 and 1.8-1.95 for the respective consequence classes, which is consistent with the provided values in the first case, but not the second.

[10] which implies that the failure probability computed from the networks corresponds to the lower bound

5 Modeling the Inspection Phase

This chapter focuses on representing the inspection phase as a risk-based decision problem. Two networks are created to represent the inspection phase for a single mooring line and system of multiple mooring lines. Since the decay of the structural integrity is time-dependent, it is preferred to model the inspection phase as a dynamic decision graph. Since GeNIe does not support dynamic decision graphs, potential solutions are explored, but subsequently abandoned when the single line network is unable to represent the reduction of the uncertainties from inspections, without considerable effort.

5.1 Inspection Policy

Two important terms for this chapter are *inspection policy* and *replacement policy*. As the name suggests, the inspection policy describes what to inspect, and when to inspect it. As an example, the mooring lines of the platform Troll B are inspected over the whole length every four years, while the upper parts are inspected every year (*Troll B ROV (våt) inspeksjon av forankringsliner* 2014). The inspection policy is normally altered to a shorter interval if any damages are reported. The benefit from inspection is to reduce the uncertainties about the state of the mooring lines, to make better informed and therefore more optimal decisions that concern their integrity.

The replacement policy dictates whether the mooring line should be replaced. The mooring lines are normally replaced if the damages are too severe; however, there is no universal metric to quantify this damage. Because of this, the decision is made on a case-by-case basis. In this chapter, the replacement policy is modeled in two ways; the first method is to model the decision explicitly, so GeNIe or the user may optimize for both inspection and replacement; the second method is to apply a decision rule for which action to take. An example of a decision rule is to replace the mooring line if it is indicated by the inspection that the mooring line is in a certain state, otherwise to keep it.

5.2 Underlying Assumptions

Similar to Chapter 4, the underlying assumptions are stated before the networks are developed. Since the purpose of the networks is to find the inspection policy that minimizes the expected costs, the decisions about the design (diameter, grade, and consequence class) are removed to reduce the number of decisions, thus simplifying the problem. The assumptions from Section 4.2.1[11] are considered to be still valid. It is assumed that uniform corrosion is the only deterioration mechanism that affects the state of the mooring line. Deterioration due to fatigue and pitting corrosion and damages caused by accidents are not covered in this Thesis.

[11] It is sufficient to look at the most loaded link, the mooring is permanent, the series and fatigue effects neglected

The networks are based on a one-year time step, with a service life of 30 years. It is assumed that a failure is discovered immediately and that the mooring line is replaced within the year the failure occurred. A replaced mooring line is assumed to be in the best state. Since the networks model the whole service life, the potential costs should be discounted to reflect present value. The annual load distribution is assumed independent between the time steps, which implies that there is no bias in the weather model, so there is no systematic under- or over-prediction of the loads. For both networks, the effects of the partial inspection are neglected, although it could be included in future work.

5.3 Single Mooring Line Network

The limit state function serves as a starting point, similar to the networks developed in Chapter 4. Therefore, *Failure* is a child of *Loads* and *Resistance*. The deterioration of *Resistance* is modeled by a decreasing diameter due to uniform corrosion. Because of this, the node *Diameter* is a parent to *Resistance*. It is clear that the diameter depends on its previous state; thus the node *Diameter* is self-referring.

In this network, each time step contains two decision nodes, namely *Inspection* and *Action*, each with two outcomes. The node *Inspection* describes the decision on whether to conduct an inspection and *Action* describes whether the mooring line should be replaced. Since the outcome of an inspection of the diameter size depends on the actual diameter, a chance node called *Outcome* is included as a child of *Inspection* and *Diameter*. It is assumed the outcome of an inspection is known before a decision about replacing the mooring lines is made; thus, an arc is drawn from *Outcome* to *Action*. If the mooring line is replaced, it influences the state of *Diameter*, and it is therefore conditional on *Action*.

The costs are added to complete the network. Intuitively, *Inspection* leads to *Inspection Cost*, *Action* leads to *Action Cost* and *Failure* leads to *Failure Cost*. In this network, the probability of having a system failure is neglected, hence the lack of the *System Failure* and *System Failure Cost* nodes which are present in the networks from Chapter 4. The final configuration of the network is shown in Figure 32. Note that *Action* should be a parent to *Inspection* the following year since an order of decisions is required. However, this is not crucial as GeNIe assumes the correct order of decisions when there is no ambiguity.

5.4 Multiple Mooring Line Network

The Single Mooring Line Network may be expanded into the Multiple Mooring Line Network by simply duplicating it as many times as needed. Figure 33 shows the rearranged Multiple Mooring Line Network for two mooring lines where *Diameter* is marginalized out to ease readability. The network also features two important additions, namely the nodes *Design* and

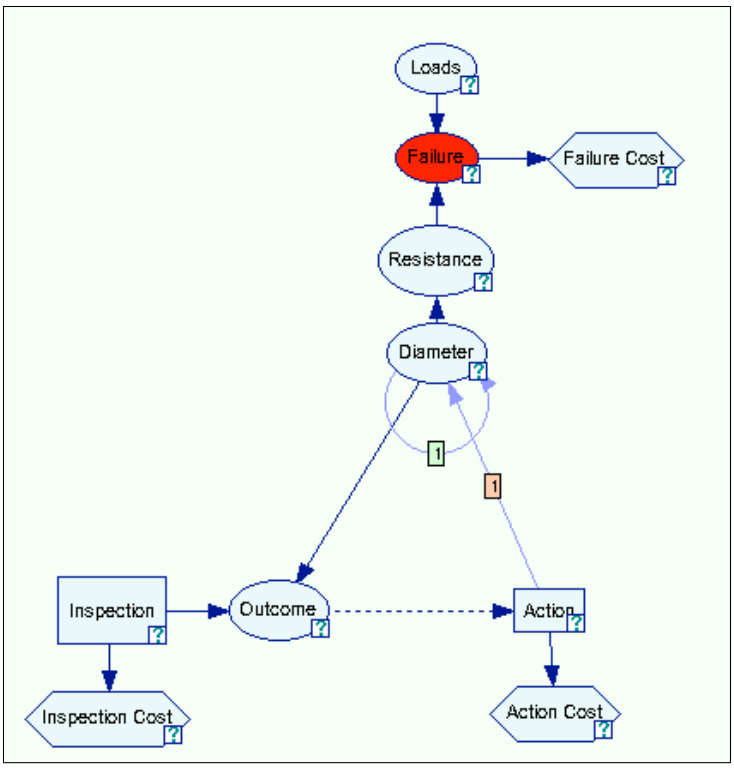

Figure 32: Single Mooring Line Network

Weather, which purpose is to account for correlation caused during manufacturing and by the loading. Since there are no common factors between the two *Resistance* nodes except for *Design*, the deterioration mechanisms are assumed to be independent. The node *Failure* is included in the network as a failure switch, which purpose is model that a failure of one mooring line will lead to an inspection of the remaining lines. Note that *Design* has a different background color in Figure 33. This is because this node is an initial condition for the resistance, and is therefore not included in the time-dependent part along the rest of the network.

It is observed that this network is flawed since the failure switch does not work as intended. This is because a decision cannot be conditional on a chance node in GeNIe[12]. As a result, GeNIe is not able to automatically model inspections for the system conditional on failure, at least for the proposed network.

5.5 Potential Solutions for the Modeling Problems

As mentioned in the introduction of the chapter, GeNIe does not currently support dynamic decision graphs, although the developer plans to incorporate this feature in the future. Instead of abandoning the second research goal, alternative modeling practices are being investigated. In the following section, two potential solutions to circumvent this problem are discussed.

[12]The dotted arcs from *Failure* to *Inspection* shows that information on *Failure* is know before a decision is made for *Inspection*

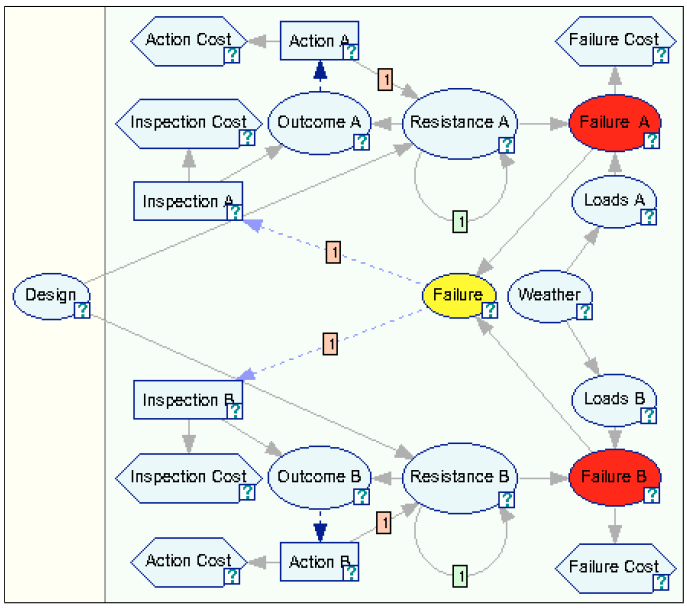

Figure 33: Multiple Mooring Line Network

5.5.1 Approach 1: Unrolled Decision Graph

One potential solution is to create the unrolled version of the decision graph, shown in Figure 34 for the Single Mooring Line Network. The idea is to use GeNIe's best policy algorithm to find the optimal inspection routine where the expected costs are minimized. This idea is tested on the unrolled network, with as few as five time steps. In this case, each time step contained the two decision nodes *Inspection* and *Action*, each with two outcomes; whether to conduct an inspection, and whether to replace the mooring line. As for all decision graphs, the order of decisions is assumed. In this case, a decision on *Inspection* is conducted before a decision on *Action*. Since the network is chronological, an arc is drawn *Action* to *Inspection* the following year.

It is found that GeNIe is unable to analyze this network. A potential explanation is that the number of combinations for the decision outcomes is too large. For this network, there are as many as many as $(2 \cdot 2)^5 = 1,024$ combinations, compared to $2 \cdot 5 \cdot 11 = 110$ combinations for the ULS Network and Progressive Failure Network from Chapter 4. The number of choices can be reduced to $2^5 = 32$ by applying a decision rule for *Action*. Therefore, the network is modified by implementing the following decision rule; if the outcome of the inspection indicated the worst state, the mooring line is replaced, if not, it is kept another year. In this case, GeNIe is able to analyze the network. A drawback of this technique is that the cost of action is to be implemented manually. This may be done by taking the sum of the probability of replacing the mooring line multiplied by the cost of the replacement, and add it to the expected costs computed by GeNIe. This network is not suitable for modeling the system effects of inspection since this would introduce additional decision nodes and therefore increase the demand on GeNIe. Consequently, further effort to circumvent the problem with this technique is abandoned.

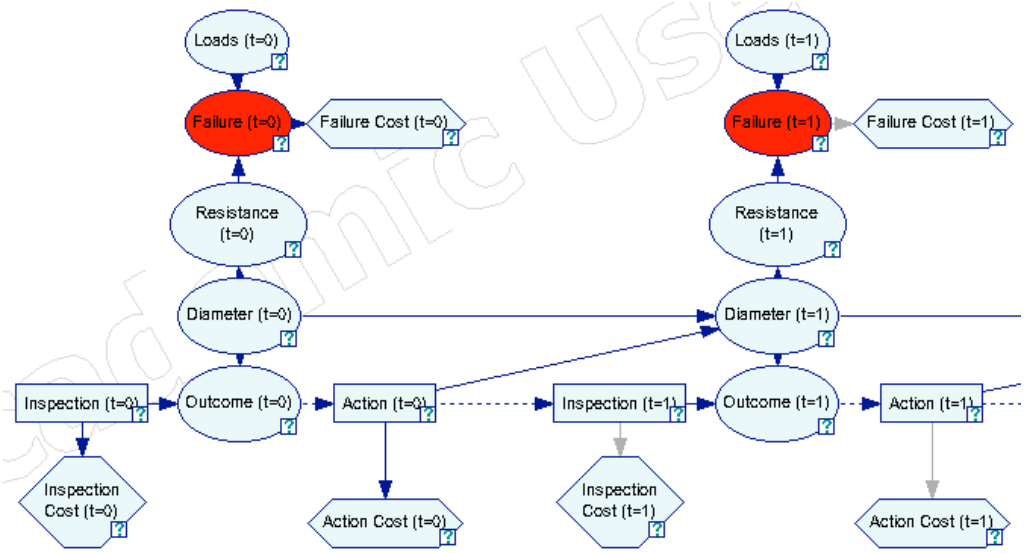

Figure 34: Unrolled decision graph for the Single Mooring Line Network

5.5.2 Approach 2: Dynamic Bayesian Network

Another potential approach is to remove the utility nodes from the dynamic decision graphs and to replace the decision nodes with chance nodes with a uniform probability for the outcomes, thus reducing the dynamic decision graph into a dynamic Bayesian network. The result for the Single Mooring Line Network is shown in Figure 35. The inspection and action policies can be accounted for through evidence about the state of the chance nodes. The costs for each policy are then manually computed by combining the direct policy cost with the risk. This is summarized in Equation (9), where C_I, C_R, C_F and P_F is inspection cost, replacement cost, failure cost and probability of failure, respectively.

$$\text{Expected Cost} = \sum_{i=1}^{n} C_{I,i}\left(t\right) + \sum_{i=1}^{n} C_{R,i}\left(t\right) + \sum_{i=1}^{n} P_{F,i}\left(R, I, t\right) \cdot C_{F,i}\left(t\right) \tag{9}$$

Figure 36(a), Figure 36(b), and Figure 36(c), show the result of the dynamic Bayesian network for different cases, where the network is quantified in accordance with the assumptions stated in Section 4.2.1 and Section 5.2, assuming a deterministic diameter and the Loads II distribution. Figure 36(a) shows the prior prediction for the decrease of the diameter, where purple is the best state and blue is the worst state, and each state covers a 2 mm interval. It is observed that there is no uncertainty about the diameter initially, however, as the decay progresses, it becomes less likely that the diameter is in the best conditions. Figure 36(b) shows the posterior prediction for the diameter when evidence from an inspection conducted 8 years after installation suggests that the diameter is in *State 4* (approximately 142 mm). The final Figure 36(c), shows how the diameter is changed when the mooring line is replaced. In this case, the mooring line is replaced 25 years after installation.

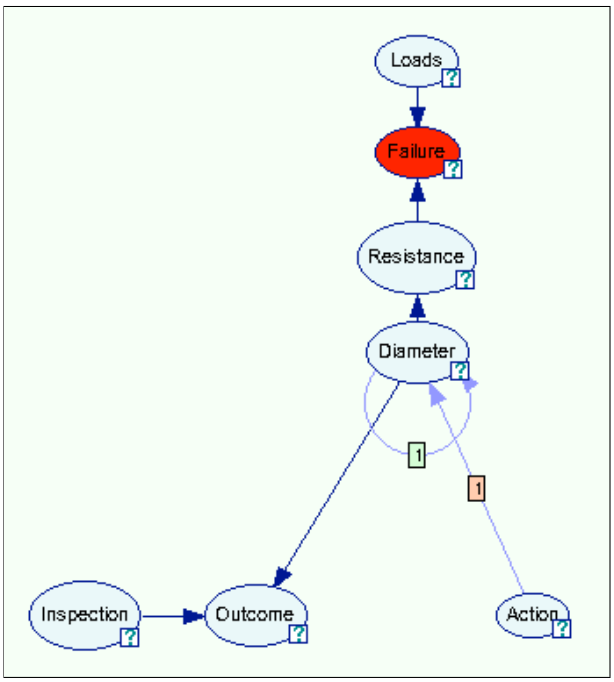

Figure 35: Dynamic Bayesian version of the Single Mooring Line Network

These actions affect the probability of failure. Figure 36(d), Figure 36(e), and Figure 36(f) illustrate how the probability changes with time and the different actions. Figure 36(d) and Figure 36(e) show the prior and posterior predictions of the probability of failure, which correspond to the policy applied to pictures above them. It is observed that an indication for *State 4* in the 8th year after installation increases the prediction of the failure probability. Similarly, Figure 36(f) shows how a replacement of the mooring line affects the probability of failure.

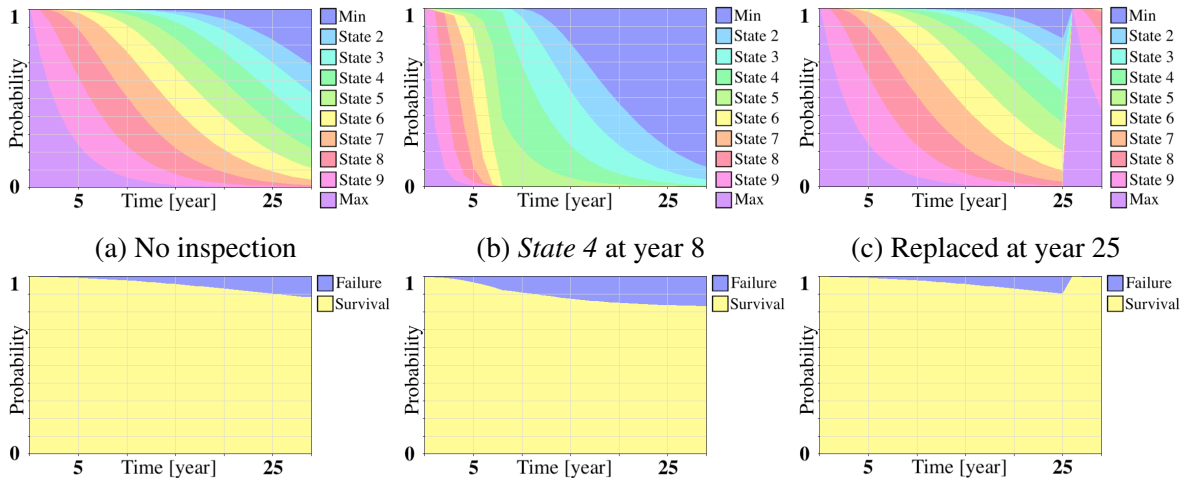

(a) No inspection (b) *State 4* at year 8 (c) Replaced at year 25

(d) No inspection (e) *State 4* at year 8 (f) Replaced at year 25

Figure 36: Predictions for the diameter and failure probability given different actions

From Figure 35 it is observed that *Inspection* and *Diameter* are both parent to *Outcome*, and together they form a converging connection. Recall from Section 3.5 that this connection is

D-separated when there is no information about the state of *Outcome*. In practice, this means that knowing an inspection has been conducted does not change our prediction of the state of *Diameter* (and thus its children), without knowing the outcome of the inspection.

As a result, the assessment of the expected costs of a policy becomes very complicated. To conduct the analysis, evidence is to be introduced into *Inspection* according to the inspection policy, followed by a systematic insertion of evidence about the state of *Outcomes* until all possible combinations have been covered. This is combined with the possible actions if a decision rule is not used. For each of these combinations, the probability of failure for all time steps is recorded to compute the risk. The expected cost of inspection is then computed by taking the sum of the expected cost of each outcome scaled by the probability of the outcome.

This approach quickly becomes very labor-intensive. To illustrate this, consider the case where the inspection with three potential outcomes is conducted once within the service life, without applying a decision rule for *Action*. The potential combinations of outcomes and costs are structured as a decision tree, shown in Figure 37. If the number of inspections to be conducted is increased to two, 64 vectors that contain the probability of failure for each time step have to be analyzed. This number can be reduced to 16 by applying a decision rule for *Action*, but it is still a demanding task. As a result, it is concluded that this approach is not a practical solution, and it is therefore not further investigated in this Thesis.

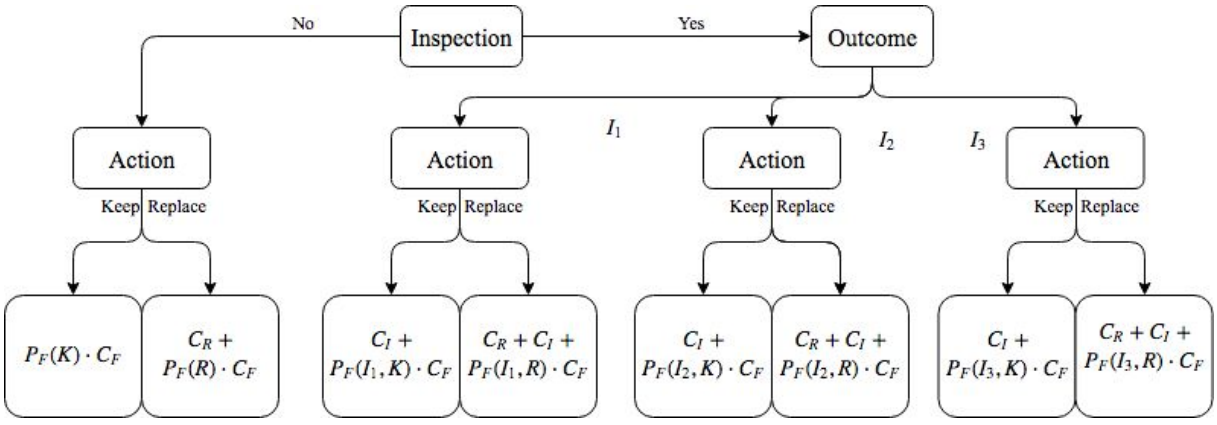

Figure 37: All combinations from an inspection with three outcomes

5.6 Summary

In this chapter, the modeling of the inspection phase is studied. The chapter opens with a brief introduction to inspection policy before it states the underlying assumptions required to model the inspection phase as a dynamic decision graph in GeNIe. The assumptions stated in Chapter 4 are still valid. In addition, it is assumed that the decay of structural integrity is only due to uniform corrosion, a failure is discovered and repaired within a year, and that a replaced mooring line is in the best state.

Two networks are made to model the inspection phase of a single mooring line and multiple mooring lines as dynamic decision graphs. However, the use of dynamic decision graphs is currently not supported by GeNIe. Therefore, two potential solutions are attempted. The first approach is to create a network that is similar to the unrolled decision graph; nonetheless, this does not work, possibly due to the high number of combinations of decisions. The second approach is to create a dynamic Bayesian network and use vectors of evidence as the inspection policy. However, the D-separation property of a crucial connection in the network makes the extraction of results very labor-intensive. As a result, further investigation of the modeling of the inspection phase is abandoned.

6 Sensitivity and Value of Information

This chapter presents sensitivity analysis with respect to the failure event for the ULS Network and the Safety Factor Network, and with respect to the system failure event for the Progressive Failure Network. This analysis is performed to identify the nodes with the most sensitive parameters[13], which are the nodes that affect the accuracy of the results from the networks. Furthermore, a value of information analysis is conducted to investigate the potential gain of acquiring additional information. The results are presented and discussed before the chapter is concluded with a summary.

6.1 Sensitivity Analysis

The sensitivity analysis in GeNIe is based on the work in Castillo et al. (1997) and implements the algorithm proposed in Kjærulff and van der Gaag (2000). In short, the sensitivity analysis computes the derivatives in the proximity of the current value, for all nodes in the network, with respect to one or more target nodes. If the sensitivity for a parameter is high, a small deviation leads to a large difference in the posterior distribution for the target node.

According to the developer, GeNIe's sensitivity function may be applied to decision graphs. In practice, GeNIe is unable to conduct the sensitivity analysis for the decisions graphs from Chapter 4. Therefore, the networks are stabilized by removing the utility nodes, and by using chance nodes as proxies for the decision nodes.

6.1.1 Sensitivity Analysis for the ULS Network

The result of the sensitivity analysis for the ULS Network is given as the tornado diagram in Figure 38. The vertical line marks the current value of the probability. This value corresponds to the prior probability if no evidence is observed for the system. The tornado diagram is developed for 10% parameter spread, which means that the diagram illustrates the effect of increasing and decreasing each parameter by 10%. The wideness of the tornado bars shows the target value range, which is the minimum and maximum posterior probabilities given the level of parameter spread. The color of the bars illustrates how a change in the parameter changes the posterior distribution for the failure event; red/green means that an increase in the probability for the parameter leads to an increase of the probability of failure, while the opposite is true for the green/red. Note that the bars in the tornado diagram are not necessarily symmetric about the current value.

The analysis shows that the probability of failure is most sensitive to the smaller diameters (80-90 mm). The second and third most sensitive parameters are medium-high loads (7000-9000 kN) and medium corrosion rates (0.4-0.6 mm/year). Note that increasing the parameter D80 in Figure 38 increases the probability of failure. This is because an increase of the parameter does

[13] In this chapter, *parameter* is used for an entry in the CPT of a node

not represent an increase of the physical diameter, but rather a bias towards this decision for the decision-maker. This illustrates that special care ought to be used when interpreting results arising from proxy chance nodes.

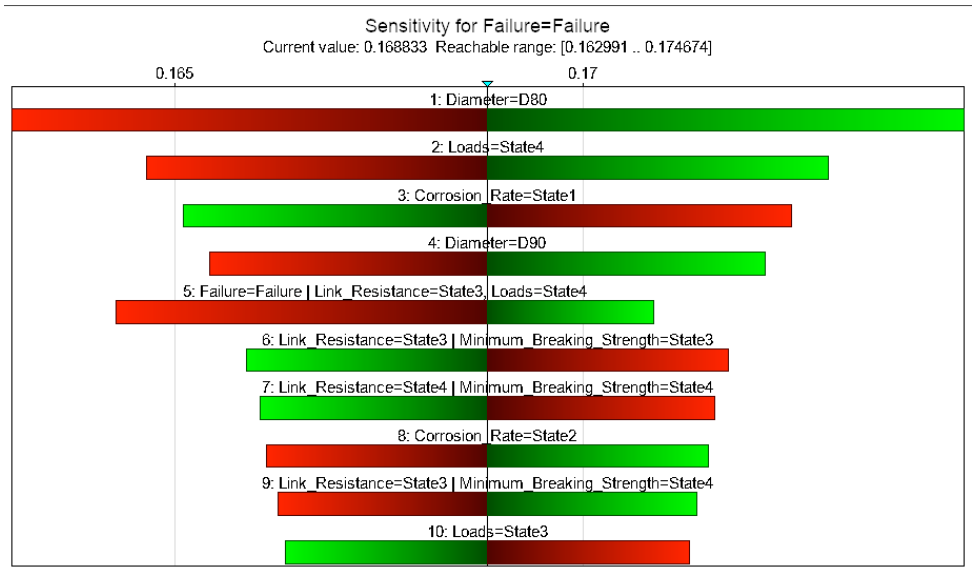

Figure 38: Tornado diagram for the ULS Network

The sensitivity plot for the ULS network is developed by conducting a sensitivity analysis for different cases where the node *Diameter* had received evidence. The resulting average[14] sensitivities are given in Figure 39(a), where a higher number indicates a greater change of the posterior for the target node. It is observed that sensitivities for *Loads*, *Grade*, *Corrosion Rate* and *Service Life* increase up to a point between 90 mm and 100 mm diameter, before it decreases for larger diameters. An explanation for this observation may be that the large diameters lead to a highly resistant chain link, with a low probability of failure. A small change in these parameters does not have a significant impact on the probability of failure since they are well within the safe domain.

6.1.2 Sensitivity Analysis for the Safety Factor Network

The sensitivity plot for the Safety Factor Network is shown in Figure 39(b) for 10% parameter spread. As expected, the sensitivity plot is almost identical to that of the ULS Network, since the Safety Factor Network is a variant of this network. It is observed that the curve for *Loads* does not have a maximum value in this range, either because the peak is out of the domain, or the discretization interval is not small enough to capture the peak. However, a safety factor below or around 1 is not realistic; therefore the location of the maximum is not interesting and therefore not further investigated. In contrast to the sensitivity plots for the ULS Network, the sensitivity of the node *Grade* is almost non-existent for the Safety Factor Network. It is

[14] Average of all parameter sensitivities for a node

concluded that this low sensitivity is caused by the quantification process, were the sensitivity of *Safety Factor* is increased at the expense of *Grade*.

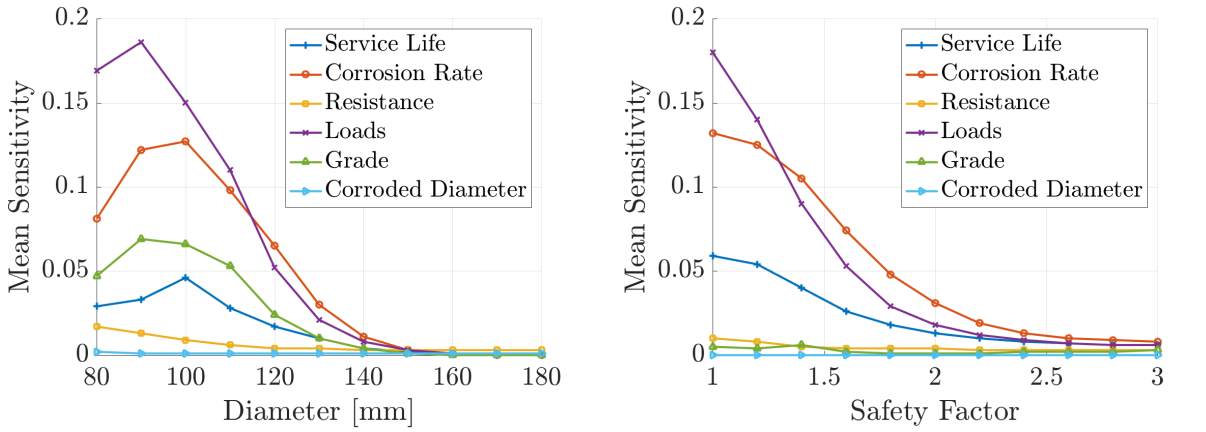

(a) Sensitivity plot for the ULS Network

(b) Sensitivity plot for the Safety Factor Network

Figure 39: Value of Information for the Progressive Failure Network

6.1.3 Sensitivity Analysis for the Progressive Failure Network

The sensitivity analysis is conducted for the Progressive Failure Network with the node *System Failure* as the target node. The resulting tornado plot for 10% parameter spread, presented in Figure 40 shows that the target node is most sensitive to the *Diameter* parameters. This observation is attributed to the assumption that the mooring lines are designed equally, so the chosen diameter greatly influences the probability of system failure.

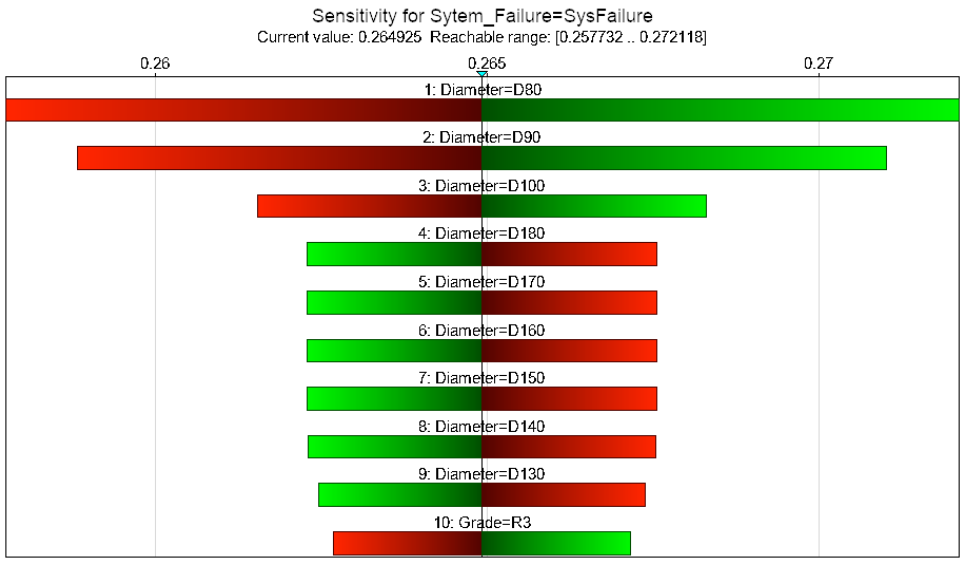

Figure 40: Tornado diagram for the Progressive Failure Network

The sensitivity plot for the Progressive Failure Network is shown in Figure 41. It is observed that the *Grade* is the most influential parameter for this network by a large margin, followed by *Corrosion Rate*, which are both linked to the resistance of each mooring line. Notice that the parameters are most sensitive between 100-110 mm, compared to 90-100 mm for the ULS Network.

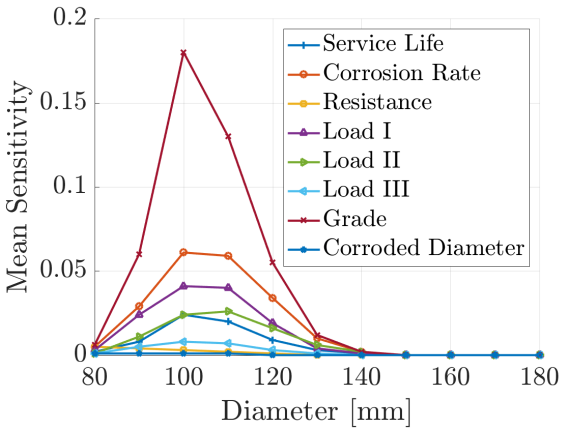

Figure 41: Sensitivity plot for the Progressive Failure Network

6.2 Value of Information

A value of information analysis is conducted for the ULS Network and the Progressive Failure Network. The analysis assesses the value of reducing uncertainty by acquiring further information. This value is estimated by taking the expected cost obtained by observing a specific node, subtracted from the expected cost obtained when the node is unobserved. It follows that the value of information cannot be negative when there are no costs associated with acquiring the information because more information reduces the uncertainty for the decision-maker. The results from the value of information analysis can be used by the decision-maker to determine whether a research project should be conducted, and the amount of resources that should be allocated.

To asses the value of information, a decision node has to be selected as the reference point. It is not possible to calculate the value of information of descendants of this node. This is because the marginal distribution of the descendant is used in the value of information analysis. However, the marginal distribution depends on the decision, which creates a circular reference. In the case for the design networks, a value of information analysis for the descendants of the decision nodes corresponds to reducing the epistemic uncertainty before the design is conducted. Note that a value of information analysis may be conducted for the descendants if the network is converted to the canonical form as described in Heckerman and Shachter (1995).

6.2.1 Value of Information Analysis for the ULS Network

The value of information analysis can be performed through a small modification of the ULS Network. The modification is conducted by adding a decision node called *Test*, which describes which test method to be used, and a chance node called *Outcome*, which describes the accuracy of the inspection method. *Outcome* depends on the state of the node the analysis is conducted for, and on the type of test conducted. Therefore, arcs are drawn from the target node and *Test* to *Outcome*. It is assumed that *Outcome* is known before the design is conducted, therefore an arc is drawn from *Outcome* to *Grade*. Finally, *Test* is placed within the decision hierarchy. In this case, it is assumed that *Test* is the second decision to be made, after *Consequence Class*. The resulting network is shown in Figure 42, where the analysis is conducted for *Loads*. In this network, it is assumed that the test yields perfect information. It is possible to include several tests with different accuracy by including additional decisions in *Test*, and by altering the CPT in *Outcome*. The value of information is then computed as the difference between the decisions *Yes* and *No*[15].

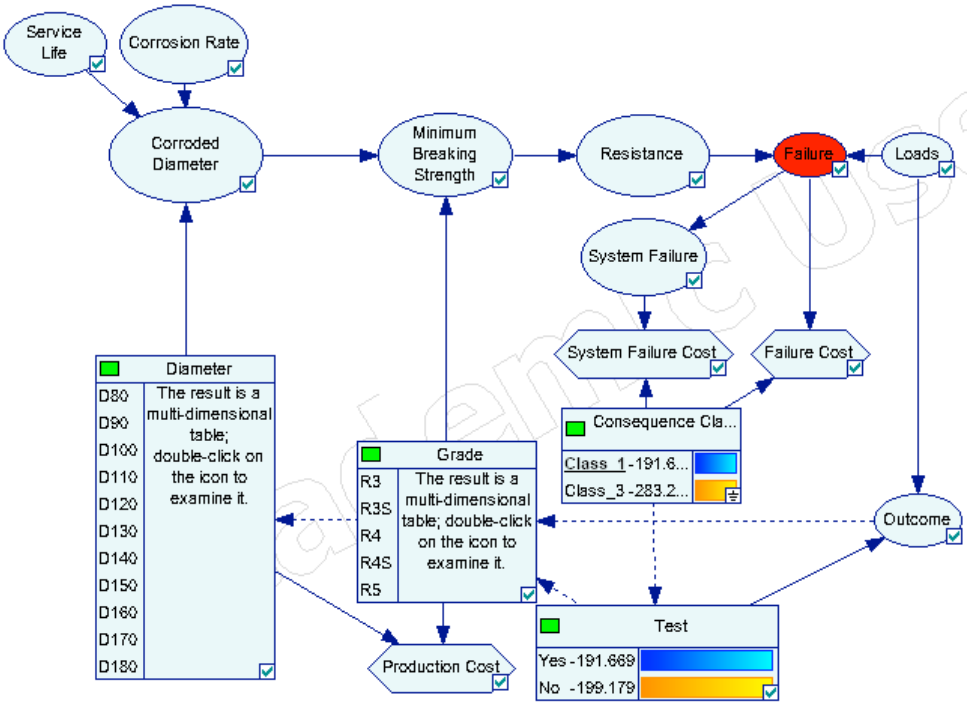

Figure 42: Value of information analysis for the ULS Network

There are three nodes in the ULS Network that are not descendants of the decision nodes and therefore suitable as target nodes, namely *Service Life*, *Corrosion Rate*, and *Loads*. Instead of altering the network for each of the target nodes, GeNIe's integrated value of information tool is used to analyze the network. The results of the analysis are given in Figure 43(a) and Figure 43(b), broken down by the node, grade and consequence class due to the ordering of

[15]The reader can verify that the *Loads* column for R4 in Figure 43(a) corresponds to the difference between the expected value for the decisions in the node *Test* in Figure 42

the decision nodes. Note that GeNIe's tool assumes perfect information about the target node. Uncertainty may be included in the analysis by adding a chance node as a child of the target node and to subsequently analyze the child node instead of the target node.

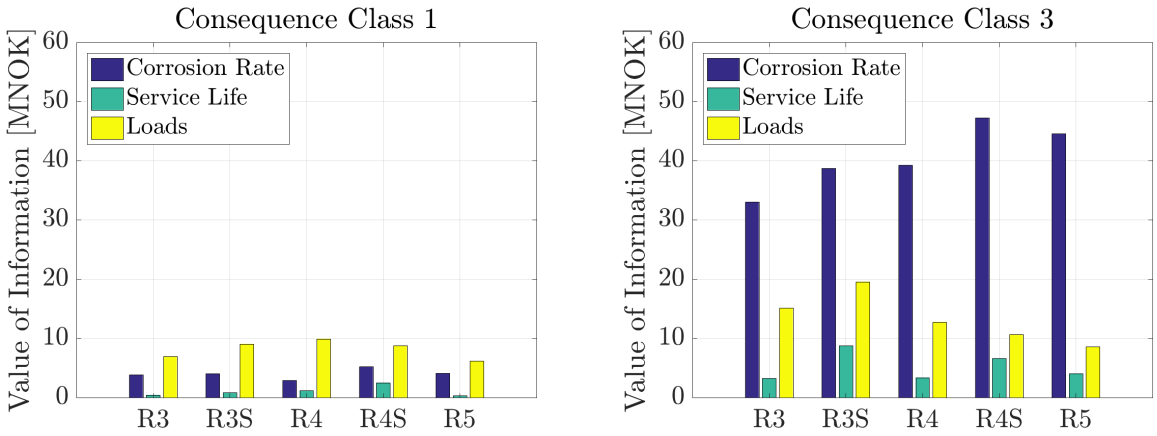

Figure 43: Value of Information Network

It is observed from Figure 43(a) that the value of information is largest for *Loads*, followed by *Corrosion Rate*. In contrast, Figure 43(b) shows that the opposite is true for consequence class 3, where observing *Corrosion Rate* is preferred. In both cases, *Service Life* has the lowest value of information.

6.2.2 Value of Information Analysis for the Progressive Failure Network

For the Progressive Failure Network, three nodes per line can be analyzed, namely *Service Life*, *Corrosion Rate*, and *Load I*[16]. In this case, there is a discrepancy between the value of information for each mooring line which is attributed to the Monte Carlo sampling method used for quantifying the network; therefore, the average of the results is presented in Figure 44(a) and Figure 44(b). Note that the *Service Life*, *Corrosion Rate*, and *Load I* nodes are assumed to be independent during the modeling phase[17], which implies that observing one of these nodes does not change the prediction for the rest.

In contrast to the results from the value of information analysis for the ULS Network, there are no clear tendencies for *Corrosion Rate* and *Service Life* observed. However, both Figure 44(a) and Figure 44(b) show that the value of information is the least for *Loads* when compared to the other nodes.

[16] *Load* for the first time step in the Progressive Failure Network
[17] ref. Section 4.3.3

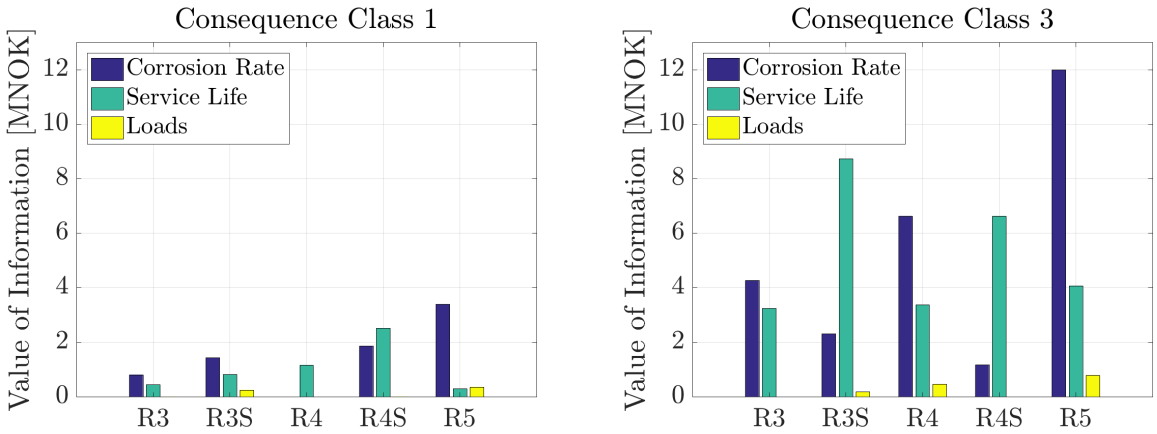

Figure 44: Value of Information for the Progressive Failure Network

6.3 Discussion

It is observed from the bar charts obtained through the value of information analysis, that the value of obtaining perfect information about nodes in the Progressive Failure Network is consistently lower compared with their respective counterparts in the ULS Network. This may be explained by the assumed independence of the relevant nodes since the outcome of a potential test for one node does not change the posterior distribution for the rest.

As argued in Section 4.7, the mooring lines are correlated to some degree in reality. In fact, the load history of each mooring line largely depends on the motion of the platform, thus ensuring a correlation between them. The mooring lines are also subjected to the same corrosive environment. Therefore, it is reasonable to suspect that there is some correlation between the lines of the mooring system. Accounting for this correlation would increase the value of information, since perfect information about one of the nodes would lead to a change in the prediction in the other nodes, thus reducing the overall uncertainty.

6.4 Summary

The chapter opens with a brief explanation of sensitivity analysis for Bayesian networks. The analysis is conducted for the ULS Network and Safety Factor Network with *Failure* as the target node, and for the Progressive Failure Network with *System Failure* as the target node. For the ULS Network and Progressive Failure Network, *Diameter* is the most sensitive node, and the *Safety Factor* is the most sensitive node for the Safety Factor Network. The sensitivity plots are developed for all the networks. The resulting plots show that the ULS Network is most sensitive to *Loads*, *Corrosion Rate*, and *Grade*, and that the Safety Factor Network is most sensitive to *Loads*, *Corrosion Rate*, and *Service Life*. In contrast to the ULS Network, the sensitivity of *Grade* is almost non-existent for the Safety Factor Network. However, for the Progressive Failure Network, *Grade* is undeniably the most important node, followed by *Corrosion Rate*

and *Load I*.

Potential gain from model enhancement by observing the nodes is computed through a value of information analysis on the ULS Network and Progressive Failure Network. For the ULS Network, the value of information is highest for either *Loads* or *Corrosion Rate*, depending on the consequence class. For the Progressive Failure Network, there is no distinct pattern except that *Loads I* gives in general lower values compared to *Corrosion Rate* and *Service Life*.

7 Conclusions and Further Research

This project aimed to investigate how aspects of mooring line design and integrity management could be coupled with decision theory, to develop networks that accurately captures features from these phases. Relevant events, decisions, consequences and the associated uncertainties had to be explored, as a prerequisite for the modeling. Three research objectives have been formulated to aid achieving this aim: (1) represent the current design practice as a decision graph; (2) represent the current inspection and maintenance routines as a decision graph; (3) conduct a sensitivity analysis and determine the value of information for the resulting networks. The overall conclusions of each research topic are presented in the section below, followed by a section on outlook to further research.

7.1 Conclusions

Two main networks were created to model the design phase, namely the ULS Network and the Progressive Failure Network. The Safety Factor Network, which is a variant of the ULS Network, was created to have the safety factor as a decision variable. The assumptions and decisions made to develop these networks were justified. The central assumptions were to neglect the series effect of the mooring line components, and not to address fatigue design. Furthermore, the probability distributions for the random variables were assumed, and the method of quantifying the nodes with Monte Carlo sampling was explained.

A parameter study was conducted to investigate how the expected cost varies with the safety factor. From the resulting cost-optimization curves for the ULS Network, it was concluded that the optimal safety factor is 1.2-1.3 and 1.8-2.05 for consequence classes 1 and 3, respectively. This is below the values provided in ISO 19901-7, which is 1.5 for the survival condition, and 2.2 for the operational condition. The optimal values found from the Progressive Failure Network are 1.5 and 1.8-1.95 for the respective consequence classes, which is sufficient in the first case, but not in the second.

In this context, the assumption of neglecting the series effect was discussed. It was concluded that when the series effect was accounted for, it would decrease the resistance, and therefore increase the probability of failure. This would lead to an increase in risk, thus making a higher safety factor the optimal solution.

It was observed from the cost-optimization curves that the optimal safety factor might depend on the steel grade. However, no conclusion was reached since the scatter may be caused by neglecting the dependency between the resistance and the loads.

Furthermore, an attempt was made to model the inspection and maintenance phase as dynamic decision graph in GeNIe. This attempt resulted in two networks; the Single Mooring Line Network, and the Multiple Mooring Line Network. Since GeNIe does not support dynamic decision graphs, two potential solutions were pursued. The first potential solution was to analyze

a created network similar to the unrolled version of the dynamic decision graph. However, it was concluded that it is not feasible in the current version of GeNIe.

The second approach was to create a dynamic Bayesian network with chance nodes as proxies for decision nodes, where the risk and policy cost would have to be computed manually. It was concluded that this approach could work; however, the D-separation property for an essential connection in the network made this a labor-intensive procedure. Therefore, it was concluded that further exploration of this procedure was to be abandoned as was too demanding to be a practical solution. Nonetheless, this work may serve as a valuable addition to the subject, and as a starting point for progressive enhancement once improved software become available.

A sensitivity analysis was conducted for the design phase networks. The failure event was used as the target node for the ULS Network and Safety Factor Network, and the system failure event was used for the Progressive Failure Network. For the ULS Network and Progressive Failure Network, the *Diameter* was the most sensitive node. The *Safety Factor* was the most sensitive node for the Safety Factor Network. An observation made in the analysis was that the sensitivity of *Grade* for the Safety Factor Network was almost non-existent, but it was the second most sensitive node for the Progressive Failure Network. It was concluded that there are two causes for this discrepancy. The first cause is that the assumption that all mooring lines are of equal design increases the sensitivity of *Grade* in the Progressive Failure Network. The second cause is that the quantification process for the Safety Factor Network increases the sensitivity of *Safety Factor* at the expense of *Grade*.

The potential gain from model enhancement by observing the state of the nodes were computed through a value of information analysis on the ULS Network and Progressive Failure Network. This could only be done for nodes that were not descendants of the decision nodes; therefore, the analysis only involved the node *Loads*, *Corrosion Rate* and *Service Life*. For the ULS Network, the value of information was highest for *Loads* and *Corrosion Rate* for consequence classes 1 and 3, respectively. For the Progressive Failure Network, there was no distinct pattern except that *Loads* gave in general lower values compared to *Corrosion Rate* and *Service Life*. It was observed that the value of information was consistently lower for the Progressive Failure Network than the ULS Network. This was attributed to the assumption that *Corrosion Rate*, *Service Life* and *Loads* were independent between the mooring lines.

7.2 Further Research

The study of the aforementioned research objectives yielded several additional objectives relevant for further studies, which are listed below:

- ***How can design for the fatigue limit state be incorporated in the existing networks?*** It is evident that the design against fatigue have to be accounted for in order to enhance the

networks. This is complicated because fatigue is dependent on time, while the accidental and ultimate limit states may be modeled as time-independent. A possible solution may be to approximate the stress range as a Weibull distribution as done in Mathisen and Larsen (2002). Another major challenge is to account for all these limit states in one node, to accommodate that the failure event is a single event, regardless of the cause.

- ***How may the load node be enhanced to capture the dependency on the selected design?*** The load node have to be expanded in to a load branch by including more of its causes, in particular pre-tension, which is typically in the range of 10-20% of the MBS. In addition, the loads depend on the motion of the structure, which again is dependent on the chosen configuration of the mooring system. Therefore, a natural enhancement for the networks is to include more decisions for the design configuration and mooring line composition such as: catenary or taut leg system, clustered or evenly spread mooring lines, and whether to use synthetic rope, steel wire rope, and studlink or studless link. The direct effects from the fluid-mooring line interaction may be modeled in further research.

- ***How can the series effect of the mooring line components be accounted for?*** For the models in this Thesis, the series effect within the mooring lines are neglected, that is, only the most loaded link is considered. A major challenge is to model this effect accurately, especially for a segmented mooring line, without making the model too complex and computational expensive.

- ***How can the consequences be elaborated, especially with respect to potential loss of human lives?*** The consequences may be modeled with a non-linear utility curve to reflect risk-averse behavior. Multiple-attribute utility theory could be used to explicitly incorporate the decision-maker's weighting of the attributes. A further development of the models could be to include the *marginal lifesaving cost* principle, so the optimal solution can be found by minimizing the costs while still ensuring a sufficient level of safety.

References

Attema, Thomas et al. (2017). "Maintenance decision model for steel bridges: a case in the Netherlands." In: *Structure and Infrastructure Engineering* 13.2, pp. 242–253.

Bache, Truls Johan Martin Braut (2017). "Numerical Investigation of 3D Scanned Mooring Chains." MA thesis. Norwegian University of Science and Technology.

BayesFusion LLC (n.d.). *GeNIe Support Forum*. Downloaded 29.05.18. URL: `https://goo.gl/1QqiD4`.

Benjamin, Jack R and C Allin Cornell (2014). *Probability, statistics, and decision for civil engineers*. Courier Corporation.

Castillo, Enrique, José Manuel Gutiérrez, and Ali S Hadi (1997). "Sensitivity analysis in discrete Bayesian networks." In: *IEEE Transactions on Systems, Man, and Cybernetics-Part A: Systems and Humans* 27.4, pp. 412–423.

Chakrabarti, Subrata (2005). *Handbook of Offshore Engineering (2-volume set)*. Elsevier.

DNVGL-OS-E302 (2015). *Offshore mooring chain - Rules and Standards*.

DNVGL-OS-E304 (2015). *Offshore mooring steel wire ropes - Rules and Standards*.

DNVGL-RU-OU-0101 (2015). *Offshore drilling and support units - Rules and Standards*.

DVNGL-OS-E301 (2015). *Position Mooring - Rules and Standards*.

Faber, Michael Havbro et al. (2002). "Risk assessment of decommissioning options using Bayesian networks." In: *Journal of Offshore Mechanics and Arctic Engineering* 124.4, pp. 231–238.

Faltinsen, Odd (1993). *Sea loads on ships and offshore structures*. Vol. 1. Cambridge university press.

Fontaine, Emmanuel et al. (2014). "Industry survey of past failures, pre-emptive replacements and reported degradations for mooring systems of floating production units." In: *Offshore Technology Conference*. Offshore Technology Conference.

Friis-Hansen, Peter (2004). "Structuring of complex systems using Bayesian network." In: *Proceedings of Two-Part Workshop at DTU*, pp. 23–25.

GeNIe (2017). Version 2.2. BayesFusion LLC. URL: `www.bayesfusion.com`.

Grädel, Erich et al. (2007). *Finite Model Theory and its applications*. Springer Science & Business Media.

Grêt-Regamey, Adrienne and D Straub (2006). "Spatially explicit avalanche risk assessment linking Bayesian networks to a GIS." In: *Natural Hazards and Earth System Science* 6.6, pp. 911–926.

Hájek, Alan (2003). "Interpretations of probability." In: *In The Stanford Encyclopedia of Philosophy (Zalta*. Citeseer.

Heckerman, David and Ross Shachter (1995). "Decision-theoretic foundations for causal reasoning." In: *Journal of Artificial Intelligence Research* 3, pp. 405–430.

Hoel, Alexander (2016). "3D Scanning of Corroded Mooring Chain." MA thesis. Norwegian University of Science and Technology.

Huckl, Jürgen (n.d.). *Fact Sheet No. WG1-1 :Introduction to Bayesian Networks*. COST TU1402: Quantifying the Value of Structural Health Monitoring.

IACS W22 (2011). *Offshore Mooring Chain*.

ISO 19901-7 (2013). *Petroleum and natural gas industries - Specific requirements for offshore structures - Part 7: Stationkeeping systems for floating offshore structures and mobile offshore units*.

Kahneman, Daniel and Amos Tversky (2013). "Prospect theory: An analysis of decision under risk." In: *Handbook of the fundamentals of financial decision making: Part I*. World Scientific, pp. 99–127.

Keeney, Ralph L and Howard Raiffa (1993). *Decisions with multiple objectives: preferences and value trade-offs*. Cambridge university press.

Keshavarz, Leila (2011). "Analysis of Mooring System for a Floating Production System." MA thesis. Norwegian University of Science and Technology.

Kjærulff, Uffe and Linda C van der Gaag (2000). "Making sensitivity analysis computationally efficient." In: *Proceedings of the Sixteenth conference on Uncertainty in artificial intelligence*. Morgan Kaufmann Publishers Inc., pp. 317–325.

Kosgodagan, Alex et al. (2015). "Bayesian networks to quantify transition rates in degradation modeling: application to a set of steel bridges in the Netherlands." In: *Proc. 12th International Conference on Applications of Statistics and Probability in Civil Engineering, ICASP12, Vancouver, Canada, July 12-15, 2015, 1-8*.

Kosgodagan, A et al. (2015). "Bayesian network-based models for bridge network management." In: *ESREL, Zurich, Switzerland, September, 7-11 2015, 1-7*.

Kvitrud, A (2014). "Anchor line failures-Norwegian Continental Shelf-2010–2014." In: *Stavanger, Norway: Petroleum Safety Authority Norway*.

Langseth, Helge, Thomas D Nielsen, et al. (2009). "Inference in hybrid Bayesian networks." In: *Reliability Engineering & System Safety* 94.10, pp. 1499–1509.

Langseth, Helge and Luigi Portinale (2007). "Bayesian networks in reliability." In: *Reliability Engineering & System Safety* 92.1, pp. 92–108.

Larsen, Kjell (2015). *Mooring for Dummies*. TEKNA Conference - DP and Mooring of Offshore Installations.

— (2017). *Lecture Notes in Stationkeeping and Mooring Systems*. University Lecture.

Ma, Kai-tung et al. (2013). "A historical review on integrity issues of permanent mooring systems." In: *Offshore technology conference*. Offshore Technology Conference.

Maersk (2011). *Gryphon Alpha Loss of Heading, Mooring System Failure and Subsequent Loss of Position*.

Mathisen, Jan and Kjell Larsen (2002). "Risk-based inspection planning for mooring chain." In: *ASME 2002 21st International Conference on Offshore Mechanics and Arctic Engineering*. American Society of Mechanical Engineers, pp. 357–366.

Nielsen, Thomas Dyhre and Finn Verner Jensen (2009). *Bayesian networks and decision graphs*. Springer Science & Business Media.

Noble Denton Europe (2006). *Floating production system JIP FPS mooring integrity*. Tech. rep. Research report 444 prepared for the Health and Safety Executive (HSE).

Norwegian Maritime Authority (2009). *Forskrift om posisjonerings- og ankringssystemer på flyttbare innretninger*.

Okkenhaug, Siril, Torfinn Hørte, and Øivind Paulshus (2017). "Summary and recommendations for safe mooring system design in ULS and ALS." In: *ASME 2017 36th International Conference on Ocean, Offshore and Arctic Engineering*. American Society of Mechanical Engineers, V03BT02A004–V03BT02A004.

Pearl, Judea (2014). *Probabilistic reasoning in intelligent systems: networks of plausible inference*. Elsevier.

Petroleum Safety Authority Norway (2016). *RNNP: Sammendragsrapport Sokkel*.

— (2017a). *Regulations relating to design and outfitting of facilities, etc. in the petroleum activities*.

— (2017b). *Regulations relation to health, safety and the environment in the petroleum activities and at certain onshore facilities*.

PSA (2018). *Trends in risk level in the petroleum activity (RNNP) 2017*.

Rämnes Bruk Product Catalogue (2018). *Top products for harsh offshore conditions*.

Russell, Stuart J and Peter Norvig (2016). *Artificial intelligence: a modern approach*. Malaysia; Pearson Education Limited,

Smedley, P and D Petruska (2014). "Comparison of Global Design Requirements and Failure Rates for Industry Long Term Mooring Systems." In: *Proceedigns of the Offshore Structural Reliability Conference*.

Straub, Daniel (2009). "Stochastic modeling of deterioration processes through dynamic Bayesian networks." In: *Journal of Engineering Mechanics* 135.10, pp. 1089–1099.

— (2015). *Lecture Notes in Engineering Risk Analysis*. University Lecture.

Straub, Daniel and Armen Der Kiureghian (2010). "Bayesian network enhanced with structural reliability methods: methodology." In: *Journal of engineering mechanics* 136.10, pp. 1248–1258.

Straub, Daniel and Iason Papaioannou (2014). "Bayesian updating with structural reliability methods." In: *Journal of Engineering Mechanics* 141.3, p. 04014134.

Tømmervåg, Kristin Hanem (2016). "Degradation Mechanisms of Chain Links in Offshore Mooring Lines." MA thesis. Norwegian University of Science and Technology.

Troll B ROV (våt) inspeksjon av forankringsliner (2014).

Von Neumann, John and Oskar Morgenstern (2007). *Theory of games and economic behavior (commemorative edition)*. Princeton university press.

A Quantifying the nodes with GeNIe

This section provides a tutorial on how the auxiliary[18] networks are established and used to quantify the discrete networks, exemplified with the ULS Network. Figure 45 shows the complete auxiliary ULS network. The proxy decision nodes are marked with **1** and treated in Section A.1. **2** marks the parent chance nodes, which are treated in Section A.2. The child chance nodes are marked with **3** and they are treated in Section A.3. Finally, Section A.4 explains two different methods for discretizing and quantifying the nodes.

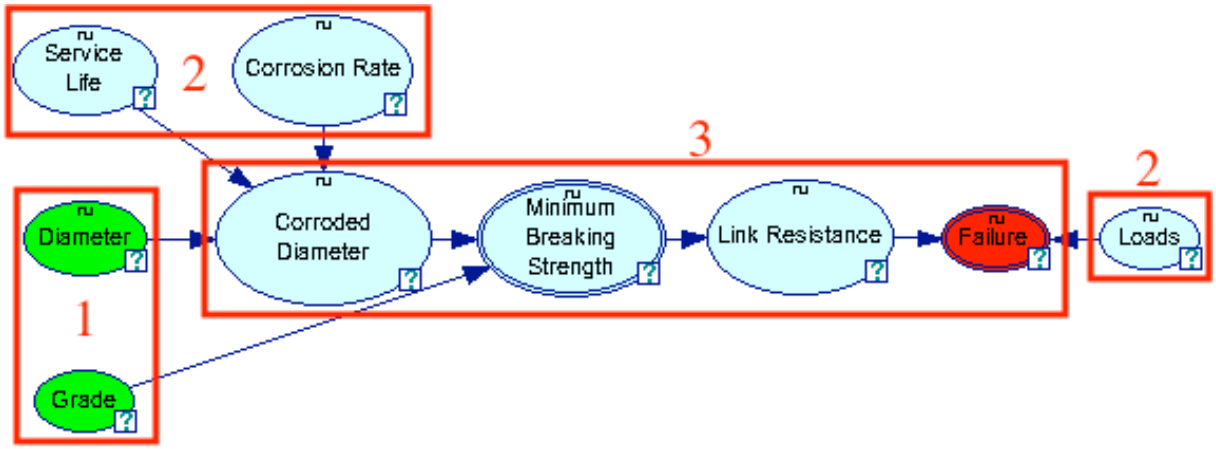

Figure 45: The auxiliary ULS Network

A.1 Model a Decision

There are two approaches to model a decision in the auxiliary networks:

- Chance node with uniform outcome probability where each state corresponds to a decision. It is the preferred option when a finer discretization of decision states does not have a physical interpretation. This is the case for *Grade* since this note contains maximum five decisions.
- Equation node with a Uniform distribution. This may be applied where a finer discretization of the decision outcome has a physical interpretation, such as for *Diameter*.

Figure 47(a) and Figure 47(b) show how *Grade* and *Diameter* is defined in the auxiliary ULS Network. The red arrow in Figure 47(b) shows where the available distributions can be found. For the equation node, the bounds must be specified as marked by the red box.

Furthermore, the equation node is discretized. The layout of the *Discretization* tab is shown in Figure 48. The buttons *Add* and *Insert* marked by **1** controls how many states the nodes are discretized in. The discretization interval is uniformized in the equation domain by the *Uniformize* button, marked with **2**. A non-uniform interval may be created by manually changing the white

[18] Hybrid Bayesian networks used to quantify their discrete counterparts

values in **4**. **5** shows the current names of the states the node is discretized in. These names can be manually changed by the user. By pressing the *Rediscretize* button marked by **3**, the CPT, marked by **6**, appears.

Notice that the symbol above *Diameter* changes throughout this process. The **C** and double lines show that the node in Figure 46(a) is a constant and deterministic, respectively. A deterministic equation node is a node where no additional uncertainty is introduced. This means that all uncertainty of this node is attributed to its parents. The symbol in Figure 46(b) shows that the equation node is distributed but not discretized. A distributed and discretized node is shown in Figure 46(c).

(a) (b) (c)

Figure 46: The different symbols for the equation nodes

A.2 Model a Parent Chance Node

The next step is to model the parent chance nodes. For the ULS Network, these are the nodes *Service Life*, *Corrosion Rate* and *Loads*. It is not recommended to model these nodes as chance nodes, even for simple CPTs, since it requires the user to write potentially time-consuming *switch* or *choose* statements to relate the states to physical values.

The nodes are discretized with the methodology explained in the previous section. It is recommended to activate the tool marked by **1** in Figure 49(a) to visually inspect that the CPT resembles the distribution. Note that a non-uniform discretization makes it harder to recognize the distribution in the CPT. Therefore, a uniform discretization interval is recommended.

Valuable information and a graphical representation of the distribution is found in the *Value* tab, as shown for *Service Life* in Figure 49(b).

A.3 Model a Child Chance Node

The relationship between a child and its parents is described by a function. The function depends on the type of the child node. There are two types of child nodes:

- Child of equation nodes: The equation is specified with operators and node identifiers. An example is given in Figure 50(a). Note that the node identifier ”Diameter” corresponds to the Uniform distribution from Figure 47(b).

- Child of proxy chance nodes: In this case, a *switch* or *choose* statement is written to convert each state to a numerical value. This is illustrated in Figure 50(b).

Note that short node identifiers are preferred, as this eases readability.

In both instances, appropriate bounds for the equation domain must be established. It is crucial to conduct a visual inspection of the CPT to ensure that the distribution is fully captured within the bounds. An unexpected Uniform distribution means that the bounds are too strict. In addition, GeNIe prompts a warning message stating that the samples are out of bounds and that several entries in the CPT are not configured. The effect of strict bounds is illustrated in Figure 51(a) and Figure 51(b).

The accuracy of the Monte Carlo sampling is dependent on the number of samples generated. The standard number of samples in GeNIe is 10,000. To increase the number, click on the *Network* menu, or right-click outside the network, and click on *Network Properties*. On the resulting pop-up window, click on the *Sampling* tab. The *Sampling* tab is shown in Figure 52.

A.4 Discretization and Quantification

The discretization may be performed in two ways:

- Using the discretization tool in the *Network* menu. This is useful for establishing the discrete network for the first time. The decision nodes are created by right-clicking on the proxy nodes, then *change type*. The discretization tool requires that all nodes are discretized with the aforementioned procedure.

- Manually copying the CPT for each node using the rediscretization tool. This is useful for minor changes in the model that can easily be implemented in the auxiliary network. Note that a change in one node requires a change of all its descendants.

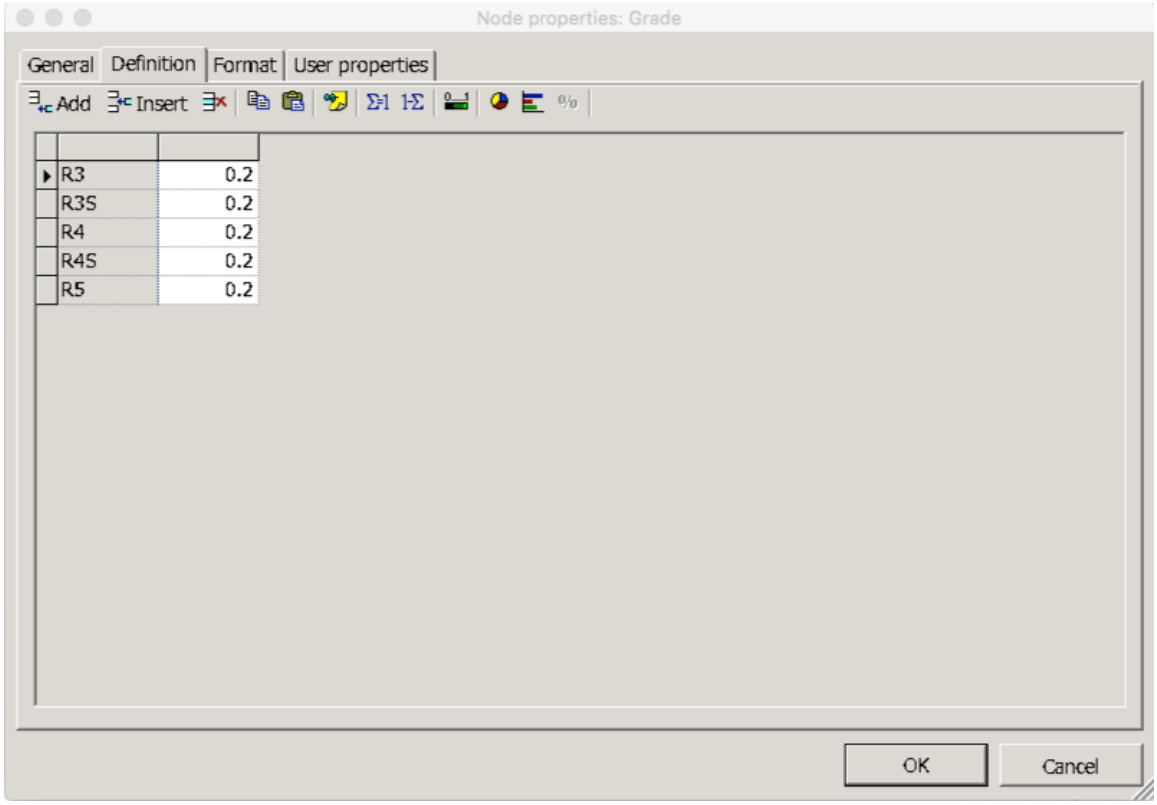

(a) Definition of *Grade*

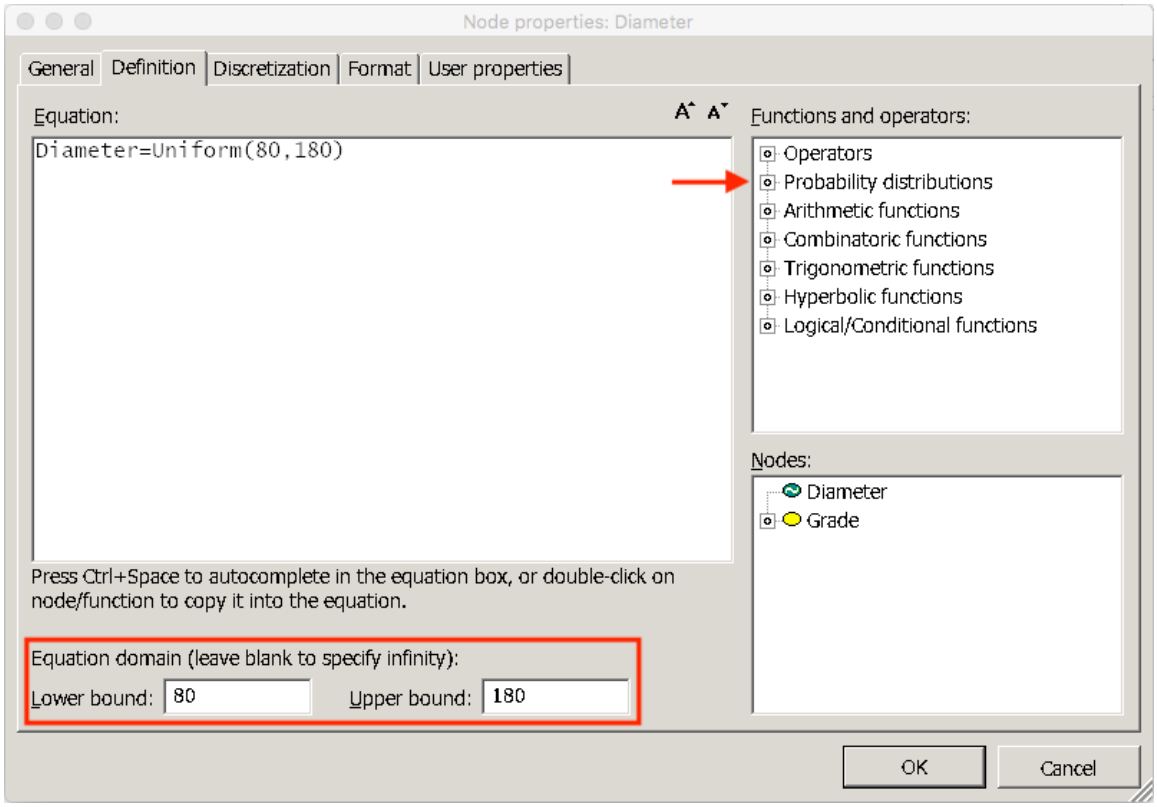

(b) Definition of *Diameter*

Figure 47: The two different approaches for modeling a decision node

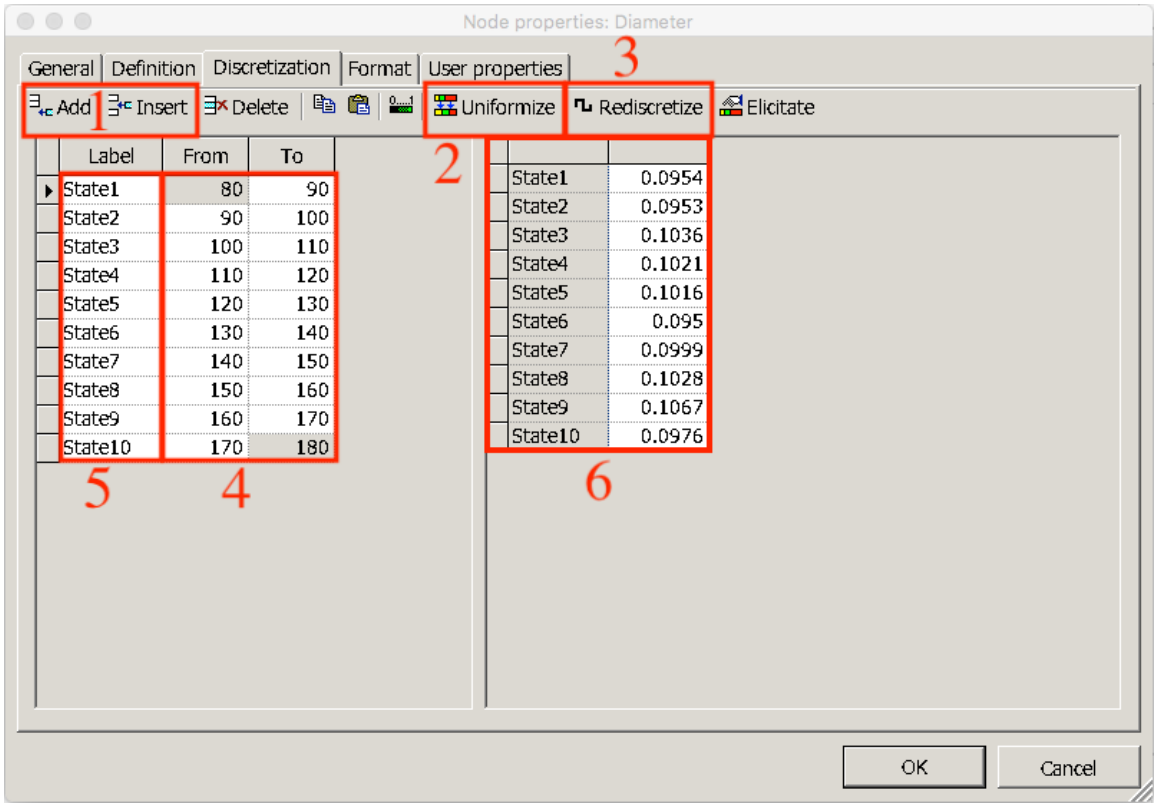

Figure 48: *Discretization* tab of an equation node

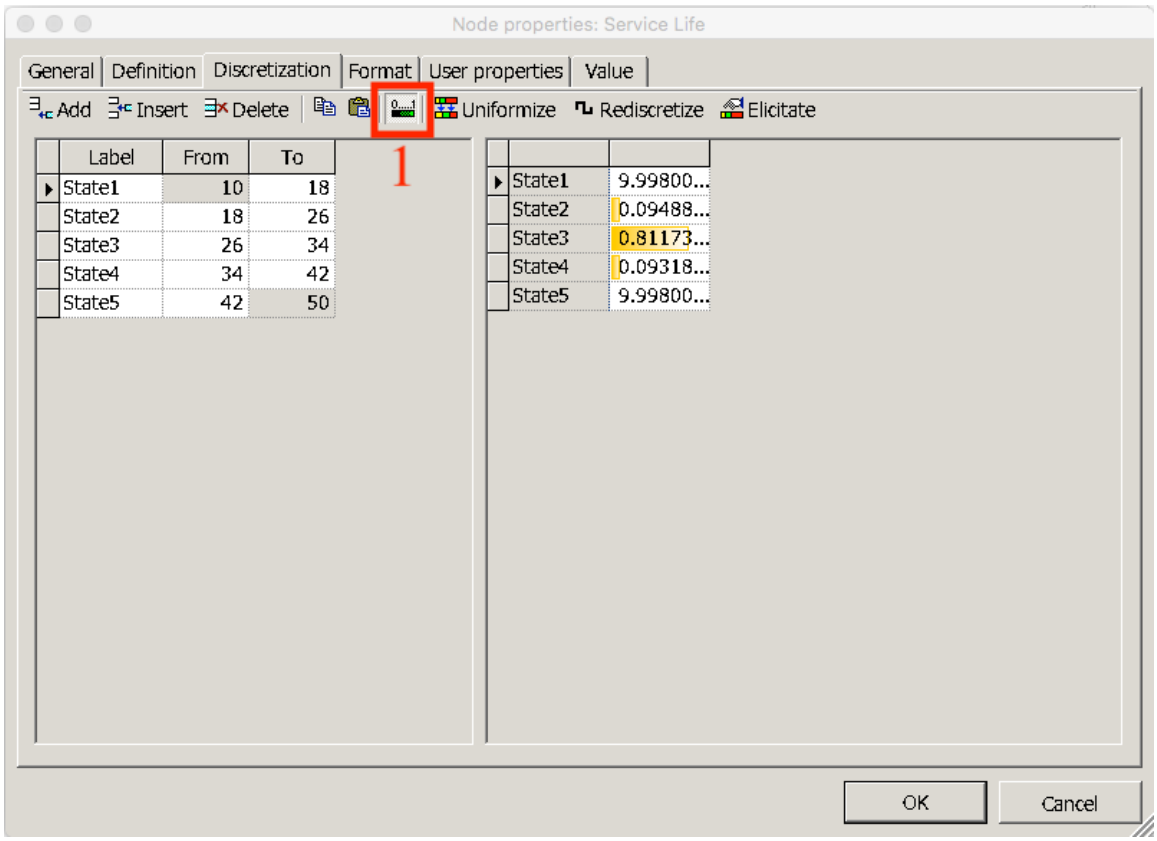

(a) The *Discretization* tab

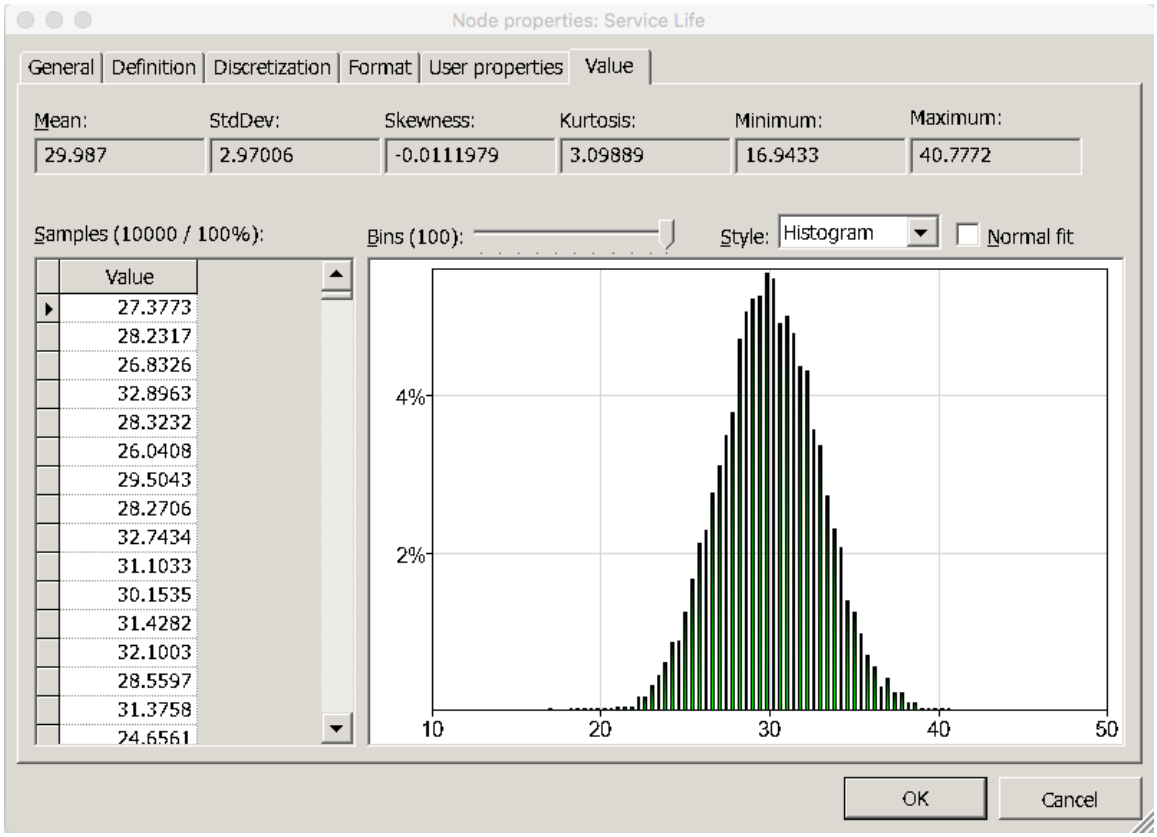

(b) The *Value* tab

Figure 49

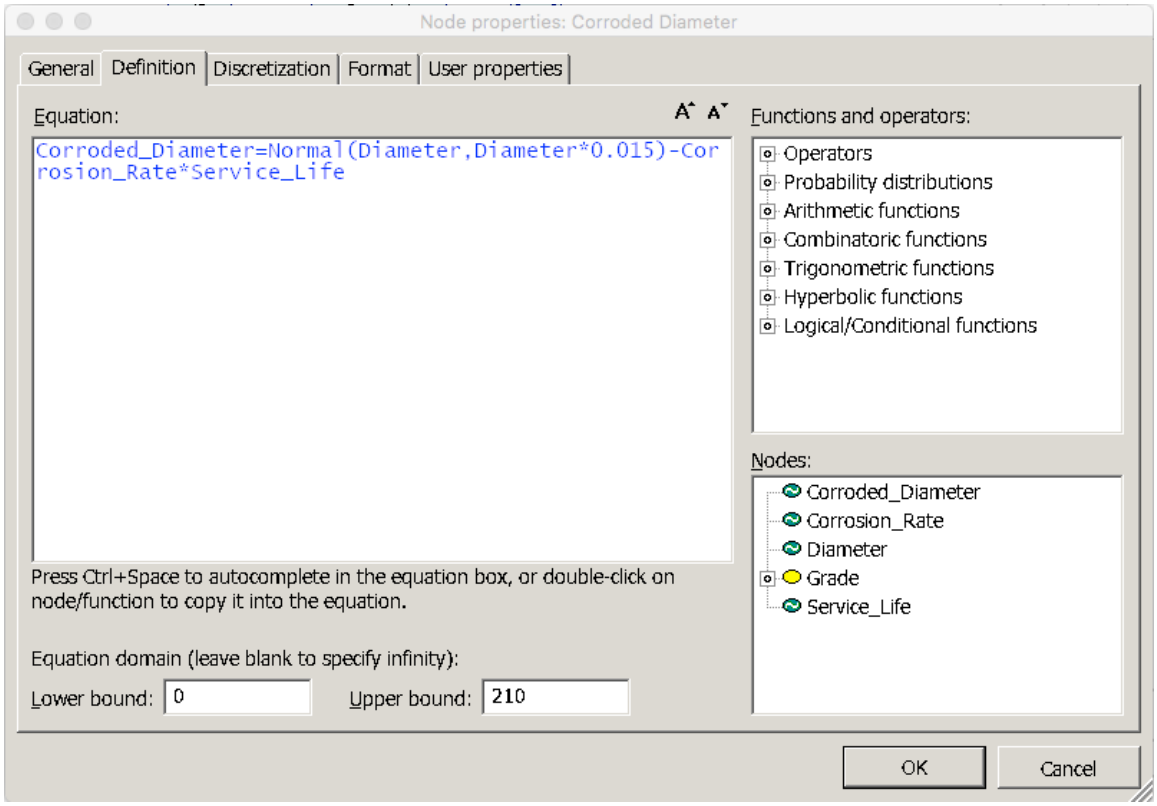

(a) Child of an equation node

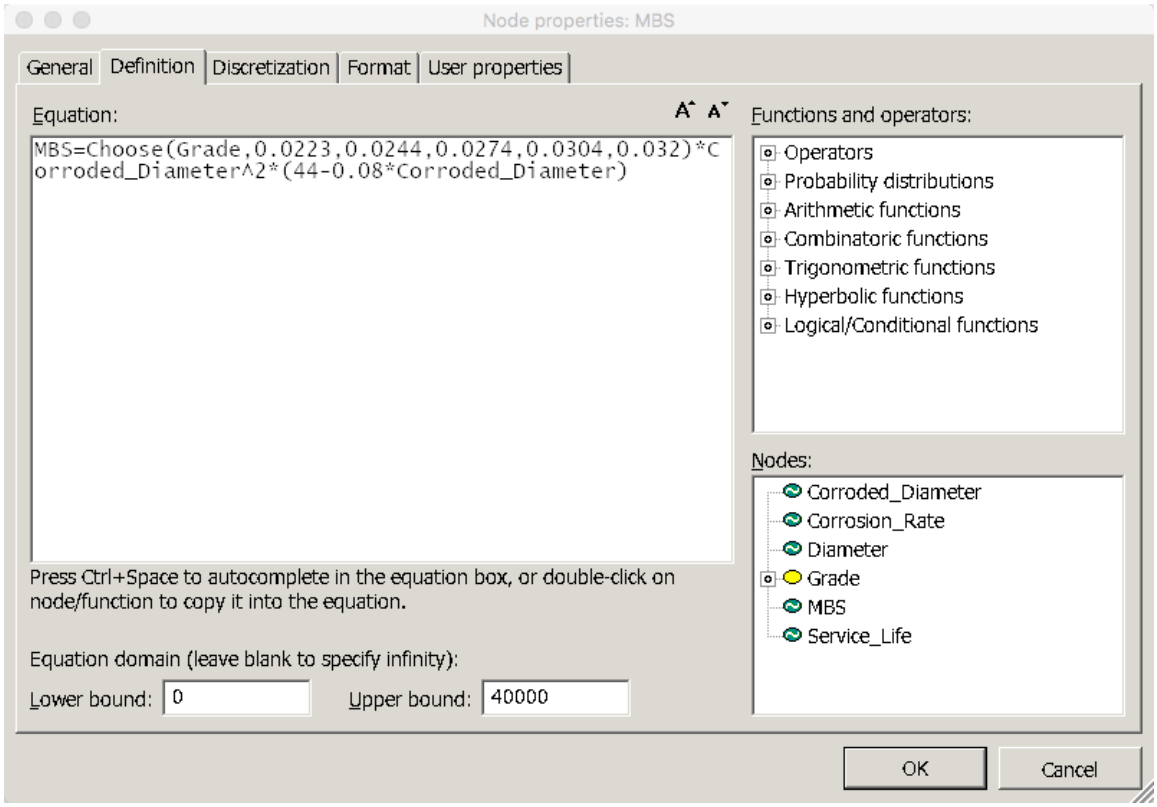

(b) Child of a proxy chance node

Figure 50: The *Definition* tab for a child chance node

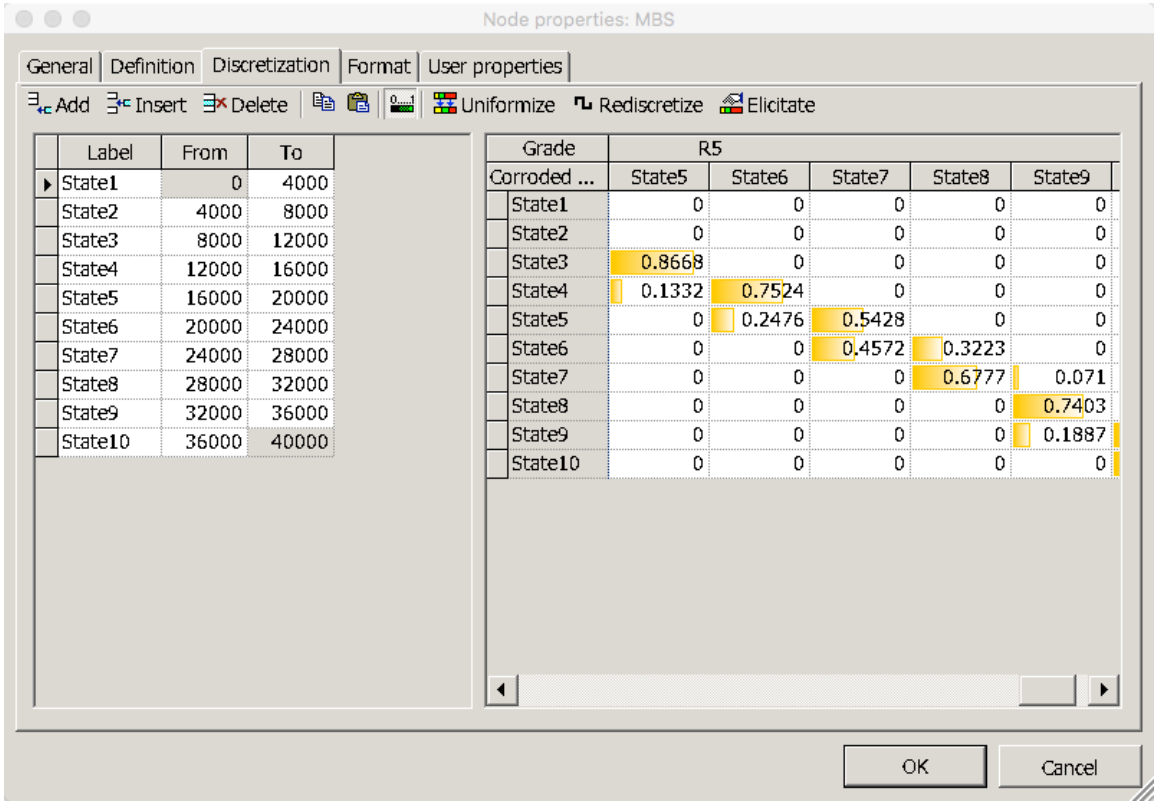

(a) Adequate bounds

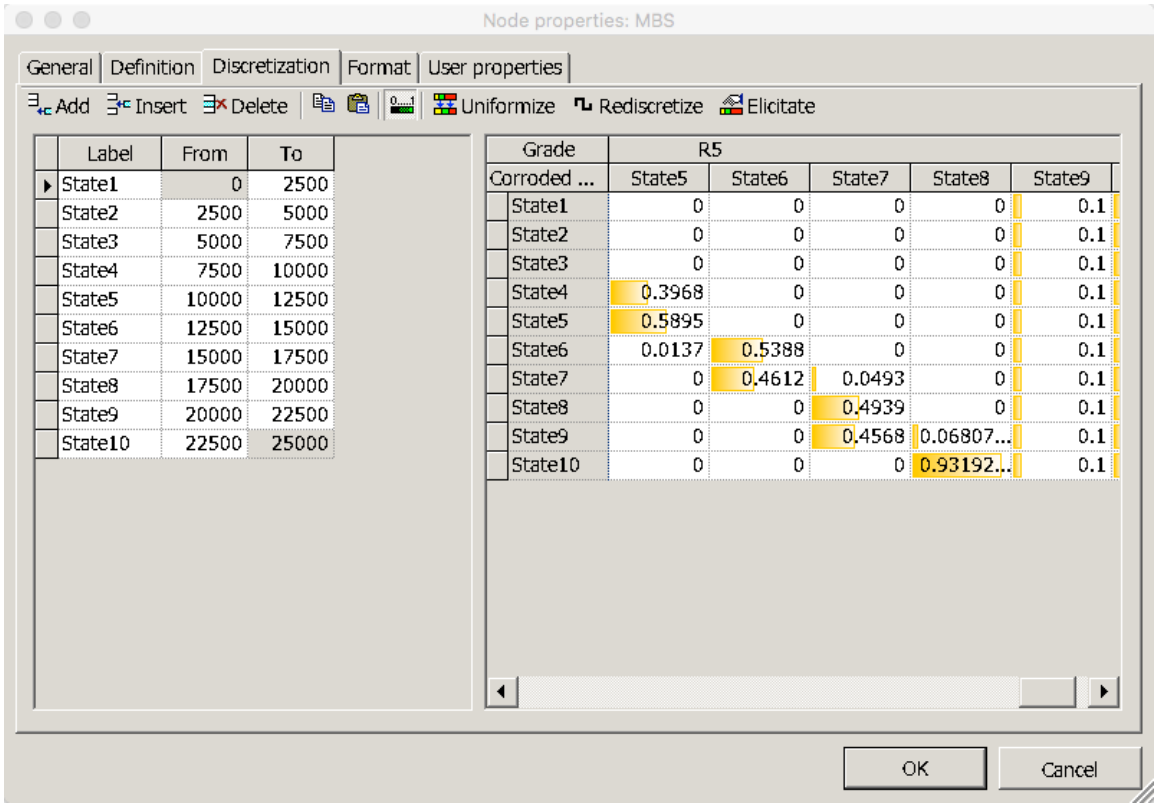

(b) Bounds too strict

Figure 51: The CPT for *Minimum Breaking Strength*

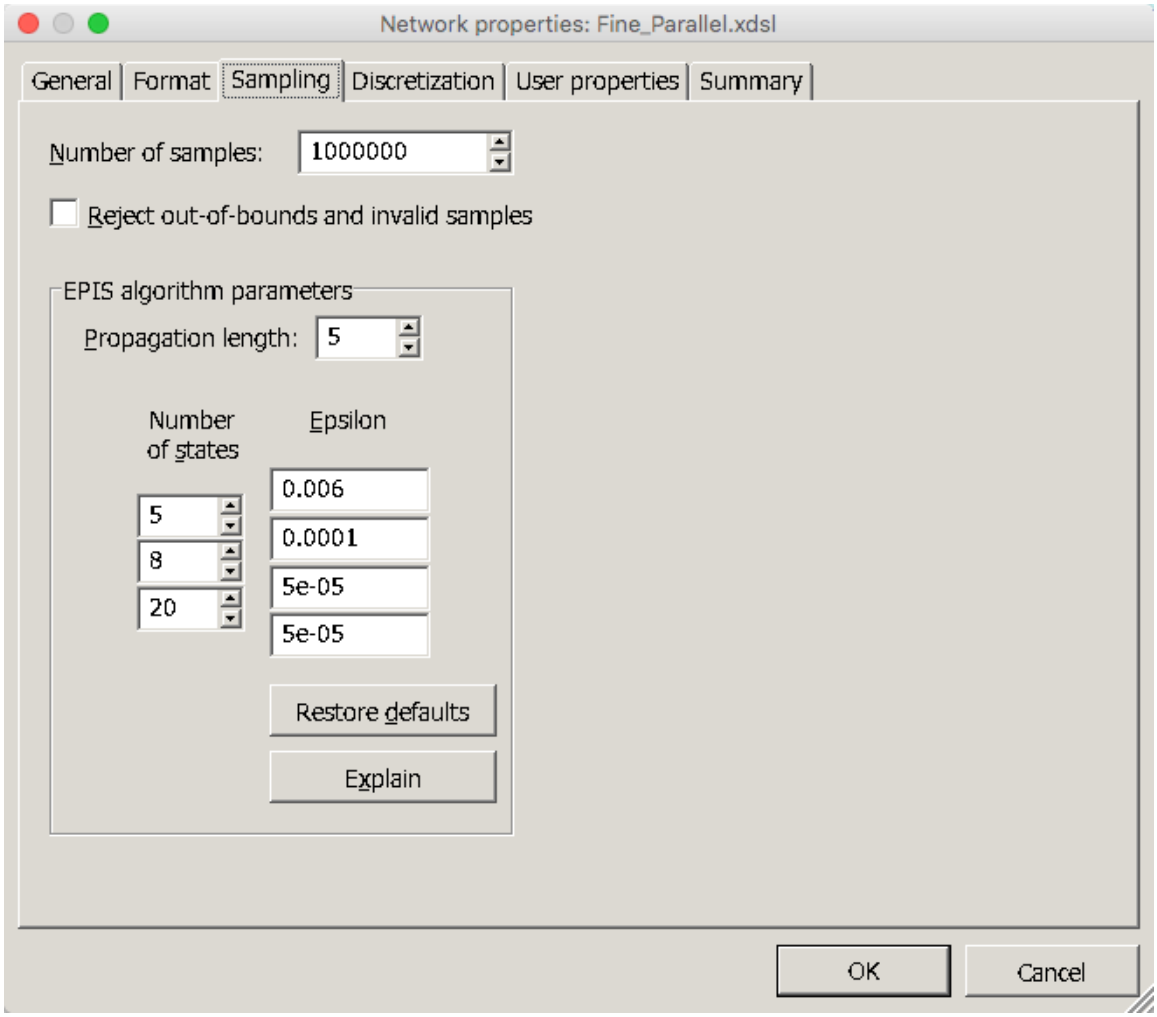

Figure 52: Layout of the *Sampling* tab